DYNAMICS OF A PERIODICALLY SUPPORTED PIPE CONVEYING FLUID

A Thesis Submitted
In Partial Fulfilment of the Requirements
for the Degree of
DOCTOR OF PHILOSOPHY

by
KULDIP SINGH

to the

DEPARTMENT OF MECHANICAL ENGINEERING
INDIAN INSTITUTE OF TECHNOLOGY KANPUR
SEPTEMBER 1977

CERTIFICATE

This is to certify that the thesis entitled "DYNAMICS OF A PERIODICALLY SUPPORTED PIPE CONVEYING FLUID" by Kuldip Singh is a record of work carried out under my supervision and has not been submitted elsewhere for a degree.

Mallik 26/9/77

Kanpur
September 1977

A.K. Mallik
Assistant Professor
Department of Mechanical Engineering
Indian Institute of Technology Kanpur

ACKNOWLEDGEMENT

I wish to express my gratitude to Dr. Asok K. Mallik for his guidance throughout the course of this work.

I am also indebted to Dr. V.K. Stokes, Dr. M.M. Oberoi, Dr. G.S. Kainth and Dr. R. Rajagopalan for their interest in this work.

I wish to thank Capt. & Mrs. K.K. Mehra for their affection and hospitality that never let me feel home-sick during the course of this study.

I am grateful to all my friends for rendering their services whenever needed.

I wish to thank Dr. K.C. Pande who was kind enough to read and criticize portions of the manuscript.

Finally, I wish to thank Mr. S.K. Tewari and Mr. G.L. Misra for typing the manuscript and Mr. D.S. Panesar for tracing the figures.

September - 1977 Kuldip Singh

CONTENTS

LIST OF FIGURES

LIST OF PRINCIPAL SYMBOLS

A_p	cross-sectional area of the pipe
C_o	viscous damping on the motion of the pipe
C_a	viscous damping of the absorber
C_v	convection velocity of the loading
EI	flexural stiffness of the pipe
E^*	coefficient of internal dissipation of the pipe
k	wave number of the loading
k_a	spring constant of the absorber
k_r	rotational stiffness at each support
ℓ	span length of the pipe
m_a	mass of the absorber
m_f	mass of the fluid per unit length of the pipe
m_p	mass of the pipe per unit length
M	bending moment at any cross-section of the pipe
$\bar{M}$	non-dimensional bending moment, $= \frac{M\ell}{EI}$
p_o	loading parameter
$\bar{p}_o$	non-dimensional loading parameter, $= \frac{p_o \ell^3}{EI}$
p_f	fluid pressure
t	time
x	co-ordinate along the length of the pipe
y	displacement of the pipe in the transverse direction
$\bar{y}_1$	non-dimensional displacement of the pipe, $= \frac{y}{\ell}$

V fluid velocity in x direction

u non-dimensional fluid velocity, $= \left(\frac{m_f}{EI}\right)^{\frac{1}{2}} V\ell$

u_o non-dimensional constant mean velocity of the fluid

α non-dimensional coefficient of internal dissipation, $= \left[\frac{I}{E(m_f+m_p)}\right]^{\frac{1}{2}} \frac{E^*}{\ell^2}$

β mass ratio parameter, $= \left(\frac{m_f}{m_f+m_p}\right)^{\frac{1}{2}}$

β_{ij} slope at section i due to unit harmonic moment at section j

γ non-dimensional fluid pressure, $= \frac{p_f A_p \ell^2}{EI}$

Γ_a mass ratio of the absorber, $= \frac{m_a}{(m_f+m_p)\ell}$

δ excitation parameter

ε phase difference between loading over length ℓ, $= -k\ell$

η_c non-dimensional viscous damping, $= \frac{C_o \ell^2}{[EI(m_f+m_p)]^{1/2}}$

η_s loss factor associated with rotational stiffness at each support

θ slope of the neutral axis of the pipe

κ_r non-dimensional rotational stiffness at each support, $= \frac{k_r \ell}{EI}$

μ $= \mu_r + i\,\mu_i$, complex propagation constant

μ_r attenuation constant

μ_i phase constant

ξ non-dimensional x co-ordinate along the pipe, $= \frac{x}{\ell}$

$\bar{\rho}$ non-dimensional curvature amplitude at mid-span

τ non-dimensional time, $= \left(\frac{EI}{m_f+m_p}\right)^{\frac{1}{2}} \frac{t}{\ell^2}$

ω frequency

ω_o reference frequency

ω_a natural frequency of the undamped absorber, $= \left(\frac{k_a}{m_a}\right)^{\frac{1}{2}}$

Ω non-dimensional frequency, $= \left(\frac{m_f + m_p}{EI}\right)^{\frac{1}{2}} \omega \ell^2$

Ω_n non-dimensional natural frequency

Ω_o non-dimensional reference frequency

$\bar{C}$ non-dimensional convection velocity of the loading,
$= \left(\frac{m_f + m_p}{EI}\right)^{\frac{1}{2}} \ell C_v$

C_c critical damping of the absorber, $= 2m_a \omega_a$

C_p non-dimensional phase velocity of the free propagating wave, $= -\frac{\Omega}{\mu_i}$

T periodic time of the harmonically varying component of the fluid velocity, $= \frac{2\pi}{\Omega}$

$\bar{y}$ non-dimensional displacement of the pipe, $= \frac{y}{\ell\, e^{i\omega t}}$

ζ_a damping ratio of the absorber, $= \frac{C_a}{C_c}$

η_b loss factor of the pipe, $= \frac{E^* \omega}{E}$

σ_a tuning ratio of the absorber, $= \frac{\omega_a}{\omega_o}$

SYNOPSIS

DYNAMICS OF A PERIODICALLY SUPPORTED PIPE CONVEYING FLUID

The Thesis Submitted

In Partial Fulfilment of the Requirements

For the Degree of

DOCTOR OF PHILOSOPHY

by

KULDIP SINGH

to the

Department of Mechanical Engineering

Indian Institute of Technology, Kanpur

September 1977

This thesis is a study of the dynamics of a periodically supported pipe conveying fluid. The work can be broadly divided into three sections :

(i) Study of the wave propagation and vibration response of a periodically supported pipe conveying fluid.

(ii) Study of the parametric instabilities of such pipes.

(iii) Investigation of the effects of dynamic absorber on the parametric instabilities of such pipes.

In the first part of the work, free harmonic wave propagation in a periodically supported infinite pipe has been studied, treating the pipe as a beam-type structure. The velocity and the pressure of the flowing fluid have been assumed to be constant throughout. We show

that there exist alternate frequency bands of attenuation and propagation of free harmonic waves. Due to the presence of the Coriolis acceleration of the fluid, the waves travel in the positive and the negative directions with different velocities. Numerical results have been computed to show the effects of different parameters like the rotational constraint at the supports, the fluid pressure and the fluid velocity.

Natural frequencies of a finite, periodically supported pipe are then determined using the 'wave approach'. Due to the difference in the velocities of the waves travelling in opposite directions, no classical normal modes (in the sense of standing modes) exist. The effect of introducing identical rotational springs at each support has also been studied. The propagation constants have been used to study the divergence instabilities of these pipes.

The response of a periodically supported infinite pipe to convected harmonic pressure fields has been determined. The resonant-type response occurs at 'coincident frequency' where the convection velocity is equal to the phase velocity of the free wave. The value of the coincident frequency depends on whether the convected pressure field travels along the direction of the fluid flow or in the opposite direction. The effects of introducing damping in the pipe and at the supports have also been studied.

The second part of the work is concerned with the case when the velocity of the flowing fluid is having a harmonic fluctuation over and above the mean constant value. This introduces 'parametric instabilities' in the pipe. Two types of parametric instabilities may

be distinguished, the so-called primary and secondary instabilities. First, the method used in previous works for single span pipes have been extended. Mode shape approximation is necessary in this method. Normally, the approximate modes are taken as those of the corresponding beam. Hence, to use this method, mode shapes of a periodically supported beam must be known in advance. Moreover, the computational effort increases with increasing number of spans.

To overcome the first problem, we present a method which does not require any mode shape approximation. This gives a set of coupled differential equations. By applying boundary conditions, a frequency equation is obtained in the form of a determinant. The zeros of this determinent gives the boundaries of the unstable regions. The size of this determinant, however, increases drastically with the increase in the number of spans of the pipe.

Another method using the wave approach has also been proposed to determine the regions of parametric instabilities. Numerical results have been presented for the primary and the secondary instability regions of a two span pipe. All the three methods have been used for the purpose of comparison and cross-checking.

The effect of various parameters like the Coriolis term, the fluid velocity and the fluid pressure on the regions of instabilities have been studied in detail. The effect of damping has also been investigated.

The last phase of the work considers the problem of controlling the regions of parametric instabilities by means of dynamic absorbers. First, single span pipes with pinned-pinned, clamped-clamped, and clamped-pinned ends have been studied. The effects of various parameters such as damping ratio, tuning ratio, and mass ratio of the absorber have been studied numerically. No attempt, however, has been made to optimise these parameters for best performance of the absorbers. Analysis has also been presented for the case when an undamped absorber is attached at the mid-point of each bay of a periodically supported finite pipe.

CHAPTER 1

INTRODUCTION

1.1 Introduction

Pipe-lines conveying fluids at high pressure and velocity are encountered in various fields of engineering. To name a few, such pipe-lines exist in different process industries, high pressure boilers, fuel-lines of air-crafts and missiles, and in nuclear reactors. A thorough understanding of the dynamics of elastic pipes conveying fluid is necessary for the proper design of these pipe-lines. An improper design of the pipe-lines may result in leakage and unsatisfactory performance of the whole system. In severe cases, excessive vibration of the pipe-lines may even cause fatigue cracks and eventual failure of the pipes.

In the past two decades, considerable amount of research work has been done in the field of flow induced vibrations. The exact analysis of the problem is complicated by the fact that the fluid flow-field and the motion of the pipe are affected by each other. In theoretical models for pipes with internal flow, fluid flow is usually assumed to be undisturbed by the motion of the pipe. Vibrations of single span pipes with different boundary conditions have already been analysed by many researchers. Some of the works analysed the free oscillation of a pipe with the fluid flowing at a constant velocity. Quite a few studies concentrated on the parametric instabilities of

a pipe for situations when the fluid velocity has harmonic fluctuations over and above a constant mean value. A historical account of all these works can be found in reference [48] . The effects of bends in a pipe have also drawn the attention of some workers [24] .

With slight modifications, the theory developed for the above mentioned problems can also be applied to various other problems. These include

(i) the dynamics of a stiff, moving wire or belt [13,52] ,

(ii) the dynamics of a moving chain or string [1,29,58] , and

(iii) the dynamics of an empty pipe submerged in a fluid flowing parallel to the axis of the pipe [60] .

With strong motivation provided by wide applications, much progress has been made in the study of dynamics of a single span pipe conveying fluid. Very often, long pipe-lines on multiple supports are used to transmit high pressure fluids. However, very little has been reported on the vibration problems of such multi-supported pipes [53] . The present thesis is an attempt to fill this gap and deals with the dynamics of an elastic pipe supported identically at regular intervals. Performance of a dynamic absorber in controlling the parametric instabilities of such pipes has also been investigated. The objective and scope of the present work is outlined in detail in a later section.

1.2 Review of Previous Work

Since the present work deals with the dynamics of pipes conveying fluids and analysis of periodic structures, a brief review of the available literature in each of these fields is given in the following sections.

1.2.1 Dynamics of Pipes Conveying Fluids

Interest in the study of dynamics of elastic pipes conveying fluids was activated by Ashley and Haviland [2] in connection with the vibration problems of Trans-Arabian pipe-line. They used an approximate power series solution. The equation used to describe the motion of the pipe did not adequately account for the governing inertia forces, as later pointed out by Feodos'yev [15] . They studied the flow induced damping in a simply supported pipe and found it to increase with the flow rate. They further studied the wave - type solutions and found that the effect of flow is to expedite the waves travelling in the flow direction and to retard the waves travelling in the opposite direction.

Housner [23] studied the same problem by developing the equation of motion using Hamilton's principle. He found that at sufficiently high flow velocities the pipe may buckle, essentially like a column subjected to axial loading. A more general study by Niordson [40] led to the same conclusions. Later on, experimental study conducted by Dodds and Runyan [14] also confirmed the conclusions about the stability of the pipe. The experimental results were in good agreement with those obtained by Housner's analysis [23] .

Long [28] also presented experimental and theoretical studies of the transverse vibration of pipe transporting fluid. He used the equation of motion as derived by Housner [23] and a power series solution was used. His solution was applicable to relatively small flow velocities. The pipes with different end conditions were also considered. He showed that in contrast to those of simply supported pipes, the motion of cantilevered pipes are damped by internal flow in a particular range of flow velocities. The conclusion of Ashley and Haviland [2] that the flow of fluid damps the motion of the simply supported pipe was due to improper selection of lesser number of terms in the power series solution.

Handelman [19] studied the nature of eigen values from the structure of the governing differential equation. No specific solution, however, was reported. Movchan [38] used Liapunov's direct method to determine the condition of stability for a simply supported pipe conveying fluid.

Benjamin [3,4] studied the dynamics of articulated pipes consisting of rigid tubes connected by flexible joints. He showed that a cantilevered system of articulated pipe is subjected to oscillatory instability. He also found that the dynamical problem is independent of the fluid friction. Later Gregory and Paidoussis [17,18] confirmed, both theoretically and experimentally, that at sufficiently high flow velocities, cantilevered pipes are subjected to oscillatory instabilities.

Benjamin [3] , using his articulated pipe representation, also concluded that buckling instability is possible in the case of a vertical

cantilevered system, where gravity is operative. On the other hand, Paidoussis [44] found that vertical continuous flexble pipes never experience buckling instability. This contradiction was later cleared by Paidoussis and Deksnis [45] . They showed that the dynamic behaviour of articulated and continuously flexible pipes are not strictly analogous. The stability of tubular cantilevered pipes has also been studied in detail by several workers [21,22, 41].

Naguleswaran and William [39] studied, both theoretically and experimentally, the effect of the fluid pressure on the dynamics of the pipe. They showed that pipes with both ends supported may buckle even at small flow velocities by the action of the fluid pressure. Stein and Torbiner [57] studied the dynamics of an infinitely long pipe resting on continuous elastic support. They studied the effect of the foundation modulus, fluid velocity, and fluid pressure on various characteristics such as the dynamic stability, the frequency response, and the wave propagation.

Srinivasan and Kamath [55] used Ritz method to study the vibration of a cantilevered pipe. They calculated the logarithmic decrement for the motion of the pipe and also derived the stability conditions. The same method has also been used for pipes with other conditions [56].

Thurman and Monte [59] presented a non-linear analysis for a pipe with simply supported ends. They used the perturbation technique and found that the importance of the nonlinear term increases with the

flow velocity. Thus, the applicability of the linear theory becomes restricted as the flow velocity increases.

Chen [9] studied the stability of a pipe with upstream end clamped and downstream end constrained by a linear spring, so that boundary conditions are intermediate between clamped-free and clamped-pinned cases. He showed that, in general, both buckling and oscillatory instabilities are possible depending on the spring constant.

Paidoussis and Issid [48] derived the most general equation for the motion of a pipe. They included the effect of axial contraction of the pipe. They also showed that with both ends supported, the pipe is subjected not only to divergence (buckling) instability but may also undergo coupled mode flutter if the flow velocity is sufficiently high. On the other hand, a cantilevered pipe is subjected only to flutter of the single degree of freedom. They also discussed the existence of the flutter in conservative system and found it to be associated with the gyroscopic (Coriolis) forces. It was shown that flutter in such systems can only be of the coupled-mode kind. Some design criteria were proposed for maximum flow velocity from the point of view of stability.

In all the above works, the pipe was treated as a beam-type structure. Paidoussis and Denise [46,47] studied the dynamics of a thin cylindrical pipe conveying fluid, treating it as a shell-type structure. The fluid forces were obtained using potential flow theory. They analysed both cantilevered and clamped-clamped pipes.

They found that in addition to the instabilities in beam modes (corresponding to those found previously by treating the pipe as a beam-type structure), instabilities in shell modes are also possible. They also showed that a clamped-clamped pipe experiences coupled-mode flutter in addition to the divergence instability. The experimental results were in confirmation with the theory. Weaver and Unny [61] obtained similar results in case of a pinned-pinned pipe.

Chen and Rosenberg [12] studied the free vibration of cylindrical shells conveying fluids. The shell motion was described by Flügge's equations and the hydrodynamic forces were derived from the linearised potential flow theory. In low frequency range, they developed a modified water-hammer theory and an approximate bounding frequency equation including the effect of fluid flow.

Liu and Monte [27] conducted experiments to compare the different existing theories. Three velocity regions, viz., low, moderate and high, were considered separately. Good agreement between theory and experiments was obtained in the low velocity region. However, discrepancy increased with higher fluid velocity. The discrepancies were attributed to the fact that the initial configuration of the pipe is not straight and it also depends on the flow velocity.

In all the above studies, the velocity of the fluid flowing through the pipe was assumed to be constant. Chen [10] studied the problem with the velocity of the flowing fluid having a harmonic fluctuation over and above the mean constant value. He found that

both parametric and combinational resonances are possible. He determined the instability regions for a simply supported pipe.

Ginsberg [16] also studied the problem of the stability of a simply supported pipe with a pulsatile flow. He used Bolotin's method to determine the parametric instabilities. It was found that damping, in general, has greater effect on the regions of instability associated with the higher natural frequencies. Similar effects of damping was also observed on the higher order regions of instability.

Paidoussis and Issid [48] determined the regions of parametric instability for pipes with various end conditions. They showed that cantilevered pipes are also subjected to parametric instabilities, provided that the flow velocity is not too small. Later Paidoussis and Sundararajan [49] determined the regions of combinational resonances for a pipe. Plaut and Huseyin [43] determined the instability regions of a pipe with an axial load.

1.2.2 Analysis of Periodic Structures

Dynamics of periodic structures has been studied by Lin [25] through calculation of the normal modes and then analysing the forced motion in each of the significant modes. Transfer matrix method has also been applied for studying the vibration of beams on many supports [26].

Wave motion in periodic systems in the field of crystals, electrical circuits, etc., has been studied for nearly 300 years, as pointed out by Brillouin [8] in his classical work. It was only

recently that wave motion in engineering periodic structures (consisting of beams, plates, etc.) has been studied. Heckl [20] considered a system of beams coupled together to form a regular grillage and demonstrated that flexural motion in periodic beam type structures can propagate in some frequency bands and not in others.

Mead [30] studied the free wave propagation in infinite beams resting on periodic supports. He also studied their possible interaction with the acoustic waves. Later, he presented a general theory for periodic structures with multiple couplings [32].

Sen Gupta [51] developed a graphical method, using wave approach, to determine the natural frequencies of a periodic beam. Mead [31] used the wave approach to determine the response of periodic structures when subjected to convected harmonic loading. He showed that 'coincidence' occurs at a frequency when the convection velocity of the pressure field is equal to the phase velocity of the free waves propagating through the structure. Natural frequencies and mode shapes of mono-coupled and multi-coupled systems have also been studied in detail [33,34].

In all the works mentioned above, periodic element was taken to be uniform. Thus, exact harmonic solution was obtained in closed form. But when the periodic element is non-uniform, one cannot find the closed form solution. So, attempts have also been made to develop approximate methods. Mead and Pujara [36] developed a space-harmonic series solution for such problems. Mead and Mallik [35]

presented an 'assumed mode' method to determine the response of infinite periodic beams with non-uniform elements. Rao and Mallik [50] extended this approximate method to calculate the response of finite periodic beams. Finite element techniques have also been used for similar problems [42].

Recently, Chen [11] used the wave approach to determine the natural frequencies of a periodic row of circular cylinders surrounded by a liquid.

1.3 Objective and Scope of the Present Work

It is seen from the available literature, that much progress has been made in the study of the dynamics and the stability of single span pipes conveying fluids. In the present thesis the dynamics of a periodically supported pipe conveying fluid has been studied. The work can be broadly divided into three sections:

(i) Study of the wave propagation and vibration response of a periodically supported pipe conveying fluid.

(ii) Study of the parametric instabilities of such pipes.

(iii) Investigation of the effect of dynamic absorbers onthe parametric instabilities of these pipes.

In the first part of the work, harmonic wave propagation in a periodically supported infinite pipe is studied, treating the pipe as a beam-type structure. It is assumed that the supports are transversely rigid and they produce no axial force. The axial contraction of the pipe has been assumed to be negligible. The velocity and the

pressure of the fluid are taken to be constant throughout.

Natural frequencies of a finite, periodically supported, pipe are then determined using a graphical method. In this approach the computational effort is independent of the number of spans of the pipe. The case with identical rotational stiffness at each support has also been investigated. Furthermore, the propagation constants are used to study the divergence instabilities of such pipes. This is followed by the response analysis of a periodically supported infinite pipe subjected to a convected harmonic pressure field. The effect of damping in the pipe and at the supports has also been investigated.

The second part of the work considers the velocity of the flowing fluid as having harmonic fluctuations superimposed on a constant mean value. This introduces 'parametric instabilities' in the pipe. Though the pipe experiences combinational instabilities as well, in the present work no attempt has been made to compute these regions of instabilities. Two types of parametric instabilities may be distinguished, namely, the primary and the secondary instabilities. Three different methods have been proposed to determine the regions of these instabilities.

In the first method, Bolotin's concept has been used in conjunction with mode shape approximation. The mode shapes used to approximate the displacement of the pipe are taken as those of a periodically supported beam. Thus, to use this method, the mode shapes of a beam with same number of spans as in the pipe under consideration must be known in advance.

In the second method, we use Bolotin's concept directly without recourse to any mode shape approximation. This gives a set of coupled differential equations. By applying appropriate boundary conditions, a frequency equation is obtained in the form of a determinant. The size of this determinant, _____ however, increases drastically with an increase in the number of spans in the pipe.

The third method uses the wave approach concept developed in the first part of the work. Instability regions are determined by using a graphical procedure similar to the one mentioned earlier. In this method, the computational effort is independent of the number of spans in the pipe.

The effect of neglecting the mass ratio parameter, β , has been studied. We also discuss the effect of damping on the regions of instabilities.

The last phase of the work considers the problem of controlling the regions of parametric instabilities by attaching viscously damped dynamic absorber to a pipe. First, single span pipes with pinned-pinned, clamped-clamped, and clamped-pinned ends have been studied. The effects of various parameters such as damping ratio, tuning ratio, and mass ratio of the absorber have been studied numerically. No attempt, however has been made to optimise these parameters for best performance of the absorber. Analysis has also been presented for the case when an undamped absorber is attached at the mid-point

of each bay of a periodically supported finite pipe. For this case the instability regions are determined via the wave approach alone.

The numerical results have always been presented in non-dimensional forms for various values of the significant parameters characterizing the problems.

CHAPTER 2

WAVE PROPAGATION AND VIBRATION RESPONSE OF A PERIODICALLY SUPPORTED PIPE CONVEYING FLUID

2.1 Introduction

A periodic structure consists of a number of identical members connected together in identical manners to form the whole structure. Examples of such structures are, a tall apartment block having identical storeys, an aeroplane fuselage structure consisting of identical curved panels reinforced at regular intervals by an orthogonal set of identical stiffeners, etc. The identical members forming the whole structure are known as 'periodic elements'.

The response of periodic beam-type structures to the convected pressure fields has been analysed in the past by calculating the principal modes of the system, and then studying the forced motion in each of the significant modes [25] . For such problems, the transfer matrix technique has also been used in which the response is obtained directly without recourse to the principal mode calculation [26].

When the structure is very long and contains many elements, a large number of modes must be included in the modal analysis making the process extremely unwieldy. This difficulty is avoided, of course, in the transfer matrix approach. However, no clear physical picture emerges out of this approach either.

It has been shown [30] that the steady state vibration of periodic structures under the influence of a harmonic source can be better understood in terms of a special kind of 'wave motions'. These waves are not of simple spatially-simusoidal form as the supports cause reflections and consequent 'near-field' effects. Vibrations of such structures to arbitrary excitations can be expressed in terms of these wave motions. In particular, the response to convected harmonic pressure fields may be readily expressed in simple closed form using this wave approach [31].

In this chapter, harmonic wave propagation in a periodically supported pipe conveying fluid has been studied, treating the pipe as a beam-type structure. The velocity and pressure of the fluid have been assumed to be constant throughout the pipe. When the pipe vibrates laterally, the fluid flow field is affected. Conversely, the fluid interacts with the wall of the pipe changing its vibration characteristics. In the present study, the effect of the fluid flow on vibration characteristics of the pipe has been taken into account. The effect of vibration of the pipe on the fluid flow characteristics, however, has been assumed to be negligible.

First, a brief discussion on the fundamentals of wave approach, developed by Mead [30] for a periodically supported beam has been presented. Then the receptance method is used to determine the propagation constants for the case of a periodically supported pipe for various values of pressure and velocity of the fluid. Next, the propagation constant versus frequency curves are used to determine the

natural frequencies of a periodically supported finite pipe. It has also been shown how these curves can be used for determining the divergence instability of such pipe-lines. At the end, the response of such pipe-lines to a convected harmonic pressure field has been obtained using this wave approach. The effect of damping, present in the pipe and in the supports, on the response has also been investigated.

2.2 Fundamentals of Wave Approach

Let us consider an infinite pipe resting on equi-spaced, identical and transversely rigid supports. The pipe is excited at a point by a harmonic force $p\, e^{i\omega t}$ (Figure 2.1), where p and ω are the amplitude and frequency of the harmonic force respectively, and t denotes the time. A form of harmonic wave motion is set up in the whole structure, propagating outwards from the point of excitation. Due to the reflections at the supports and the consequent 'near-field' effects, this wave motion is not of a simple spatially-sinusoidal form. However, on examining the motion at corresponding points in any pair of adjacent bays excluding the excited one (for example points F and G in Figure 2.1), it is found that the phase difference, μ_i, and the amplitude ratio, e^{μ_r}, between the motions of such points are same for any pair of adjacent bays throughout the pipe. Thus, in particular, μ_i represents the phase difference in the motion between two consecutive supports, and μ_r represents the decay rate over the same distance. μ_r is termed as the attenuation constant and μ_i is known as the phase

constant. The propagation constant, μ, is defined as $\mu_r + i\,\mu_i$. The propagation constant with negative value of μ_r corresponds to the wave that is travelling from left to right. Likewise, propagation constant with positive value of μ_r corresponds to the wave that is travelling from right to left.

Outside the excited bay, the wave motion is entirely free and is governed only by the free wave equation subject to the boundary conditions imposed by the supports. The propagation constant is determined from this wave equation and the appropriate boundary conditions. Therefore, a propagation constant is a function only of the frequency and the pipe/support physical characteristics and is independent of the nature of the loading in the loaded bay. Associated with the propagation constant is a unique mode of transverse vibration of a free bay of the pipe. All free bays vibrate in identical modes differing only in phase and amplitude.

2.2.1 Determination of Propagation Constants

Figure 2.1 shows an infinite pipe resting on identical supports at a distance ℓ apart; k_r denotes the rotational stiffness provided by each support. Considering any span, say AB in Figure 2.1, one can write for free harmonic waves in such periodic structure [30]

$$\theta_B = \theta_A\, e^{\mu} \quad , \tag{2.1a}$$

$$\bar{M}_B = \bar{M}_A\, e^{\mu} \quad , \tag{2.1b}$$

where θ and $\bar{M}$ denote the slope and the non-dimensional bending

moment, respectively, at sections indicated by the subscripts A and B. The non-dimensional bending moment, $\bar{M}$, is defined as $M\ell/EI$ where M is the bending moment and EI is the flexural stiffness of the pipe.* Again, θ_B and θ_A can be expressed in terms of the moments $\bar{M}_B$ and $\bar{M}_A$ through the receptance relationships as follows:

$$\theta_B = \beta_{BA} \bar{M}_A + \beta_{BB} \bar{M}_B \quad , \tag{2.2a}$$

$$\theta_A = \beta_{AA} \bar{M}_A + \beta_{AB} \bar{M}_B \quad , \tag{2.2b}$$

where β_{XY} is the slope at the section X due to a unit harmonic moment at the section Y. From equations (2.1) and (2.2), by eliminating θ_A, θ_B, $\bar{M}_A$ and $\bar{M}_B$, the following equation for the propagation constant, μ, is obtained:

$$\beta_{AB} e^{2\mu} + (\beta_{AA} - \beta_{BB}) e^{\mu} - \beta_{BA} = 0 \tag{2.3}$$

Since the receptances β_{XY} are functions of the frequency, μ is strongly frequency dependent. Obviously, from equation (2.3), for each value of the frequency, two roots for e^{μ} are obtained. One of these roots corresponds to the positive going wave and the other to the negative going wave. Receptances to be used in equation (2.3) are derived from ___ equation of the motion of a pipe conveying fluid (see Appendix 1).

If $\mu = \mu_r + i\,\mu_i$ is a solution of equation (2.3), then

$$\mu = \mu_r + i\,(\mu_i \pm 2n\pi), \quad n = 0,1,2,\ldots \tag{2.4}$$

---

* Hereafter, all bending moments will refer to the non-dimensional values.

is also a solution. The propagation constants corresponding to $n = 0$ in equation (2.4) are called the primary values of the propagation constant. Thus, the wave motion travelling in each direction can be thought of as wave groups, each having infinite components corresponding to integer values of n in equation (2.4). The wave components corresponding to $n = 0$ are called the primary waves [30].

As noted in earlier works on beams on periodic supports [30], in the present case also there exist alternate frequency bands of attenuation and propagation of free waves. The only difference in this case from that of an ordinary beam will be that the values of μ_i for the positive and the negative going waves will not be the negative of each other. This loss of symmetry is due to the Coriolis term (due to the fluid flowing in a curved path) in the equation of motion of the pipe (see Appendix 1).

When the waves propagate without attenuation, i.e., with $\mu_r = 0$, the non-dimensional phase velocities of these waves are given by

$$C_p^+ = -\Omega / \mu_i^+ \quad \text{for the positive going wave,}$$

$$\text{and} \quad C_p^- = -\Omega / \mu_i^- \quad \text{for the negative going wave,}$$

where Ω is the non-dimensional frequency, and μ_i^+ and μ_i^- are the phase constants for the positive and the negative going waves, respectively.

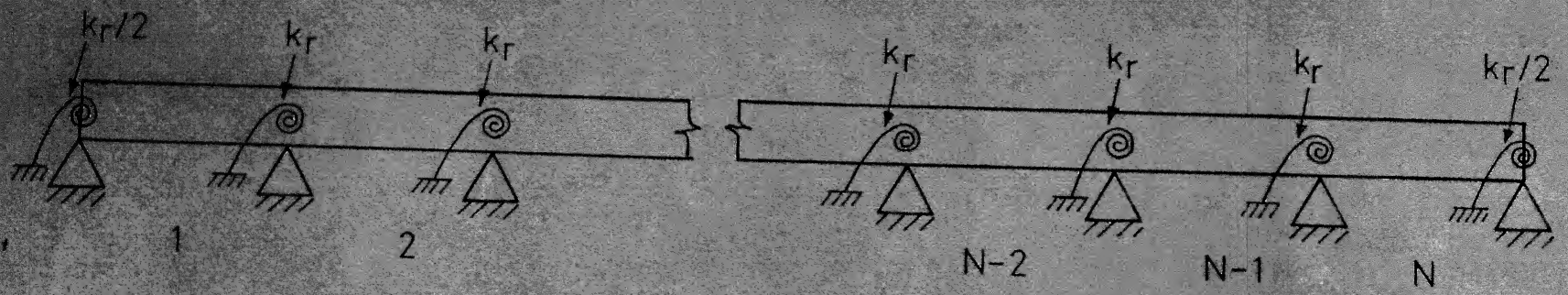

Figure 2.2 - An N-span periodically supported pipe.

2.3 Natural Frequencies of a Periodically Supported Finite Pipe

Sen Gupta [51] developed a graphical method based on wave approach to determine the natural frequencies of periodically supported finite beams. He showed that natural frequencies of an N-span beam can be obtained by dividing the range of μ_i (in the propagation band) into N equal divisions. Since in the case of a pipe, μ_i^+ and μ_i^- have different numerical values, a slight modification of the above mentioned approach is necessary.

Figure 2.2 shows an N-span pipe periodically supported on transversely rigid supports; the periodic element being a single span of the pipe with rotational stiffness $k_r/2$ at each end (Figure 2.3). To determine the natural frequencies, any dynamic disturbance is considered in terms of two opposite going waves and only propagating waves (with $\mu_r = 0$) need to be considered [51] . Let $\bar{M}_+$ and $\bar{M}_-$ be the moments due to the positive and the negative going waves at the extreme left support. If μ_i^+ and μ_i^- are phase constants for these two waves, then the respective bending moments at the last support will be $\bar{M}_+ e^{iN\mu_i^+}$ and $\bar{M}_- e^{iN\mu_i^-}$. Since the total moments at the end supports must vanish, one obtains

$$\bar{M}_+ + \bar{M}_- = 0 \qquad (2.5a)$$

$$\bar{M}_+ e^{iN\mu_i^+} + \bar{M}_- e^{iN\mu_i^-} = 0 \qquad (2.5b)$$

Substitution of equation (2.5a) in equation (2.5b) gives

$$e^{iN\mu_i^+} - e^{iN\mu_i^-} = 0$$

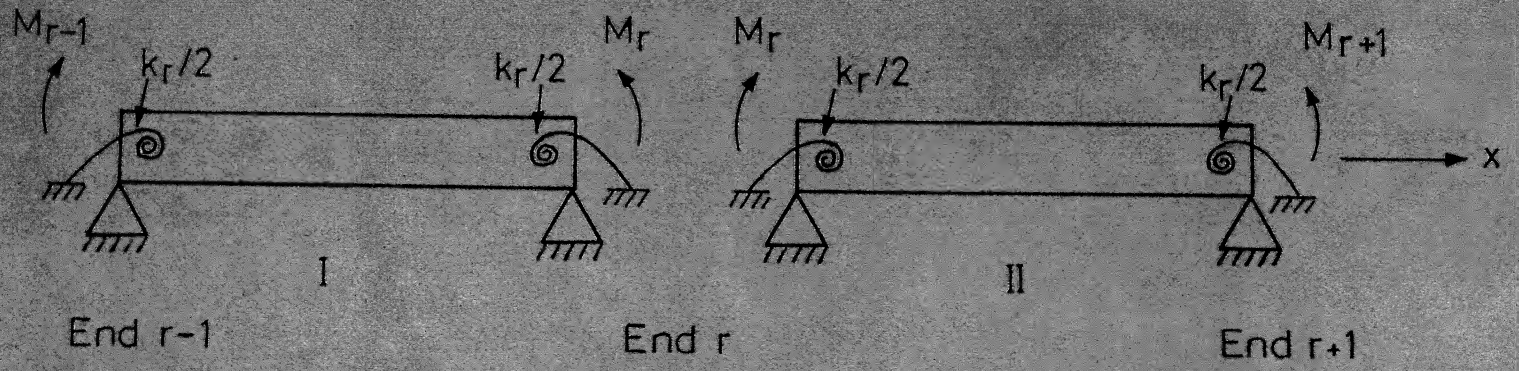

Figure 2.3 - Two consecutive periodic elements of the infinite pipe shown in Figure 2.1

or,

$$\mu_i^+ - \mu_i^- = \pm 2j\pi/N \ , \ j = 0,1,2,\ldots,N \qquad (2.6)$$

For primary values (i.e., with $n = 0$ in equation (2.4)) in any propagation band, the values of $|\mu_i^+ - \mu_i^-|$ vary between 0 and 2π. Hence admissible values of μ_i^+ and μ_i^- to satisfy the boundary conditions during free vibration, as given by equation (2.6), can be written as

$$\mu^* = |\mu_i^+ - \mu_i^-| = 2j\pi/N, \ j = 0,1,2,\ldots,N \qquad (2.7)$$

Frequencies within the propagation bands where condition (2.7) is fulfilled are the natural frequencies of the N-span pipe.

Thus, once the propagation constants are obtained in the manner outlined in section 2.2.1, one can draw a curve of μ^* versus frequency for each propagation band. The value of μ^* varies between 2π and 0 in each of these bands. Then, dividing this range of μ^* into N equal divisions, one obtains the natural frequencies of an N-span pipe in each propagation band. Thus it would appear that there are $(N+1)$ natural frequencies in each propagation band for an N-span pipe, but this is not so, as explained in reference [51]. The highest natural frequency in each propagation band, obtained from equation (2.7) happens to be the natural frequency of the individual bays with both ends clamped. Since the ends are not clamped in the present case, the highest natural frequency obtained from equation (2.7) cannot be a possible natural frequency.

The main advantage of this graphical approach over the frequency determinant method is that the computational effort remains independent of the number of spans in the pipe. Once the curve of μ^* versus frequency has been obtained, natural frequencies of the pipe with any number of spans are determined by dividing the range of μ^* into the same number of equal divisions as the number of spans in the pipe. In frequency determinant method, however, the computational effort increases drastically with the number of spans. This will be apparent from Appendix 2 which presents the frequency determinant formulation for just two spans.

It should be noted, however, that at these natural frequencies no classical normal modes exist. This is due to the fact that the positive and the negative going waves travel at different speeds (as implied by different numerical values of μ_i^+ and μ_i^-) and hence cannot be superimposed to give rise to standing modes. Thus, at these natural frequencies the modes of the pipe will be complex.

2.3.1 Natural Frequencies of a Finite Pipe on Equi-Spaced Supports with Equal Rotational Stiffness

In section 2.3, natural frequencies of a periodically supported pipe were calculated using the wave approach. Due to the periodicity of the structure, the rotational stiffnesses at the intermediate supports were different from those at the ends as indicated in Figure 2.2. However, if all the supports are identical, i.e., having equal rotational stiffness, minor modification of the wave approach presented

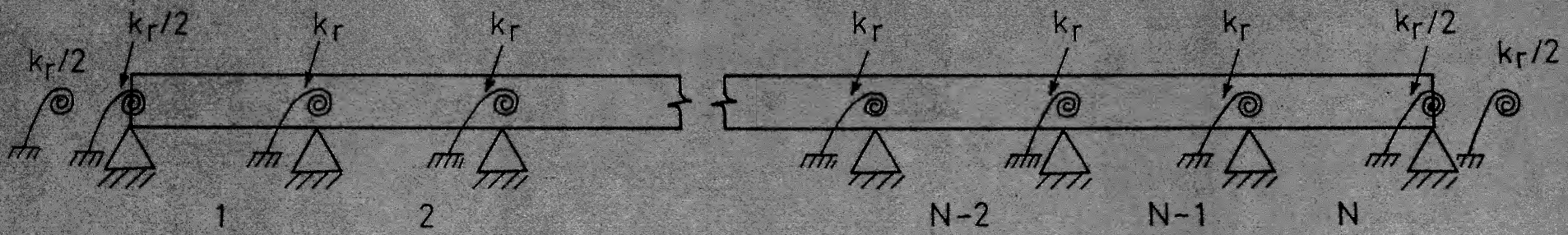

Figure 2.4 - An N-span pipe on identical supports at regular interval.

in section 2.3 is necessary for determining the natural frequencies. This modification is presented in this section.

Consider an N-span pipe resting on equi-spaced and transversely rigid supports, each having a rotational stiffness k_r. If the periodic element is taken as a single span of the pipe with rotational stiffness $k_r/2$ at each end, then extra rotational stiffnesses $k_r/2$ are left out at the extreme ends as shown in Figure 2.4.

First, let us consider any one bay of the periodically supported pipe neglecting the extra stiffness $k_r/2$ at extreme ends. The transverse displacement of this bay, $\bar{y}(\xi)$, during free vibration, can be written as (see Appendix-1)

$$\bar{y}(\xi) = \sum_{n=1}^{4} C_n e^{i\lambda_n \xi}, \qquad (2.8)$$

where the λ's are the roots of the characteristic polynomial given by equation (A-1.5), the C_n's are the unknown constants to be determined from the boundary conditions, and ξ is the non-dimensional co-ordinate along the length of the pipe.

For free harmonic waves in the bay under consideration, the boundary conditions are

$$\bar{y}(0) = 0 , \qquad (2.9a)$$

$$\bar{y}(1) = 0 , \qquad (2.9b)$$

$$\bar{y}'(1) = e^{\mu} \bar{y}'(0), \qquad (2.9c)$$

where primes denote differentation with respect to ξ, and μ is the propagation constant.

Using the above boundary conditions, constants C_2, C_3 and C_4 can be determined in terms of C_1. Let $C_n = q_n C_1$, n=1,2,3,4, where obviously $q_1 = 1$.

Thus, the displacement of any bay of the pipe, due to the positive and the negative going waves can be written separately as

$$\bar{y}_+(\xi) = C_1^+ \sum_{n=1}^{4} q_n^+ e^{i\lambda_n \xi}, \qquad (2.10a)$$

$$\bar{y}_-(\xi) = C_1^- \sum_{n=1}^{4} q_n^- e^{i\lambda_n \xi} \qquad (2.10b)$$

The positive and the negative signs used as subscripts and superscripts refer to the positive and the negative going waves, respectively.

As stated in section 2.3, only the propagating waves (with $\mu_r = 0$) need to be considered for the determination of the natural frequencies. Let $\bar{M}_+$ and $\bar{M}_-$ be the non-dimensional moments at the extreme left support due to the positive and the negative going waves, respectively. The slopes due to these waves at the same support are $\bar{y}'_+(0)$ and $\bar{y}'_-(0)$, respectively. If μ_i^+ and μ_i^- are the phase constants for these two waves, then respective bending moments and slopes at the last support will be $\bar{M}_+ e^{iN\mu_i^+}$, $\bar{M}_- e^{iN\mu_i^-}$ and $\bar{y}'_+(0) e^{iN\mu_i^+}$, $\bar{y}'_-(0) e^{iN\mu_i^-}$. The total bending moments at the end supports will no longer be zero, as given by equations (2.5). Due to the presence of extra stiffness $k_r/2$ at these ends, the modified boundary conditions are

$$\bar{M}_+ + \bar{M}_- = -\frac{\kappa_r}{2}\{\bar{y}'_+(0) + \bar{y}'_-(0)\} , \tag{2.11a}$$

$$\bar{M}_+ e^{iN\mu_i^+} + \bar{M}_- e^{iN\mu_i^-} = \frac{\kappa_r}{2}\{\bar{y}'_+(0)\, e^{iN\mu_i^+} + \bar{y}'_-(0)\, e^{iN\mu_i^-}\} , \tag{2.11b}$$

where κ_r is the non-dimensional rotational stiffness.

The bending moments $\bar{M}_+$ and $\bar{M}_-$ can be written as

$$\bar{M}_+ = -\bar{y}''_+(0) + \frac{\kappa_r}{2}\bar{y}'_+(0) , \tag{2.12a}$$

$$\bar{M}_- = -\bar{y}''_-(0) + \frac{\kappa_r}{2}\bar{y}'_-(0) \tag{2.12b}$$

Substituting equations (2.10) and (2.12) into equations (2.11), one gets

$$C_1^+ \sum_{n=1}^{4} q_n^+ (\lambda_n^2 + i\,\kappa_r\lambda_n) + C_1^- \sum_{n=1}^{4} q_n^- (\lambda_n^2 + i\,\kappa_r\lambda_n) = 0 \tag{2.13a}$$

$$C_1^+ e^{iN\mu_i^+} \sum_{n=1}^{4} q_n^+ \lambda_n^2 + C_1^- e^{iN\mu_i^-} \sum_{n=1}^{4} q_n^- \lambda_n^2 = 0 \tag{2.13b}$$

For non-trivial solution of C_1^+ and C_1^-

$$\begin{vmatrix} \sum_{n=1}^{4} q_n^+ (\lambda_n^2 + i\,\kappa_r\lambda_n) & \sum_{n=1}^{4} q_n^- (\lambda_n^2 + i\,\kappa_r\lambda_n) \\ e^{iN\mu_i^+} \sum_{n=1}^{4} q_n^+ \lambda_n^2 & e^{iN\mu_i^-} \sum_{n=1}^{4} q_n^- \lambda_n^2 \end{vmatrix} = 0$$

or

$$e^{iN\mu_i^+}\Big[\sum_{n=1}^{4} q_n^+ \lambda_n^2\Big]\Big[\sum_{n=1}^{4} q_n^- (\lambda_n^2 + i\,\kappa_r\lambda_n)\Big] - e^{iN\mu_i^-}\Big[\sum_{n=1}^{4} q_n^+ (\lambda_n^2 + i\,\kappa_r\lambda_n)\Big]\Big[\sum_{n=1}^{4} q_n^- \lambda_n^2\Big] = 0 \tag{2.14}$$

The left hand side of equation (2.14) is strongly frequency dependent and in general, it will be complex. Frequencies in each propagation band, where equation (2.14) is satisfied, are the natural frequencies of the pipe. For this case, the graphical approach presented in section 2.3 can no longer be used. However, once the propagation constants (and corresponding λ_n's and q_n's) are obtained, natural frequencies for any number of spans in the pipe can be determined using equation (2.14). It is interesting to note that in this case also the computational effort is independent of the number of spans in the pipe.

Natural frequencies of a periodically supported finite pipe on rigid supports without rotational stiffness can be determined considering $\kappa_r = 0$ in either of the methods presented in sections 2.3 or 2.3.1.

2.3.2 Buckling (Divergence) Instability

A careful examination of equation (A-1.2) reveals that the coefficient of the term $\frac{\partial^2 y}{\partial x^2}$ is equivalent to an axial load on the pipe. Hence it is apparent that an increase in the velocity or pressure of the fluid beyond certain critical values will cause static buckling of the pipe [48] . This static buckling is also termed as "Divergence Instability". Bolotin [6] has shown that static buckling can be considered as a special case of dynamic instability. Buckling is implied when at certain critical values of the parameters, one of the natural frequencies of the system is reduced to zero.

Natural frequencies of a periodically supported pipe can be obtained following the method developed in section 2.3. If, for certain combinations of parameters any one of the natural frequencies is zero, it will imply the onset of static buckling of the pipe-line in the corresponding mode. Hence, combinations of fluid velocity, fluid pressure, and rotational stiffness, which make the pipe to buckle in a particular mode can easily be determined.

2.4 Response of an Infinite Periodically Supported Pipe to a Convected Harmonic Pressure Field

Mead [31] studied the response of periodically supported beams to a convected harmonic pressure field using the wave approach. He showed that coincidence occurs at a frequency when the velocity of the free harmonic waves travelling in the beam is equal to the velocity of the convected loading. In the present section, the response of a periodically supported infinite pipe to a convected harmonic pressure field has been studied.

Consider an infinite periodically supported pipe resting on transversely rigid supports and excited by a convected harmonic pressure field which exerts a force

$$p_e(x,t) = p_o\, e^{i(\omega t - kx)} , \qquad (2.15)$$

per unit length of the pipe. The convection velocity, C_v, is ω/k and the phase difference between loading at points a distance ℓ apart is $\epsilon = -k\ell$. The equation of motion for transverse

vibration of the pipe, between any two consecutive supports, is (see Appendix 1)

$$EI \frac{\partial^4 y}{\partial x^4} + (m_f V^2 + p_f A_p) \frac{\partial^2 y}{\partial x^2} + 2 m_f V \frac{\partial^2 y}{\partial x \partial t} + (m_f + m_p) \frac{\partial^2 y}{\partial t^2}$$

$$= p_o e^{i(\omega t - kx)} \qquad (2.16)$$

On substituting $y = \ell \bar{y} e^{i\omega t}$, equation (2.16) can be put in the following non-dimensional form

$$\frac{d^4 \bar{y}}{d\xi^4} + (u^2+\gamma) \frac{d^2 \bar{y}}{d\xi^2} + i2 \beta u \Omega \frac{d\bar{y}}{d\xi} - \Omega^2 \bar{y} = \bar{p}_o e^{i\varepsilon\xi} \qquad (2.17)$$

where the non-dimensional loading parameter, $\bar{p}_o = \frac{p_o \ell^3}{EI}$.

ε can be written as $\varepsilon = -\Omega/\bar{C}$, where $\bar{C}$ is the non-dimensional convection velocity of the loading, defined as

$$\bar{C} = \left(\frac{m_f + m_p}{EI} \ell^2 \right)^{1/2} C_v \qquad (2.18)$$

The solution of equation (2.17) is

$$\bar{y}(\xi) = \sum_{n=1}^{4} C_n e^{i\lambda_n} + \frac{\bar{p}_o e^{i\varepsilon\xi}}{\varepsilon^4 - (u^2+\gamma) \varepsilon^2 - 2\beta u \Omega \varepsilon - \Omega^2}, \qquad (2.19)$$

where the λ_n's are the roots of the polynomial

$$\lambda^4 - (u^2+\gamma) \lambda^2 - 2\beta u \Omega \lambda - \Omega^2 = 0 \qquad (2.20)$$

The C_n's in equation (2.19) are to be determined from the boundary conditions as discussed below.

Consider any two adjacent elements of the pipe as shown in Figure 2.3. By virtue of the forced wave property, the slopes and

moments at end r of the element II and at end r-1 of the element I are related as [31]

$$\bar{y}'_r = e^{i\varepsilon}\, \bar{y}'_{r-1} \quad , \tag{2.21a}$$

$$\bar{M}_r = e^{i\varepsilon}\, \bar{M}_{r-1} \quad , \tag{2.21b}$$

where primes denote differentiation with respect to ξ. Now, the displacements at the supports are zero, i.e.,

$$\bar{y}_r = 0 \quad ,$$

$$\bar{y}_{r-1} = 0 \tag{2.22}$$

The bending moments M_r and M_{r-1} of equation (2.21b) can be written as

$$\bar{M}_r = -\bar{y}''(1) - \frac{\kappa_r}{2}\, \bar{y}'(1) \quad , \tag{2.23a}$$

$$\bar{M}_{r-1} = -\bar{y}''(0) + \frac{\kappa_r}{2}\, \bar{y}'(0) \tag{2.23b}$$

Use of equations (2.19), (2.21), (2.22) and (2.23) yields the following system of equations for the coefficients C_n's used in equation (2.19).

$$\sum_{n=1}^{4} C_n = -\frac{\bar{p}_o}{\varepsilon^4 - (u^2+\gamma)\,\varepsilon^2 - 2\beta u \Omega \varepsilon - \Omega^2} \quad , \tag{2.24a}$$

$$\sum_{n=1}^{4} C_n e^{i\lambda_n} = -\frac{\bar{p}_o e^{i\varepsilon}}{\varepsilon^4 - (u^2+\gamma)\varepsilon^2 - 2\beta u \Omega \varepsilon - \Omega^2} \quad , \tag{2.24b}$$

$$\sum_{n=1}^{4} C_n \lambda_n e^{i\lambda_n} = e^{i\varepsilon} \sum_{n=1}^{4} C_n \lambda_n \quad , \tag{2.24c}$$

$$\sum_{n=1}^{4} C_n\left(\lambda_n^2 - \frac{\kappa_r}{2} i\lambda_n\right) e^{i\lambda_n} = e^{i\varepsilon}\left[\sum_{n=1}^{4} C_n\left(\lambda_n^2 + \frac{\kappa_r}{2} i\lambda_n\right) + \frac{i\kappa_r \varepsilon \bar{p}_o}{\varepsilon^4 - (u^2+\gamma)\varepsilon^2 - 2\beta u \Omega \varepsilon - \Omega^2}\right] \qquad (2.24d)$$

Once the C_n's have been obtained from equations (2.24a)-(2.24d), the response of the pipe to the convected harmonic pressure field can be determined from equation (2.19). Hysteretic type damping in the pipe and at the supports can easily be incorporated by replacing EI in equation (2.16) by $EI(1+i\eta_b)$ and κ_r in equation (2.23) by $\kappa_r(1+i\eta_s)$, where η_b and η_s are the loss factors of the pipe and the supports, respectively. It should be noted that the introduction of damping will change equations (2.17), (2.19), (2.20) and (2.24) accordingly.

2.5 Results and Discussions

2.5.1 Computations Performed

The following computations have been performed using the analyses developed in previous sections. All the results are expressed in terms of non-dimensional quantities.

(a) Curves of propagation constants, $\mu\ (=\mu_r + i\mu_i)$, versus frequency, Ω, have been obtained for an undamped pipe with different combinations of fluid velocity, u, fluid pressure, γ, rotational stiffness, κ_r, and mass ratio parameter, β. Equation (2.3) was used to determine the propagation constants. Phase velocities of the primary waves have also been computed.

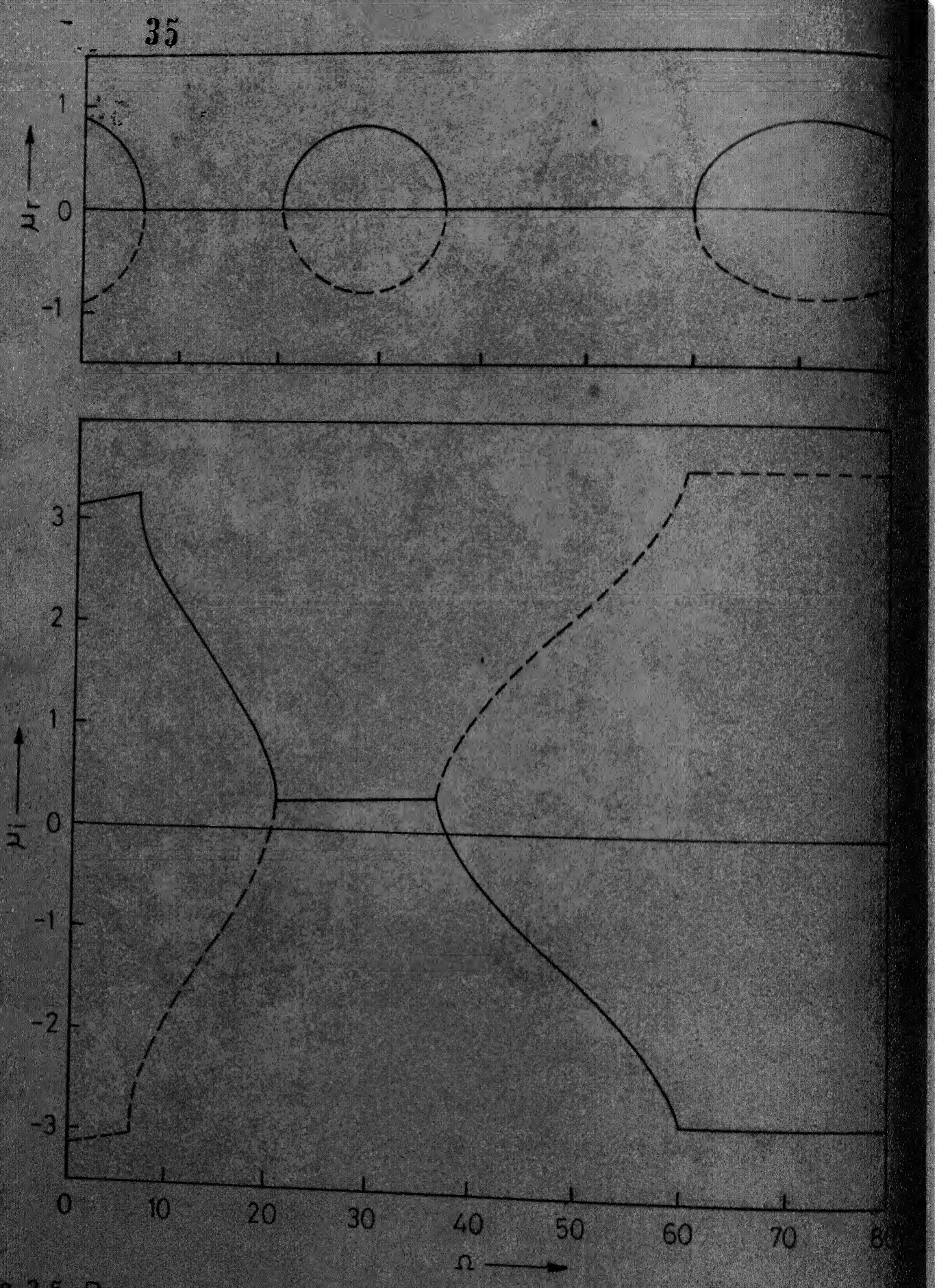

Figure 2.5 -Propagation constant versus frequency curve for $u=2$, $\gamma=2$, $\beta=0.5$ and $K_r=0$;---Positive going wave, —— Negative going wave.

(b) Numerical values of the first two natural frequencies of a two span pipe, with $\kappa_r = 0$, have been determined using the method discussed in section 2.3. As a check, same values were computed using the frequency determinant given in Appendix 2.

The first two natural frequencies of a two span pipe of the type discussed in section 2.3.1 have been calculated using equation (2.14). Variations of these two frequencies with the value of κ_r have also been shown.

Various combinations of the first critical values of the fluid velocity and the fluid pressure to cause buckling of the pipe have been presented.

(c) The response of an infinite pipe, to convected harmonic pressure field with different convection velocities, has been obtained using equation (2.19). The response is expressed in terms of the non-dimensional curvature $\bar{\rho}$ $(= \frac{d^2\bar{y}}{d\xi^2})$ at the mid-point of a bay. The effect of variation in the damping of the pipe, η_b, and at the supports, η_s, on the level of the response has also been discussed. The non-dimensional loading parameter, $\bar{p}_o$, has been taken as unity in all the cases.

2.5.2 Propagation Constants

Using equation (2.3), the propagation constant, μ, has been calculated for different values of the frequency, Ω. Figure 2.5 shows the variation of μ with Ω for $u=2$, $\gamma=2$, $\beta=0.5$ and $\kappa_r=0$. When $\mu_r=0$, free waves can travel through the pipe without attenuation and the ranges of Ω over which $\mu_r = 0$, are called the "propagation bands". It is seen from Figure 2.5 that there are alternate attenuation

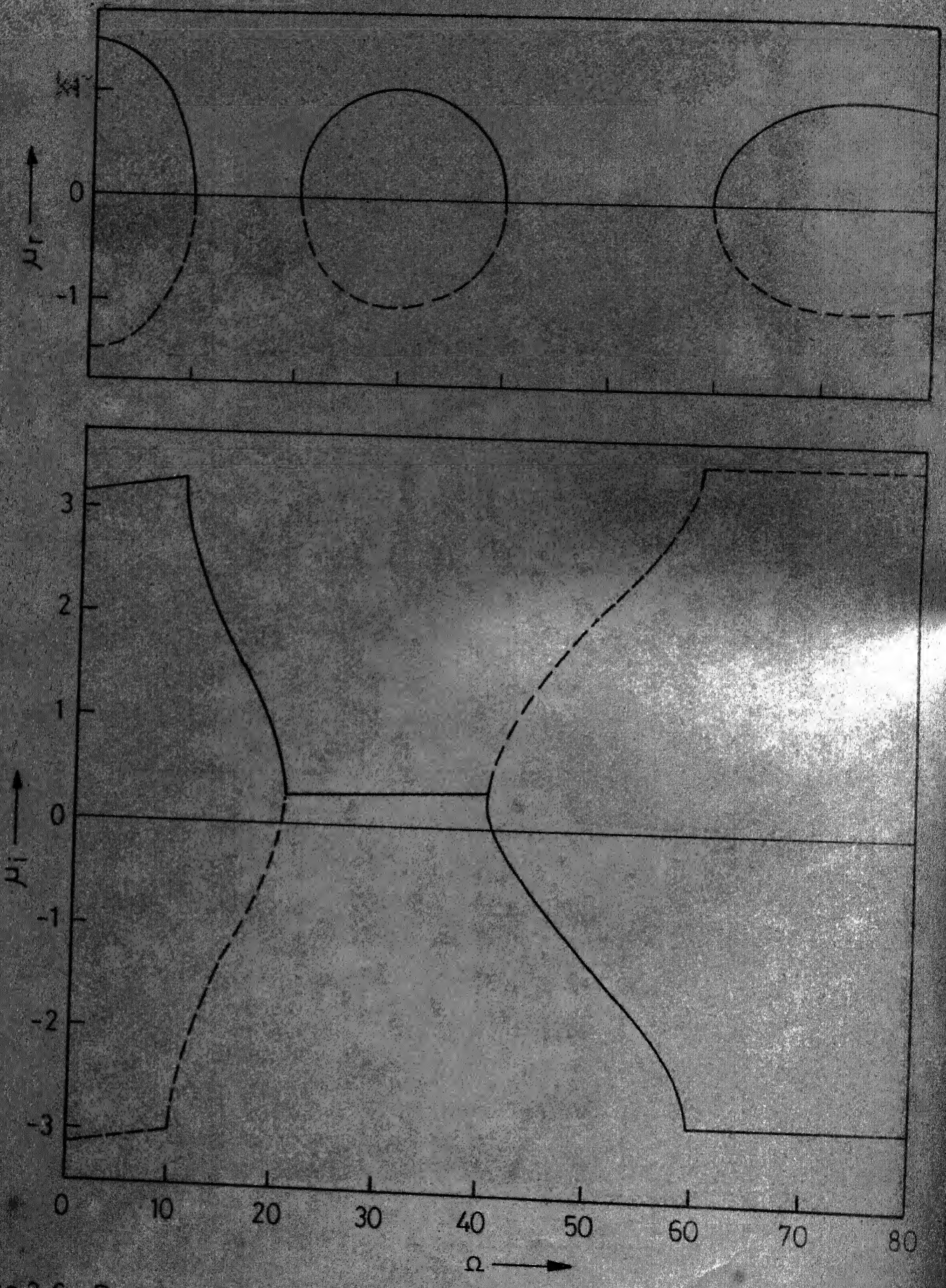

Figure 2.6 - Propagation constant versus frequency curve for $u=2$, $\gamma=2$, $\beta=0.5$ and $K_r=4$. ---- Positive going wave, —— Negative going wave

and propagation bands. It is found that the lower bounding frequency of the nth propagation band is identical with the nth natural frequency of the single bay periodic element shown in Figure 2.3. The upper bounding frequency of the nth propagation band is identical to the nth natural frequency of the same periodic element when its ends are clamped. It is clear from Figure 2.5 that in general, the values of μ_i^+ and μ_i^- are different. This is due to the Coriolis acceleration of the fluid while flowing in a curved path. As the Coriolis term is proportional to V (and not to V^2 like the centrifugal force term), the system loses symmetry along x-direction. Hence, waves travelling in the direction of the fluid (called positive going waves) have different velocities then those travelling in the opposite direction. The values of the phase constant, μ_i, vary in the attenuation bands. However, the variation is found to be decreasing with successive attenuation zones.

To study the effect of parameters like κ_r, γ, u, and β on the propagation constant, calculations were performed for different combinations of these parameters. These results, shown in Figures 2.5-2.8, can be summarised as follows:

(a) Figures 2.5 and 2.6 show the propagation constant for different values of κ_r, the other parameters being same in both the cases. It is seen from these graphs that the effect of increasing the rotational stiffness, κ_r, is to shift the start of the propagation bands to higher frequencies. However, the ends of the propagation bands remain unaffected. As noted earlier, the lower bounding frequencies of each

propagation band correspond to the natural frequencies of the single bay element of Figure 2.3. That is why, these shift towards higher values with increasing value of κ_r. However, the upper bounding frequencies of each propagation band correspond to the natural frequencies of the single bay element of Figure 2.3 when its ends are clamped and as such remain independent of the value of κ_r.

(b) Figures 2.6 and 2.7 show the effect of increasing the fluid pressure, γ, with the other parameters remaining the same. The curves show that the effect of increasing the fluid pressure, γ, is to shift both ends of the propagation bands to lower frequencies.

(c) Figures 2.6 and 2.8 show the effect of increasing the fluid velocity, u. The increase in the fluid velocity, like that in the fluid pressure, shifts both ends of the propagation bands to lower frequencies. However, the fluid velocity has more pronounced effect than the fluid pressure. It can be seen from Figures 2.6 and 2.8 that increase in the value of u from 2 to 4 shifts the end of the first propagation band from $\Omega = 20.6$ to $\Omega = 16.4$ approximately. On the other hand, for the same increase in the fluid pressure, this shift is from $\Omega = 20.6$ to $\Omega = 19.8$ only, as seen from Figures 2.6 and 2.7.

(d) The curve of μ versus Ω changes very insignificantly with changes in β in its physical range, i.e., $0 \leq \beta \leq 1$. Keeping in mind that the non-dimensional frequency, Ω, includes m_f, the above statement should not, however, be confused with the effect of the fluid mass, m_f, on the value of the propagation constant.

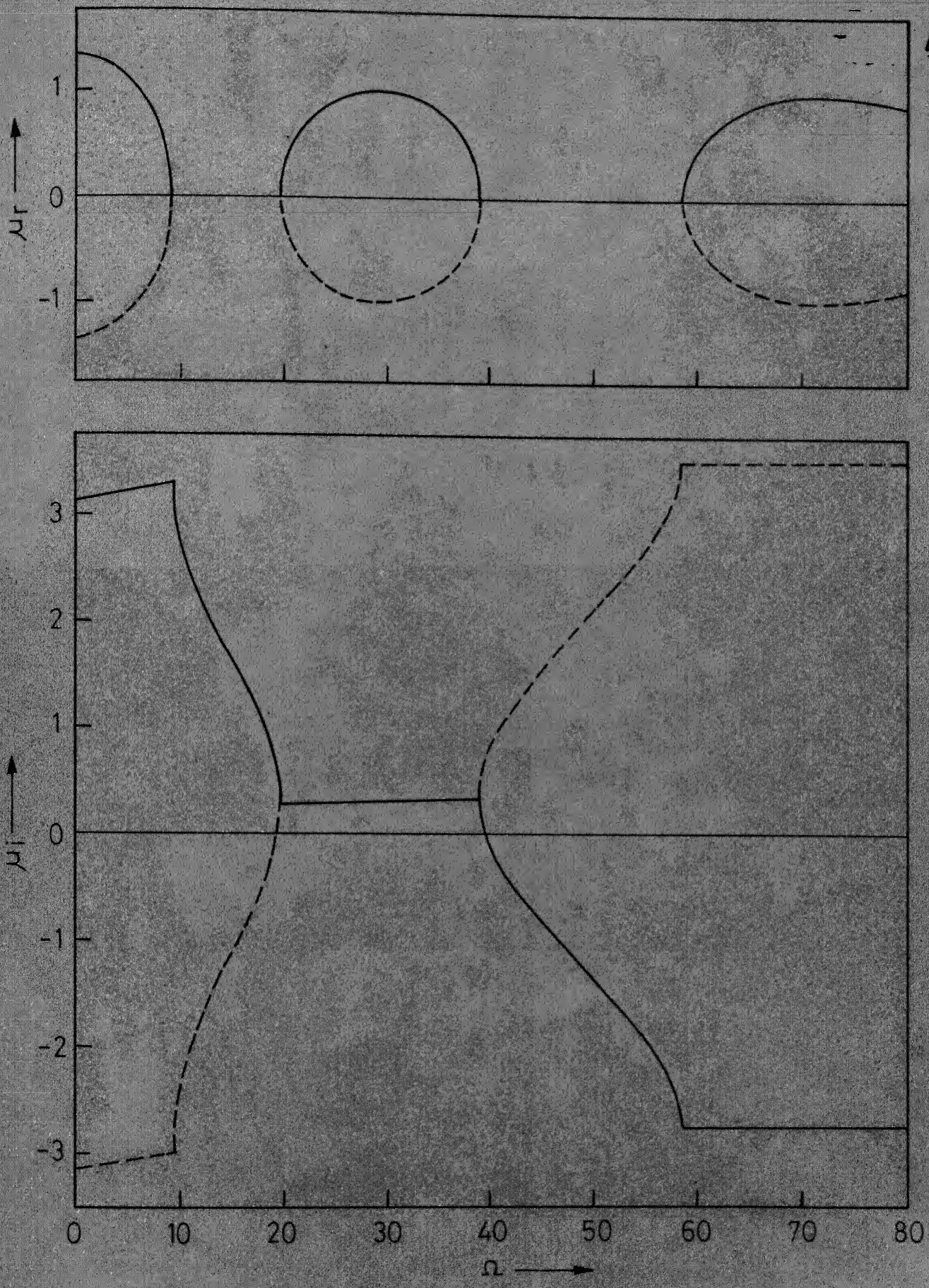

Figure 2.7 - Propagation constant versus frequency curve for $u=2, \gamma=4$, $\beta=0.5$ and $K_r=4$. ---- Positive going wave, —— Negative going wave.

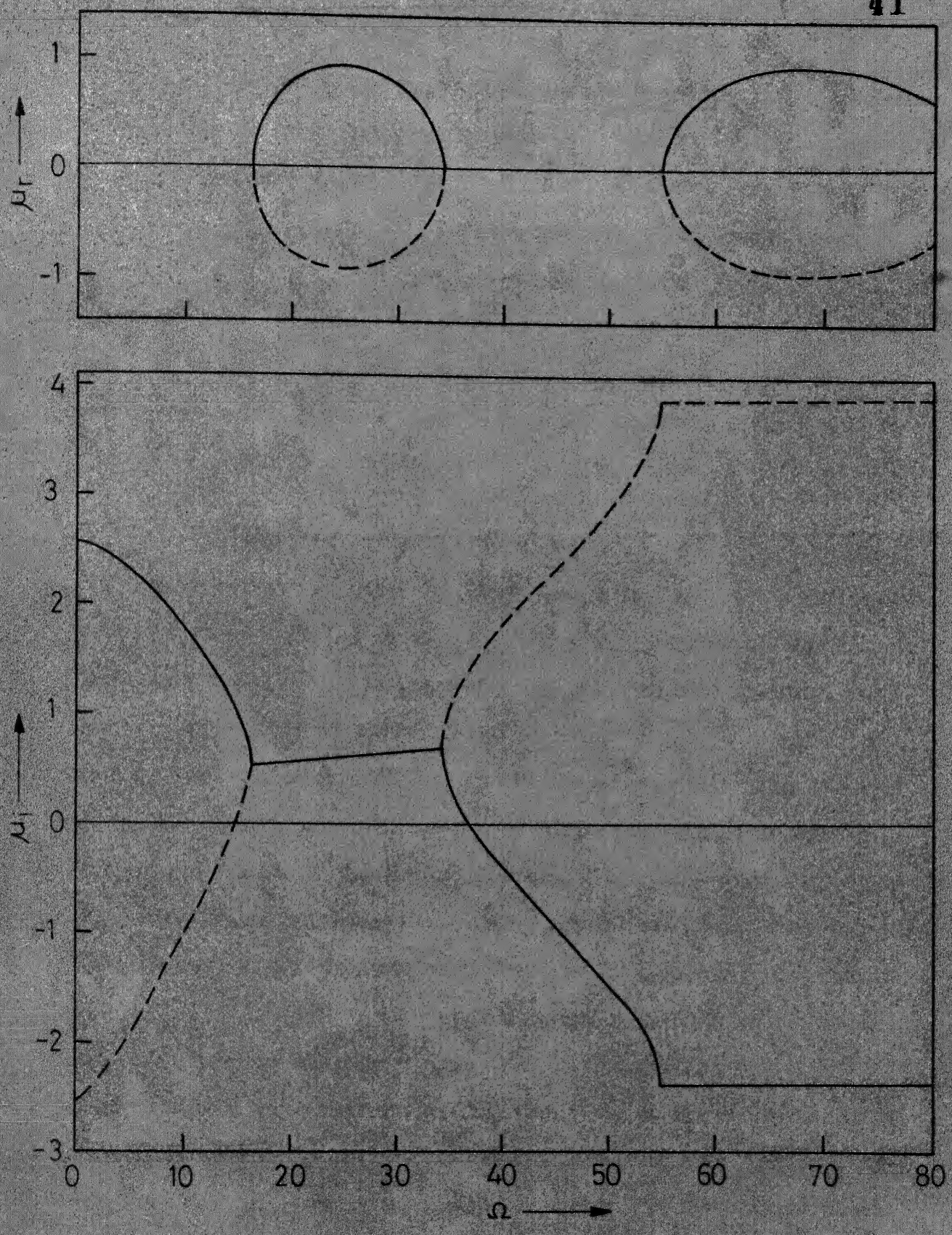

Figure 2·8 - Propagation constant versus frequency curve, for $u=4$, $\gamma=2$, $\beta=0.5$ and $K_r=4$. ---- Positive going wave, —— Negative going wave.

Figure 2.9 shows the phase velocities of the primary waves propagating in the positive and the negative directions. To save space, the negative of the phase velocity of the negative going wave has been plotted. It is seen from the graph that for primary waves, the velocity of the positive going wave goes to infinity at a frequency when $\mu_i^+ = 0$. Beyond this frequency, the sign of μ_i^+ changes, so there is no more positive going primary wave. Both the primary waves travel in the negative direction and their velocities finally attain the same finite value as indicated in Figure 2.9.

2.5.3 Natural Frequencies

As discussed in section 2.3, to determine the natural frequencies of an N-span pipe, the graph of $\mu^* (= |\mu_i^+ - \mu_i^-|)$ versus Ω is plotted in Figure 2.10. A frequency range covering only the first propagation band has been considered. Values of μ_i^+ and μ_i^- have been taken from Figure 2.5. For an N-span pipe this range of μ^* is divided into N equal intervals. The first N points of this division correspond to the first N natural frequencies of the pipe. First two natural frequencies of a two span pipe with simply supported ends are indicated in Figure 2.10. These values come out as $\Omega_{n1} = 6.11$ and $\Omega_{n2} = 12.82$, and are in very good agreement with those obtained from the frequency determinant, discussed in Appendix 2. The slight error can be attributed to the difficulty of reading the values very accurately from the graph. It has also been checked that Ω_{n2} is the first natural frequency of the single bay when one of the ends is pinned and the other clamped. As stated earlier, Ω_{n1} is the first natural frequency of a single bay with both ends simply supported.

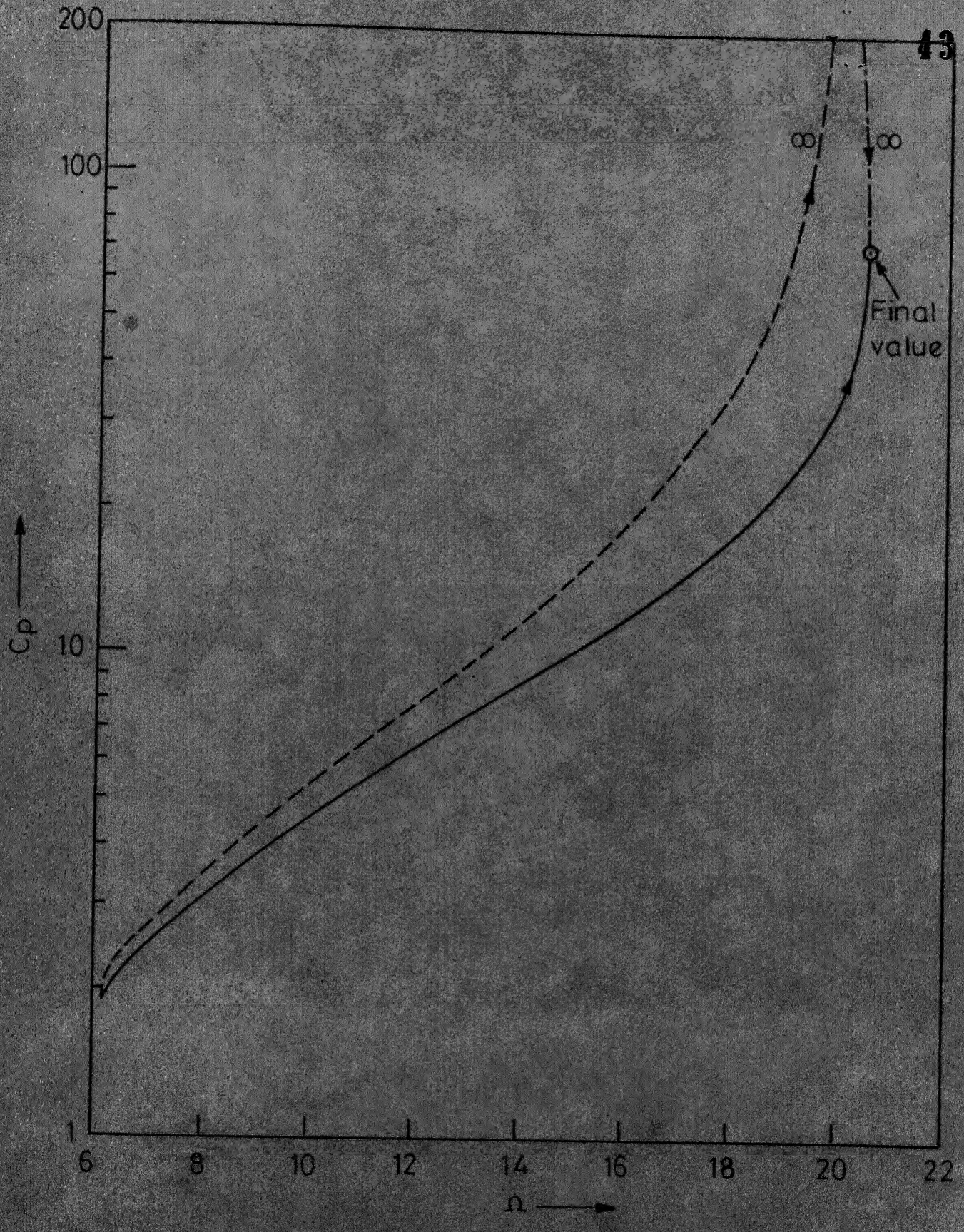

Figure 2.9 - Non-dimensional phase velocity of the primary free waves versus frequency curve. ---- Positive going wave, ——, and —·—·—, Negative going waves (negative of the velocity has been shown) $u=2$, $\gamma=2$, $\beta=0.5$ and $K_r=0$.

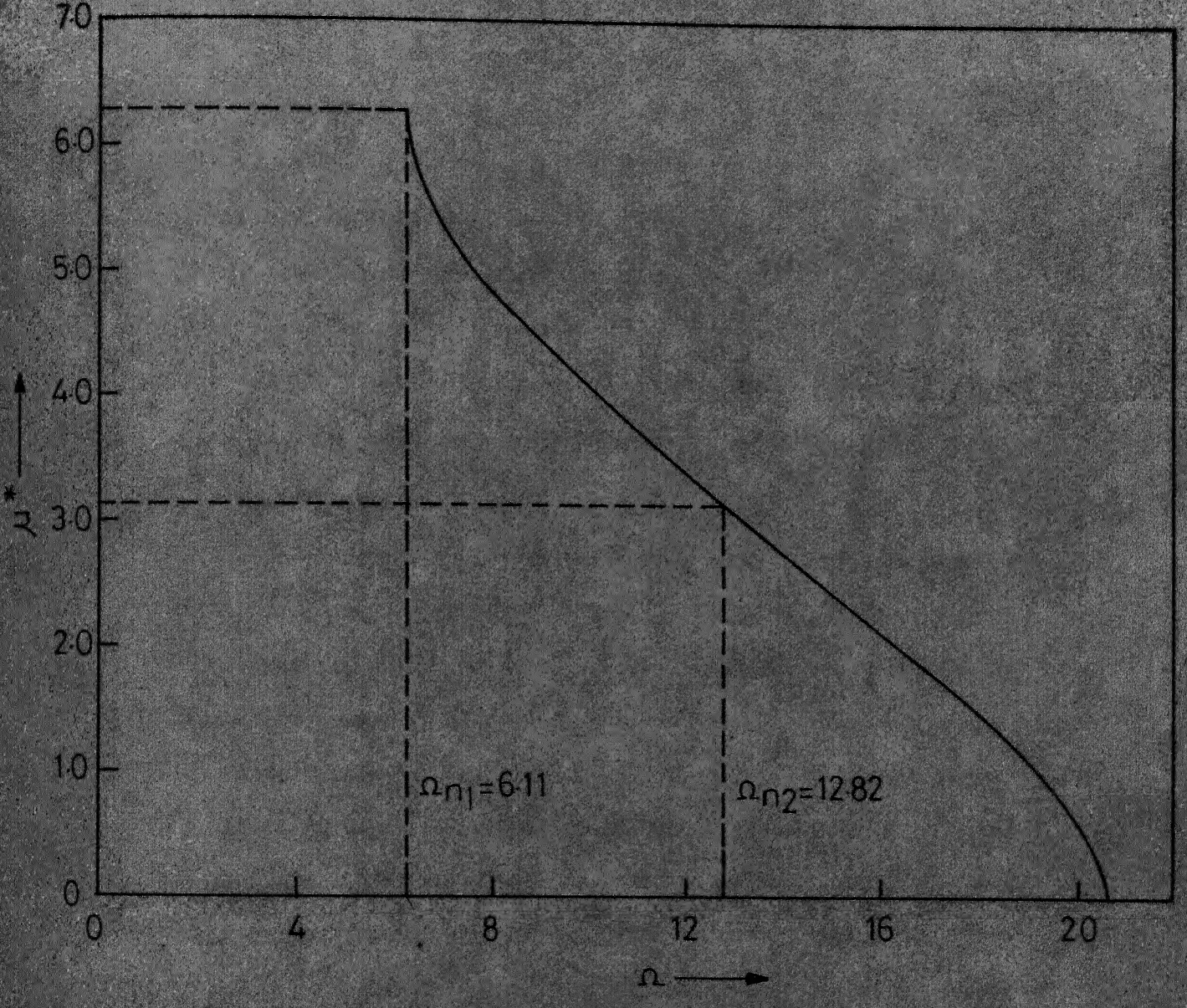

Figure 2·10 – Curve showing μ^* versus frequency in the first propagation band for $u = 2, \gamma = 2, \beta = 0.5$ and $K_r = 0$.

To study the effect of rotational stiffness, κ_r, on natural frequencies of a pipe resting on identical supports at regular intervals, first two natural frequencies of a two span pipe have been determined using equation (2.14). Figure 2.11 shows the effect of κ_r on the first two natural frequencies of the pipe. As expected, it is seen that increase in κ_r increases both the natural frequencies. However, the difference in their values reduces with increasing value of κ_r. In the limiting case when κ_r is infinite, both frequencies converge to the first natural frequency of a clamped-clamped pipe implying independent vibration of the two bays.

As discussed earlier in section 2.3.2, if any one of the natural frequencies of the system is reduced to zero, it implies the onset of the static buckling in the corresponding mode. Moreover, the first natural frequency of a periodically supported pipe with any number of spans, is given by the start of the first propagation band. The combinations of the fluid pressure, γ, and the fluid velocity, u, for a given value of the rotational stiffness, κ_r, are determined which make the first propagation band to start at zero frequency. In other words, the minimum values of γ and u necessary for the onset of static buckling of such pipe-lines are obtained. These results are shown in Figure 2.12. It is found that the equation of the curves shown in Figure 2.12 is given by $u^2+\gamma=$ constant, where the value of the constant depends upon that of κ_r. Values of this constant for $\kappa_r = 0$ and ∞ are π^2 and $4\pi^2$, respectively. The analogy between the buckling of a pipe and that of an ordinary beam

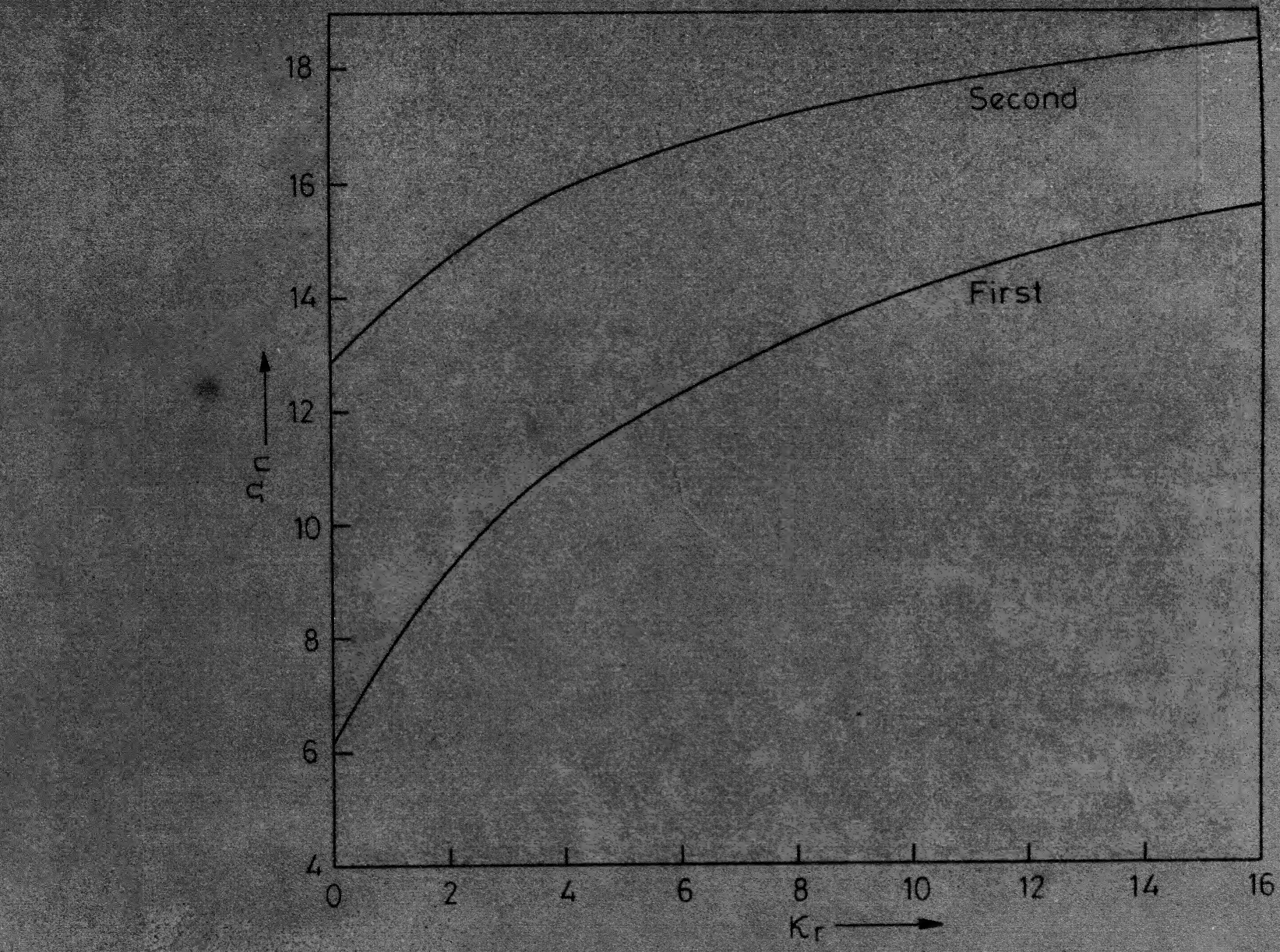

Figure 2.11 - Variation of natural frequencies with rotational stiffness, for a two span pipe on identical supports at regular interval $u = 2$, $\gamma = 2$ and $\beta = 0.5$

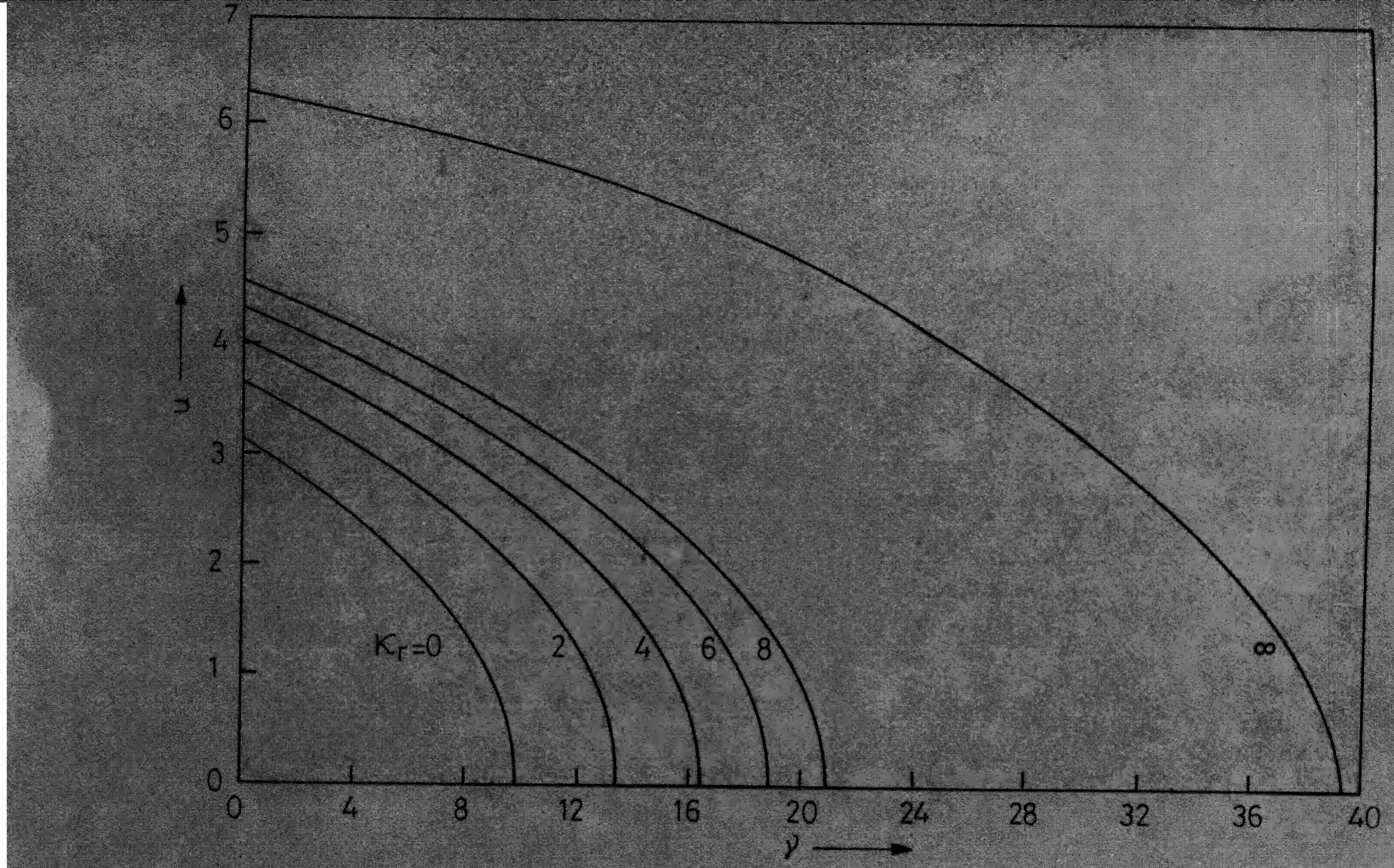

Figure 2-12 - Limits of fluid velocity (u) and fluid pressure (γ) for the onset of buckling for the rotational stiffness (K_r) at the supports.

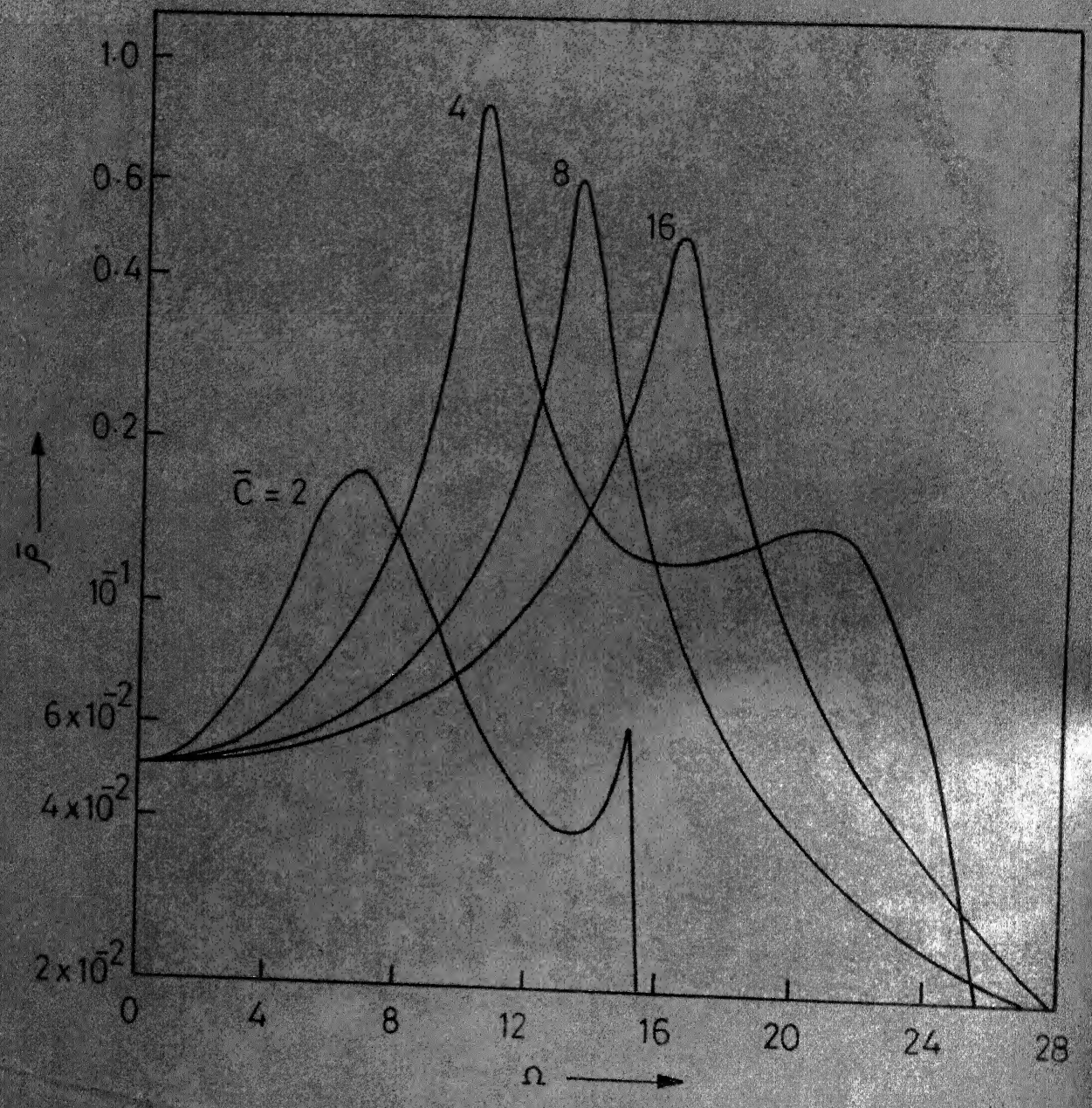

Figure 2·13 - Non-dimensional curvature amplitude ($\bar{P}$) at the mid-span for different values of the convection velocity of the loading. $u=2$, $\gamma=2$, $\beta=0.5$, $K_r=4.0$, $\bar{P}_0=1.0$, $\eta_b=0.1$, $\eta_s=0$.

can be sought by taking axial load on the beam equal to $u^2+\gamma$; and $\kappa_r = 0$ corresponds to the pinned-pinned beam and $\kappa_r = \infty$ to the clamped-clamped beam.

2.5.4 Response to a Convected Harmonic Pressure Field

Using the analysis presented in section 2.4, the response of a periodically supported infinite pipe to a convected harmonic pressure field is calculated. The response has been expressed in terms of the non-dimensional curvature amplitude, $\bar{\rho}$, at the centre of any bay.

Figure 2.13 shows the response of the pipe for different velocities of convection, $\bar{C}$, of the pressure field. A frequency range covering only the first propagation band of the corresponding undamped pipe has been considered. From Figure 2.13, it is seen that the response attains maxima at certain frequencies. Inspection of equation (2.19) shows that this will occur if

(a) C_n's assume very large values. This happens when the phase difference, ε, between pressures at distance ℓ apart is equal to the phase constant, μ_i, for free wave motion (in absence of damping). In other words, resonant-type response occurs when the convection velocity of the pressure field equals the phase velocity of one of the free wave components. This phenomenon is termed as 'coincidence'.

(b) The denominator of the second term of the right hand side of equation (2.19) has absolute minimum value which will be zero if there is no damping in the pipe. The frequency at which this occurs is the so-called resonant frequency given by $\Omega = \bar{C}^2$. Depending

upon the value of $\bar{C}$, coincidence may occur at a frequency lower than the resonant frequency.

As observed in the case of a beam, Figure 2.13 also shows that an increase in the convection velocity shifts the coincidence frequency to higher values [31].

It should be noted that for the pipe, the free wave phase velocities are different for the positive and the negative going waves. Hence the coincidence frequency depends on whether the convected pressure field travels along the direction of fluid flow (as assumed in section 2.4) or in the opposite direction.

Figure 2.14 shows the effect of damping in the pipe (η_b) on the level of the response. It is seen that the damping suppresses the response and peaks are reduced considerably. Damping in the pipe is effective in reducing both 'coincidence' and 'resonance' peaks.

Figure 2.15 shows the effect of damping in the support (η_s) on the response of the pipe. It is seen that only the 'coincidence' peaks are effectively reduced by the damping present in the supports. However, the resonant peaks are not affected much by η_s.

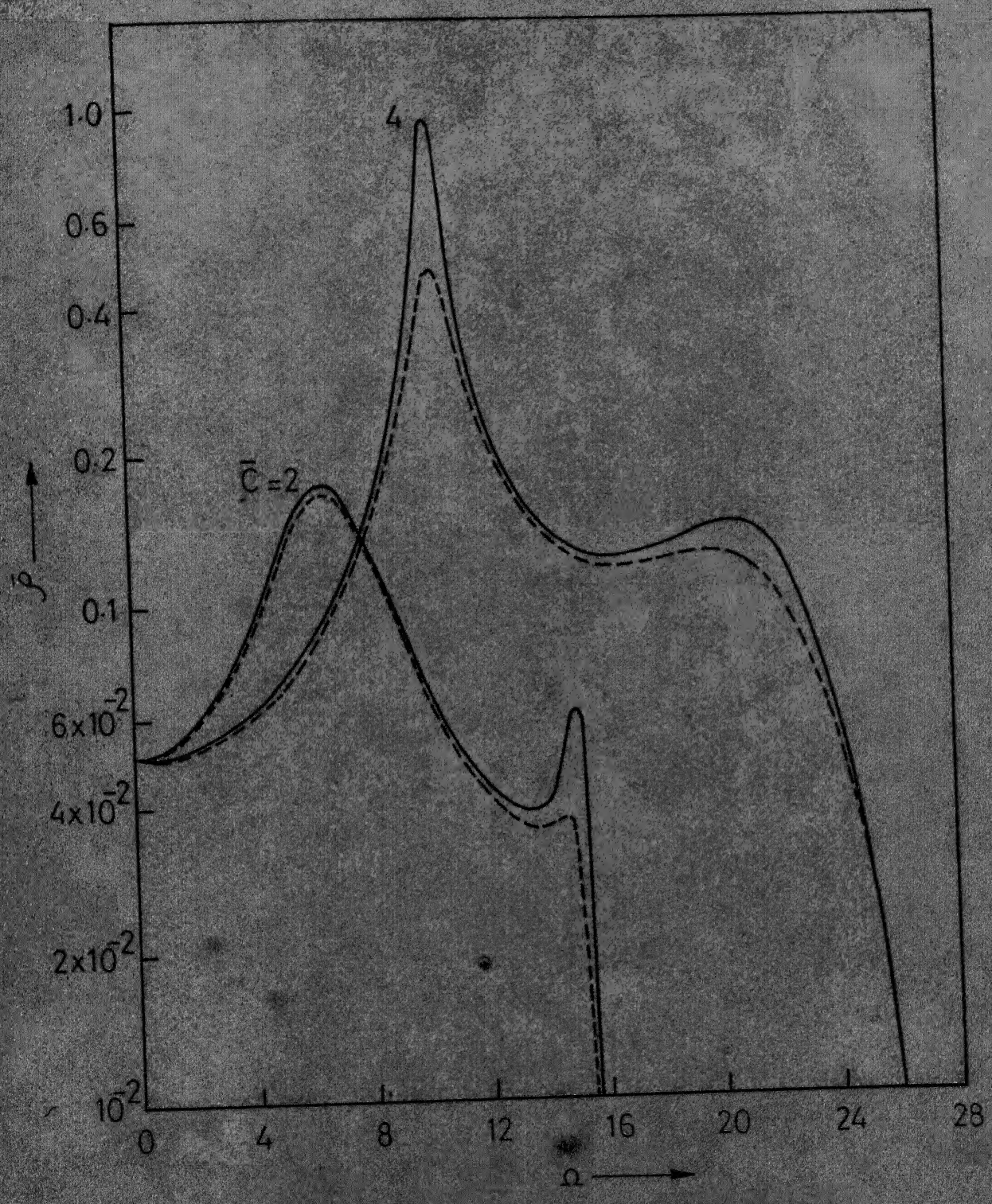

Figure 2·14 - The effect of η_b on the non-dimensional curvature amplitude ($\bar{\rho}$) at the mid-span. $u=2$, $\gamma=2$, $\beta=0.5$, $Kr=0$, $\bar{p}_o=1.0$, $\eta_s=0$; ——, $\eta_b=0.1$; - - - -, $\eta_b=0$

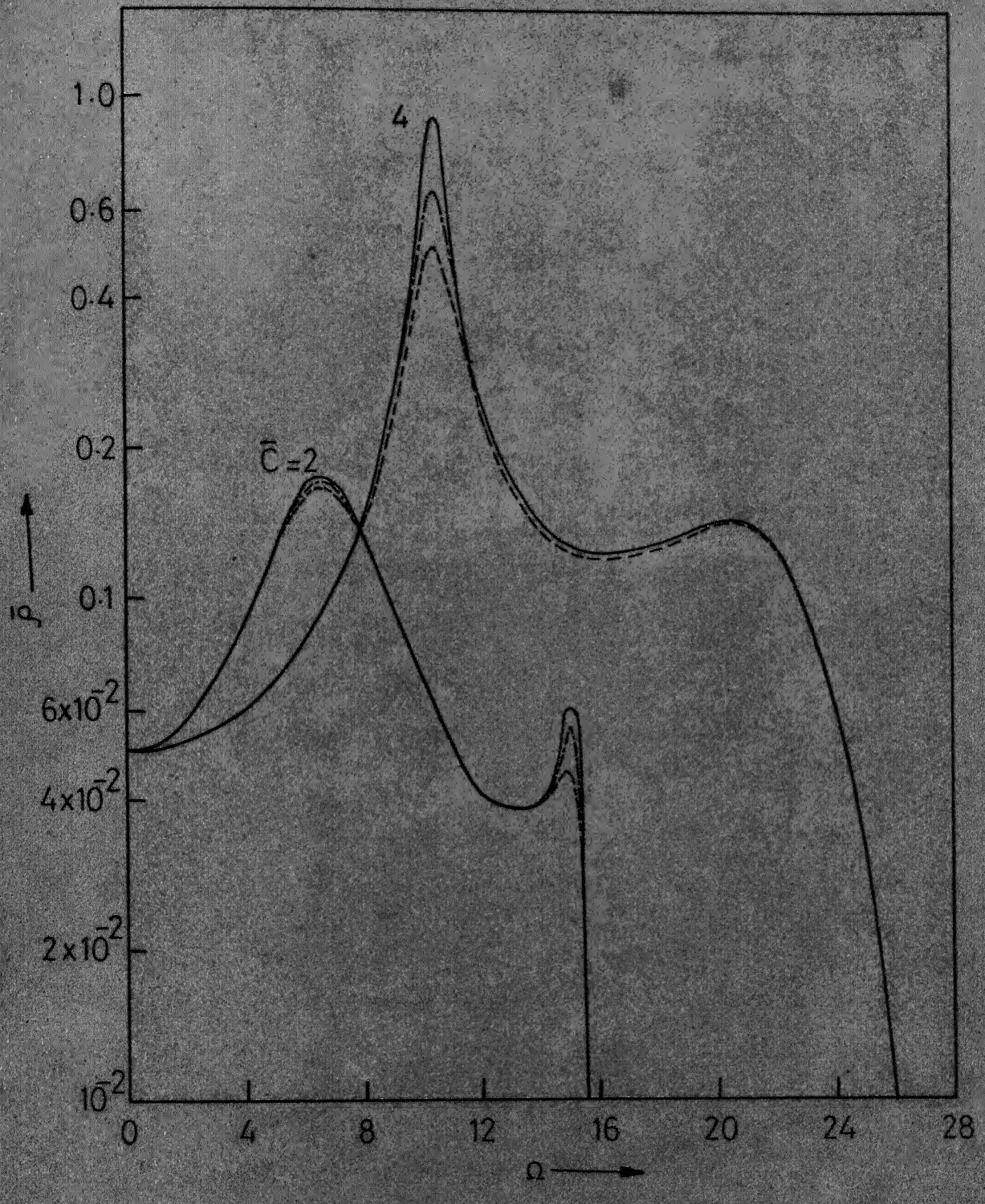

Figure 2.15 - The effect of η_s on the non-dimensional curvature amplitude ($\bar{P}$) at the mid-span. $u=2$, $\gamma=2$, $\beta=0.5$, $Kr=4.0$, $\bar{P}_0=1.0$, $\eta_b=0.1$; ——, $\eta_s=0$; — — —, $\eta_s=0.1$; - - - -, $\eta_s=0.2$.

CHAPTER 3

PARAMETRIC INSTABILITIES OF A PERIODICALLY-SUPPORTED PIPE CONVEYING FLUID

3.1 Introduction

It is well known that if the velocity of the fluid flowing through a pipe is not constant and is having harmonic fluctuations over and above a constant mean value, then the pipe experiences parametric instabilities. This phenomenon is similar to that of a beam when subjected to a periodic axial force [7]. Parametric instabilities differ from the more familiar instabilities, such as elasto-static buckling and forced vibration response, in the following aspects :

(i) It occurs over a range of parameter space and not at discrete points.

(ii) It can occur in a direction normal to the excitation.

(iii) It may occur at frequencies other than the natural frequencies of the system.

Two types of parametric instabilities may be distinguished, namely the primary and the secondary instabilities. For a system with natural frequencies given by Ω_n $(n = 1,2,3,\ldots)$, primary instabilities occur at $\Omega = \frac{2}{K}\Omega_n$ with $K = 1,3,5,\ldots$, as the excitation parameter is reduced to zero, where Ω is the frequency of the periodically varying parameter. Likewise, secondary instabilities occur at $\Omega = \frac{2}{K}\Omega_n$ with $K = 2,4,6,\ldots$ as the excitation parameter is reduced to zero. Instabilities corresponding

to K = 1 and 2 are known as the principal primary and the principal secondary instability, respectively. Bolotin [7] has shown that of all the instabilities, the principal primary instability is the most critical and has, therefore, greatest importance. This region of instability is also known as the principal region of dynamic instability.

The instability regions of a single span pipe with different boundary conditions have so far been studied in detail [10,16,48]. In all these works, comparison functions† [37] were used to represent the motion of the pipe. Thereafter, Bolotin's method [7] was used for the determination of the instability regions. In this chapter, we discuss the parametric instabilities of a periodically supported pipe. The supports are taken as transversely rigid and without any rotational stiffness. For the determination of the instability regions, following three methods have been attempted :

(i) The method used in earlier works (mentioned in the above paragraph) has been extended for the present problem.

(ii) Bolotin's concept is used directly without taking recourse to any mode shape approximation. In this method, the problem reduces to finding the zeros of a determinant. The size of this determinant, however, increases drastically with the number of spans in the pipe.

(iii) A method has been developed using the concept of wave approach presented in Chapter 2. In this method, the amount of computation is independent of the number of spans in the pipe.

---

† satisfying all the boundary conditions (geometric and natural).

Numerical results have been computed for the primary and the secondary instabilities associated with the first two modes of a two span pipe. In all cases, only the principal regions have been determined. The results obtained by all the three methods are found to be in excellent agreement with one another. The effects of various terms, like mass ratio parameter, β , mean fluid velocity and fluid pressure, on the regions of instabilities have been studied. The effect of damping in the pipe has also been investigated. All the instability regions are shown as plots of the non-dimensional frequency, Ω , versus the excitation parameter. The excitation parameter has been taken as the ratio of the amplitude of the harmonically varying component to the mean value of the fluid velocity.

3.2 Equation For Transverse Motion of the Pipe

Consider an N-span pipe identically supported on transversely rigid supports at distance 'ℓ' apart. The rotational stiffness at each support has been assumed to be zero. The equation for transverse motion of the pipe in any span is (see Appendix 1)

$$EI \frac{\partial^4 y}{\partial x^4} + (m_f V^2 + p_f A_p) \frac{\partial^2 y}{\partial x^2} + 2m_f V \frac{\partial^2 y}{\partial x \partial t} + m_f \frac{\partial V}{\partial t} \frac{\partial y}{\partial x} + (m_f + m_p) \frac{\partial^2 y}{\partial t^2} = 0 \qquad (3.1)$$

Equation (3.1) can be put in the following non-dimensional form :

$$\frac{\partial^4 \bar{y}_1}{\partial \xi^4} + (u^2 + \gamma) \frac{\partial^2 \bar{y}_1}{\partial \xi^2} + 2\beta u \frac{\partial^2 \bar{y}_1}{\partial \xi \partial \tau} + \beta \frac{\partial u}{\partial \tau} \frac{\partial \bar{y}_1}{\partial \xi} + \frac{\partial^2 \bar{y}_1}{\partial \tau^2} = 0, \qquad (3.2)$$

where the non-dimensional displacement of the pipe, $\bar{y}_1 = \frac{y}{\ell}$, the non-dimensional time, $\tau = \left(\frac{EI}{m_f + m_p}\right)^{1/2} \frac{t}{\ell^2}$, and other symbols have already

been defined in Chapter 2.

Let the non-dimensional velocity of the fluid, u, be of the form

$$u = u_o (1 + \delta \cos \Omega\tau), \tag{3.3}$$

where u_o is the constant mean velocity of the fluid,

δ is the excitation parameter,

and Ω is the non-dimensional frequency.

Substituting equation (3.3) into equation (3.2), one gets

$$\frac{\partial^4 \bar{y}_1}{\partial \xi^4} + \{u_o^2(1 + \delta \cos \Omega\tau)^2 + \gamma\} \frac{\partial^2 \bar{y}_1}{\partial \xi^2} + 2\beta u_o(1 + \delta \cos \Omega\tau) \frac{\partial^2 \bar{y}_1}{\partial \xi \partial \tau}$$

$$- \beta u_o \Omega\delta \sin \Omega\tau \frac{\partial \bar{y}_1}{\partial \xi} + \frac{\partial^2 \bar{y}_1}{\partial \tau^2} = 0 \tag{3.4}$$

Since equation (3.4) contains periodic coefficients, it may have unbounded solutions even for small value of the excitation parameter, δ [7]. The unbounded solutions will occur over a range of frequencies. These regions of instabilities are of interest to us and can be determined as discussed in the following sections.

3.3 Determination of Regions of Parametric Instabilities

Bolotin [7] has shown that the regions of unbounded solutions, of equations of type (3.4), are separated from the regions of bounded solutions by the periodic solutions with periods T and 2T, where $T = 2\pi/\Omega$ (see Appendix 3). In other words, two solutions of identical periods bound the region of instability, and two solutions of different periods bound the region of stability. The regions enclosed by solutions having

period 2T, correspond to 'primary instabilities', whereas, 'secondary instability' regions are enclosed by solutions having period T.

Three different methods to determine the solutions of equation (3.4) with periods 2T and T, i.e., the regions of primary and secondary instabilities, are discussed below.

3.4 First Method

In previous works, Bolotin's method was used in conjunction with mode shape approximation for determining the regions of parametric instability of a single span pipe with different boundary conditions [10,16,48]. In this section, the same method has been used to compute the instability regions of the pipe considered in section 3.2. The transverse displacement of the pipe is approximated by the mode shapes of a periodically supported beam. Hence, to use this method mode shapes of an N-span beam must be known in advance.

Let the displacement of the pipe, $\bar{y}_1$ in the transverse direction be approximated as

$$\bar{y}_1(\xi,\tau) = \sum_r \phi_r(\xi)\ q_r(\tau), \qquad (3.5)$$

where q_r's are the generalised co-ordinates (functions of time), and ϕ_r's are the comparison functions satisfying the boundary conditions. For the pipe in question, ϕ_r's can be taken as the normalised modes of an N-span beam. Hence, ϕ_r's satisfy the equation $\frac{d^4\phi_r}{d\xi^4} = \lambda_r^4 \phi_r$. Substituting equation (3.5) into equation (3.4), one gets

$$\sum_r \left[\phi_r \ddot{q}_r + 2\beta u_o(1 + \delta \cos \Omega\tau)\, \phi_r' \dot{q}_r + \{\phi_r'''' + (u_o^2 (1 + \delta \cos \Omega\tau)^2 + \gamma)\, \phi_r'' - \beta u_o \Omega\delta \sin \Omega\tau\, \phi_r'\}\, q_r \right] = 0, \qquad (3.6)$$

where primes and dots denote differentiation with respect to ξ and τ, respectively.

Multiplying equation (3.6) by $\frac{1}{N} \phi_s$ and integrating over the non-dimensional length of the pipe, N, one gets

$$\ddot{\underset{\sim}{Q}} + 2\beta u_o(1 + \delta \cos \Omega\tau) [P] \dot{\underset{\sim}{Q}} + \{ [S] + (u_o^2 (1 + \delta \cos \Omega\tau)^2 + \gamma) [R] - \beta u_o \Omega\delta \sin \Omega\tau [P] \} \underset{\sim}{Q} = 0, \qquad (3.7)$$

where $\underset{\sim}{Q}$ is a vector $\begin{bmatrix} q_1 \\ q_2 \\ \vdots \end{bmatrix}$, and the elements of the matrices P, R, and S are given by

$$p_{mn} = \frac{1}{N} \int_0^N \phi_m \phi_n' \, d\xi ,$$

$$r_{mn} = \frac{1}{N} \int_0^N \phi_m \phi_n'' \, d\xi ,$$

and $$s_{mn} = \frac{1}{N} \int_0^N \phi_m \phi_n'''' = \frac{\lambda_n^4}{N} \int_0^N \phi_m \phi_n \, d\xi$$

$$= \lambda_n^4 \delta_{mn} \text{ (by making use of orthogonality of the modes),}$$

where $\delta_{mn} = 1$ if $m = n$

$= 0$ if $m \neq n$

Thus, the matrices, P, R, and S can be determined if the mode shapes are known.

As stated earlier, the regions of primary instability are separated by solutions having period 2T. For these solutions, vector $\underset{\sim}{Q}$ can be written as

$$\underset{\sim}{Q} = \sum_{K=1,3,5,\cdots} \{\underset{\sim}{a}_K \sin(\tfrac{K}{2}\Omega\tau) + \underset{\sim}{b}_K \cos(\tfrac{K}{2}\Omega\tau)\}\ , \qquad (3.8)$$

where $\underset{\sim}{a}_K$ and $\underset{\sim}{b}_K$ are unknown vectors.

Substituting equation (3.8) into equation (3.7), one obtains

$$\sum_{K=1,3,5,\cdots} \Big[\{-(\tfrac{K\Omega}{2})^2 \underset{\sim}{a}_K - 2\beta u_o [P](\tfrac{K\Omega}{2}) \underset{\sim}{b}_K + ([S] + (u_o^2 + \gamma + \frac{u_o^2\delta^2}{2})[R]) \cdot \underset{\sim}{a}_K\} \sin(\tfrac{1}{2}K\Omega\tau)$$

$$+ \{-(\tfrac{K\Omega}{2})^2 \underset{\sim}{b}_K + 2\beta u_o [P](\tfrac{K\Omega}{2}) \underset{\sim}{a}_K + ([S] + (u_o^2+\gamma+\frac{u_o^2\delta^2}{2})[R])\underset{\sim}{b}_K\}\cos(\tfrac{1}{2}K\Omega\tau)$$

$$+ \{-\beta u_o \delta [P](\tfrac{K\Omega}{2})\underset{\sim}{b}_K + u_o^2\delta[R]\underset{\sim}{a}_K - \tfrac{1}{2}\beta u_o \delta\Omega[P]\underset{\sim}{b}_K\} \sin(\tfrac{K+2}{2}\Omega\tau)$$

$$+ \{\beta u_o \delta [P](\tfrac{K\Omega}{2})\underset{\sim}{a}_K + u_o^2\delta[R]\underset{\sim}{b}_K + \tfrac{1}{2}\beta u_o \delta\Omega[P]\underset{\sim}{a}_K\} \cos(\tfrac{K+2}{2}\Omega\tau)$$

$$+ \{-\beta u_o \delta [P](\tfrac{K\Omega}{2})\underset{\sim}{b}_K + u_o^2\delta[R]\underset{\sim}{a}_K + \tfrac{1}{2}\beta u_o \delta\Omega[P]\underset{\sim}{b}_K\} \sin(\tfrac{K-2}{2}\Omega\tau)$$

$$+ \{\beta u_o \delta [P](\tfrac{K\Omega}{2})\underset{\sim}{a}_K + u_o^2\delta[R]\underset{\sim}{b}_K - \tfrac{1}{2}\beta u_o \delta\Omega[P]\underset{\sim}{a}_K\} \cos(\tfrac{K-2}{2}\Omega\tau)$$

$$+ \frac{u_o^2\delta^2}{4}[R]\{\underset{\sim}{a}_K \sin(\tfrac{K+4}{2}\Omega\tau) + \underset{\sim}{b}_K\cos(\tfrac{K+4}{2}\Omega\tau) + \underset{\sim}{a}_K\sin(\tfrac{K-4}{2}\Omega\tau)$$

$$+ \underset{\sim}{b}_K \cos(\tfrac{K-4}{2}\Omega\tau)\}\Big] = 0 \qquad (3.9)$$

Equating coefficients of the terms $\sin(\frac{1}{2}\Omega\tau)$, $\cos(\frac{1}{2}\Omega\tau)$, $\sin(\frac{3}{2}\Omega\tau)$, $\cos(\frac{3}{2}\Omega\tau)$ and the like from both sides of equation (3.9), one gets

$$\begin{bmatrix} D_{11} & D_{12} & D_{13} & D_{14} \cdots\cdots \\ D_{21} & D_{22} & D_{23} & D_{24} \cdots\cdots \\ D_{31} & D_{32} & D_{33} & D_{34} \cdots\cdots \\ D_{41} & D_{42} & D_{43} & D_{44} \cdots\cdots \\ \vdots & \vdots & \vdots & \vdots \end{bmatrix} \begin{Bmatrix} \underset{\sim}{a}_1 \\ \underset{\sim}{b}_1 \\ \underset{\sim}{a}_3 \\ \underset{\sim}{b}_3 \\ \vdots \end{Bmatrix} = 0, \quad (3.10)$$

where $D_{11} = -\frac{\Omega^2}{4}[I] + [S] + (u_o^2 + \gamma + \frac{u_o^2\delta^2}{2} - u_o^2\delta)\ [R]$,

$D_{12} = -\beta u_o \Omega\ [P]$,

$D_{13} = (u_o^2\delta - \frac{u_o^2\delta^2}{4})\ [R]$,

$D_{14} = -\beta u_o \delta \Omega [P]$,

$D_{21} = \beta u_o \Omega\ [P]$,

$D_{22} = -\frac{\Omega^2}{4}[I] + [S] + (u_o^2 + \gamma + \frac{u_o^2\delta^2}{2} + u_o^2\delta)\ [R]$,

$D_{23} = \beta u_o \delta \Omega [P]$,

$D_{24} = (u_o^2\delta + \frac{u_o^2\delta^2}{4})[R]$,

$D_{31} = (u_o^2\delta - \frac{u_o^2\delta^2}{4})[R]$,

$D_{32} = -\beta u_o \delta\Omega [P]$,

$D_{33} = -\frac{9\Omega^2}{4}[I] + [S] + (u_o^2 + \gamma + \frac{u_o^2\delta^2}{2})\ [R]$,

$D_{34} = -3\beta u_o \Omega [P]$,

$D_{41} = \beta u_o \delta\Omega [P]$,

$$D_{42} = \left(u_o^2 \delta + \frac{u_o^2 \delta^2}{4}\right) [R],$$

$$D_{43} = 3\beta u_o \Omega [P],$$

$$D_{44} = \frac{9\Omega^2}{4} [I] + [S] + \left(u_o^2 + \delta + \frac{u_o^2 \delta^2}{2}\right) [R],$$

and $[I]$ is the identity matrix.

Frequencies bounding the instability regions are obtained by setting the determinant of the coefficient matrix, $[D]$, of equation (3.10) equal to zero. Of course, the determinant is of infinite order, but it belongs to the class of normal determinants and is absolutely convergent [7]. Hence, the approximate boundaries of the instability regions may be obtained by truncating the series in equation (3.8) at $K = 1$. That is, by equating to zero the determinant shown circumscribed with dashed lines in equation (3.10). This is known as $K = 1$ approximation, which necessarily yields only principal region of instability. A better approximation and as well as higher order instability regions would be obtained if the series in equation (3.8) is truncated at higher values of K. Of course, the series in equation (3.5) must be truncated at adequately high value of r, which defines the order of D_{ij}. Bolotin [7] has shown that in the case of a beam subjected to a periodic axial force, for values of δ even upto 0.3, the regions of principal primary instability obtained by $K = 1$ approximation, are within one percent of those obtained by $K = 3$ approximation.

Now, the regions of secondary instability, which are separated by solutions of period T, may be obtained by expressing

$$\underset{\sim}{Q} = \sum_{K=0,2,4,\ldots} \{\underset{\sim}{a}_K \sin(\tfrac{1}{2}K\Omega\tau) + \underset{\sim}{b}_K \cos(\tfrac{K}{2}\Omega\tau)\} \quad , \tag{3.11}$$

which substituted into equation (3.7), yields once again equation (3.9), but with summation now being over $K = 0,2,4,\ldots$. Equating coefficients of similar terms as before, one is led to a matrix equation, equivalent to equation (3.10), but with a vector $\begin{Bmatrix} b_o \\ a_2 \\ b_2 \\ \vdots \end{Bmatrix}$ and thence to a vanishing determinant which yields the boundaries of the secondary instability. The determinant obtained for $K = 2$ approximation is given by

$$\begin{vmatrix} D_{11} & D_{12} & D_{13} \\ D_{21} & D_{22} & D_{23} \\ D_{31} & D_{32} & D_{33} \end{vmatrix} \quad , \tag{3.12}$$

where $D_{11} = [S] + (u_o^2 + \gamma + \frac{u_o^2\delta^2}{2})[R]$,

$D_{12} = \frac{1}{2}\beta u_o \delta\Omega[P]$,

$D_{13} = u_o^2 \delta[R]$,

$D_{21} = -\beta u_o \delta\Omega [P]$,

$D_{22} = [S] + (u_o^2 + \gamma + \frac{u_o^2\delta^2}{2})[R] - \Omega^2$,

$D_{23} = -2\beta u_o \Omega [P]$,

$D_{31} = 2 u_o^2 \delta [R]$,

$D_{32} = 2\beta u_o \Omega [P]$,

$D_{33} = [S] + (u_o^2 + \gamma + \frac{u_o^2\delta^2}{2})[R] - \Omega^2$

3.5 Second Method

In this section, Bolotin's concept is directly used without recourse to any mode shape approximation. To determine the regions of primary instability, which are bounded by periodic solutions with period 2T, the displacement, $\bar{y}_1$, can be expressed as

$$\bar{y}_1(\xi,\tau) = \sum_{K=1,3,5,\ldots} \bar{X}_K(\xi)\sin(\tfrac{1}{2}K\Omega\tau) + \bar{Y}_K(\xi)\cos(\tfrac{1}{2}K\Omega\tau), \qquad (3.13)$$

where $\bar{X}_K$ and $\bar{Y}_K$ are unknown functions of ξ.

Substituting $\bar{y}_1$ from equation (3.13) into equation (3.4), one obtains

$$\sum_{K=1,3,5..} \Big[\Big\{ \frac{d^4\bar{X}_K}{d\xi^4} + (u_o^2+\gamma+\frac{u_o^2\delta^2}{2})\frac{d^2\bar{X}_K}{d\xi^2} - (\frac{K}{2})^2\Omega^2\bar{X}_K - \beta u_o \Omega K \frac{d\bar{Y}_K}{d\xi} \Big\}\sin(\tfrac{1}{2}K\Omega\tau)$$

$$+ \Big\{ \frac{d^4\bar{Y}_K}{d\xi^4} + (u_o^2+\gamma+\frac{u_o^2\delta^2}{2})\frac{d^2\bar{Y}_K}{d\xi^2} - (\frac{K}{2})^2\Omega^2\bar{Y}_K + \beta u_o\Omega K \frac{d\bar{X}_K}{d\xi} \Big\}\cos(\tfrac{1}{2}K\Omega\tau)$$

$$+ \Big\{ -(\frac{K\Omega}{2})\beta u_o\delta\frac{d\bar{Y}_K}{d\xi} + u_o^2\delta\frac{d^2\bar{X}_K}{d\xi^2} - \frac{1}{2}\beta u_o\delta\Omega\frac{d\bar{Y}_K}{d\xi} \Big\}\sin(\frac{K+2}{2}\Omega\tau)$$

$$+ \Big\{ (\frac{K\Omega}{2})\beta u_o\delta\frac{d\bar{X}_K}{d\xi} + u_o^2\delta\frac{d^2\bar{Y}_K}{d\xi^2} + \frac{1}{2}\beta u_o\delta\Omega\frac{d\bar{X}_K}{d\xi} \Big\}\cos(\frac{K+2}{2}\Omega\tau)$$

$$+ \Big\{ -(\frac{K\Omega}{2})\beta u_o\delta\frac{d\bar{Y}_K}{d\xi} + u_o^2\delta\frac{d^2\bar{X}_K}{d\xi^2} + \frac{1}{2}\beta u_o\delta\Omega\frac{d\bar{Y}_K}{d\xi} \Big\}\sin(\frac{K-2}{2}\Omega\tau)$$

$$+ \Big\{ (\frac{K\Omega}{2})\beta u_o\delta\frac{d\bar{X}_K}{d\xi} + u_o^2\delta\frac{d^2\bar{Y}_K}{d\xi^2} - \frac{1}{2}\beta u_o\delta\Omega\frac{d\bar{X}_K}{d\xi} \Big\}\cos(\frac{K-2}{2}\Omega\tau)$$

$$+ \frac{u_o^2\delta^2}{4} \frac{d^2\bar{X}_K}{d\xi^2} \{\sin\left(\frac{K+4}{2}\Omega\tau\right) + \sin\left(\frac{K-4}{2}\Omega\tau\right)\}$$

$$+ \frac{u_o^2\delta^2}{4} \frac{d^2\bar{Y}_K}{d\xi^2} \{\cos\left(\frac{K+4}{2}\Omega\tau\right) + \cos\left(\frac{K-4}{2}\Omega\tau\right)\}] = 0 \qquad (3.14)$$

As stated earlier, the regions of principal primary instability can be obtained quite accurately by truncating the series in equation (3.13) only at K=1. Thus, equating coefficients of $\sin(\frac{1}{2}\Omega\tau)$ and $\cos(\frac{1}{2}\Omega\tau)$ from both side of equation (3.14), one gets

$$\frac{d^4\bar{X}_1}{d\xi^4} + (u_o^2 + \gamma + \frac{u_o^2\delta^2}{2} - u_o^2\delta) \frac{d^2\bar{X}_1}{d\xi^2} - \frac{1}{4}\Omega^2\bar{X}_1 - \beta u_o \Omega \frac{d\bar{Y}_1}{d\xi} = 0, \qquad (3.15a)$$

and

$$\frac{d^4\bar{Y}_1}{d\xi^4} + (u_o^2 + \gamma + \frac{u_o^2\delta^2}{2} + u_o^2\delta) \frac{d^2\bar{Y}_1}{d\xi^2} - \frac{1}{4}\Omega^2\bar{Y}_1 + \beta u_o \Omega \frac{d\bar{X}_1}{d\xi} = 0. \qquad (3.15b)$$

It should be noted that equations (3.15a) and (3.15b) are coupled differential equations and their solutions can be written as

$$\psi_i(\xi) = C_i e^{\lambda\xi} \quad , i = 1,2, \qquad (3.16)$$

where $\psi_1 \equiv \bar{X}_1$ and $\psi_2 \equiv \bar{Y}_1$.

Substituting equation (3.16) into equations (3.15), one gets

$$\{\lambda^4 + (u_o^2 + \gamma + \frac{u_o^2\delta^2}{2} - u_o^2\delta)\lambda^2 - \frac{1}{4}\Omega^2\} C_1 - \beta u_o \Omega\lambda C_2 = 0, \qquad (3.17a)$$

$$\{\lambda^4 + (u_o^2 + \gamma + \frac{u_o^2\delta^2}{2} + u_o^2\delta)\lambda^2 - \frac{1}{4}\Omega^2\} C_2 + \beta u_o \Omega\lambda C_1 = 0. \qquad (3.17b)$$

For non-trivial solutions of C_1 and C_2,

$$\begin{vmatrix} \lambda^4 + (u_o^2 + \gamma + \frac{u_o^2\delta^2}{2} - u_o^2\delta)\lambda^2 - \frac{1}{4}\Omega^2 & -\beta u_o \Omega\lambda \\ \beta u_o \Omega\lambda & \lambda^4 + (u_o^2 + \gamma + \frac{u_o^2\delta^2}{2} + u_o^2\delta)\lambda^2 - \frac{1}{4}\Omega^4 \end{vmatrix} = 0 \qquad (3.18)$$

From equation (3.18), eight values of the λ's are obtained. Hence, the general solution of equations (3.15) is given by

$$\psi_i(\xi) = \sum_{j=1}^{8} C_{ij} e^{\lambda_j \xi}, \quad i=1,2 \qquad (3.19)$$

Equations (3.15) hold good for any span of the pipe. The solution for any span of the pipe, say the nth span, can be written as

$$\psi_i^n(\xi) = \sum_{j=1}^{8} C_{ij}^n e^{\lambda_j \xi}, \quad \begin{matrix} i=1,2 \\ n=1,2,\ldots,N \end{matrix} \qquad (3.20)$$

The unknown coefficients C_{ij}^n can be determined using the boundary conditions imposed by the supports. These boundary conditions are as follows:

(i) for zero deflection at all the supports

$$\psi_i^n(0) = 0, \qquad (3.21a)$$

$$\psi_i^n(1) = 0, \qquad (3.21b)$$

for $i = 1,2$,

and $n = 1,2,\ldots,N$

(ii) for zero moment at the end supports

$$\psi_i''^{1}(0) = 0, \tag{3.21c}$$

$$\psi_i''^{N}(1) = 0, \tag{3.21d}$$

for $i = 1,2$

where primes denote differentiation with respect to ξ.

(iii) for continuity of slopes and moments at each intermediate support :

$$\psi_i'^{n}(1) = \psi_i'^{n+1}(0) \quad , \tag{3.21e}$$

$$\psi_i''^{n}(1) = \psi_i''^{n+1}(0) \quad , \tag{3.21f}$$

for $i = 1,2,$

and $n = 1,2,\ldots,N-1$

Moreover, using equation (3.17a), C_{ij} and C_{2j} can be related as

$$C_{ij} = \frac{\beta u_o \Omega \lambda_j}{\lambda_j^4 + (u_o^2 + \gamma + \frac{u_o^2\delta^2}{2} - u_o^2\delta)\lambda_j - \frac{1}{4}\Omega^2} C_{2j}, \quad j=1,2,\ldots,8 \tag{3.22}$$

Substituting equations (3.20) and (3.22) into equations (3.21), one obtains 8N homogeneous equations in 8N unknowns. For non-trivial solutions of the constants C_{ij}'s (and consequently C_{2j}'s), determinant of the coefficients of the resulting homogeneous equations must vanish. Frequencies giving zeros of this determinant define the boundaries of the primary instability regions.

Now, to determine the regions of secondary instability, the displacement, $\bar{y}_1$ is expressed as

$$\bar{y}_1(\xi,\tau) = \sum_{K=0,2,4,\ldots} \bar{X}_K(\xi)\sin(\tfrac{1}{2}K\Omega\tau) + \bar{Y}_K(\xi)\cos(\tfrac{K}{2}\Omega\tau) \qquad (3.23)$$

Substitution of equation (3.23) into equation(3.4)results in equation (3.14) with summation now being over $K = 0,2,4,\ldots$. The regions of principal secondary instability can be predicted with reasonable accuracy by truncating the series in equation (3.23) at $K = 2$. Equating the constant term, and the coefficients of $\sin(\Omega\tau)$ and $\cos(\Omega\tau)$ terms from both sides of the resulting equation, one gets

$$\frac{d^4\bar{Y}_o}{d\xi^4} + (u_o^2+\gamma+\frac{u_o^2\delta^2}{2})\frac{d^2\bar{Y}_o}{d\xi^2} + u_o^2\delta\frac{d^2\bar{Y}_2}{d\xi^2} + \frac{1}{2}\beta\, u_o\delta\Omega\frac{d\bar{X}_2}{d\xi} = 0, \qquad (3.24a)$$

$$\frac{d^4\bar{X}_2}{d\xi^4} + (u_o^2+\gamma+\frac{u_o^2\delta^2}{2})\frac{d^2\bar{X}_2}{d\xi^2} - \Omega^2\bar{X}_2 - 2\beta\, u_o\Omega\frac{d\bar{Y}_2}{d\xi} - \beta u_o\delta\Omega\frac{d\bar{Y}_o}{d\xi} = 0, \qquad (3.24b)$$

$$\frac{d^4\bar{Y}_2}{d\xi^4} + (u_o^2+\gamma+\frac{u_o^2\delta^2}{2})\frac{d^2\bar{Y}_2}{d\xi^2} - \Omega^2\bar{Y}_2 + 2\beta u_o\Omega\frac{d\bar{X}_2}{d\xi} + 2u_o^2\delta\frac{d\bar{Y}_o}{d\xi} = 0 \qquad (3.24c)$$

Solutions of the coupled differential equations (3.24) can be written as

$$\psi_i = C_i e^{\lambda\xi}, \quad i = 0,1,2, \qquad (3.25)$$

where $\psi_o \equiv \bar{Y}_o$, $\psi_1 \equiv \bar{X}_2$, and $\psi_2 \equiv \bar{Y}_2$.

Substituting equation (3.25) into equations (3.24), one gets

$$\{\lambda^4 + (u_o^2 + \gamma + \frac{u_o^2\delta^2}{2})\lambda^2\} C_o + \frac{1}{2}\beta u_o \delta\Omega\lambda C_1 + u_o^2\delta\lambda^2 C_2 = 0 \qquad (3.26a)$$

$$\{\lambda^4 + (u_o^2 + \gamma + \frac{u_o^2\delta^2}{2})\lambda^2 - \Omega^2\} C_1 - 2\beta u_o \Omega\lambda C_2 - \beta u_o \delta\Omega\lambda C_o = 0 \qquad (3.26b)$$

$$\{\lambda^4 + (u_o^2 + \gamma + \frac{u_o^2\delta^2}{2})\lambda^2 - \Omega^2\} C_2 + 2\beta u_o \Omega\lambda C_1 + 2u_o^2\delta\lambda C_o = 0 \qquad (3.26c)$$

For non-trivial solutions of C_o, C_1, and C_2

$$\begin{vmatrix} \lambda^4 + (u_o^2+\gamma+\frac{u_o^2\delta^2}{2})\lambda^2 & \frac{1}{2}\beta u_o \delta\Omega\lambda & u_o^2\delta\lambda^2 \\ -\beta u_o \delta\Omega\lambda & \lambda^4 + (u_o^2+\gamma+\frac{u_o^2\delta^2}{2})\lambda^2 - \Omega^2 & -2\beta u_o \Omega\lambda \\ 2u_o^2\delta\lambda & 2\beta u_o \Omega\lambda & \lambda^4+(u_o^2+\gamma+\frac{u_o^2\delta^2}{2})\lambda^2-\Omega^2 \end{vmatrix} = 0 \qquad (3.27)$$

From equation (3.27), twelve values of the λ's are obtained. It is obvious that two values of the λ's (say the first two values) are zero. So general solution of equations (3.24) can be written as

$$\psi_o = C_{o1} + C_{o2}\xi + \sum_{j=3}^{12} C_{oj} e^{\lambda_j \xi} \qquad (3.28a)$$

$$\psi_i = \sum_{j=3}^{12} C_{ij} e^{\lambda_j \xi}, \quad i = 1,2 \qquad (3.28b)$$

As implied from equations (3.26b) and (3.26c) the coefficients C_1 and C_2 corresponding to zero values ot the λ's are zero. For

remaining ten values of the λ_j's, C_{1j} and C_{2j} can be expressed in terms of C_{oj}, using equations (3.26).

Now, the solution for any span of the pipe, say the nth span, can be written as

$$\psi_o^n = C_{o1}^n + C_{o2}^n \xi + \sum_{j=3}^{12} C_{oj}^n e^{\lambda_j \xi} \tag{3.29a}$$

$$\psi_i^n = \sum_{j=3}^{12} C_{ij}^n e^{\lambda_j \xi}, \quad i = 1,2 \tag{3.29b}$$

$$\text{for } n = 1,2,\ldots,N$$

The unknown coefficients C_{oj}'s can be determined, using the boundary conditions given by equations (3.21). Of course, the subscript i will now have three values 0,1, and 2. Substituting equations (3.29) into the boundary conditions, and equating the determinant of the coefficients of the resulting equation to zero (for non-trivial solution of C_{oj}'s), one gets the frequencies defining the boundaries of the secondary instability regions.

3.6 Third Method

In Chapter 2, natural frequencies of a periodically supported pipe were obtained using the propagation constants of free harmonic waves travelling in a similar infinite structure. The same concept can also be used to determine the regions of instability discussed in previous sections. It has already been seen that frequencies, Ω's, at which equations (3.15) are satisfied with appropriate boundary conditions of an N-span pipe, give the boundaries of the primary instability regions.

Likewise, frequencies at which equations (3.24) are satisfied with appropriate boundary conditions of an N-span pipe, give the boundaries of the secondary instability regions.

Comparing equations (3.15) with equation of free vibration of a system, frequencies Ω's (defining the instability regions) can be thought of as the natural frequencies of a periodically supported pipe, motion of which in each bay is governed by coupled differential equations (3.15)† . Use of wave approach to determine the boundaries of the instability regions is presented in this section.

Let us assume the pipe under consideration being infinite in length. First of all, we discuss the primary instability regions only. For $K = 1$ approximation, using equation (3.13), the displacement of the pipe in any bay, $\bar{y}_1$, can be written as

$$\bar{y}_1 = \bar{X}_1 \sin\left(\frac{1}{2}\Omega\tau\right) + \bar{Y}_1 \cos\left(\frac{1}{2}\Omega\tau\right), \qquad (3.30)$$

where $\bar{X}_1$ and $\bar{Y}_1$ satisfy equations (3.15). Since these are coupled differential equations, displacement $\bar{y}_1$, in general, will contain both $\sin\left(\frac{1}{2}\Omega\tau\right)$ and $\cos\left(\frac{1}{2}\Omega\tau\right)$ terms. We associate two different propagation constants to these two terms. As it will be shown later, for the determination of natural frequencies (i.e., defining the regions of instability), these propagation constants need to be calculated under restricted conditions. Considering any span of the pipe, say AB (Figure 2.1), for periodic structures, one can write

---

† Hereafter, these frequencies, Ω, defining the boundaries of the instability regions will be referred to as natural frequencies.

$$\theta_B = \theta_{Bx} \sin(\tfrac{1}{2}\Omega\tau) + \theta_{By} \cos(\tfrac{1}{2}\Omega\tau)$$

$$= \theta_{Ax} e^{\mu_x} \sin(\tfrac{1}{2}\Omega\tau) + \theta_{Ay} e^{\mu_y} \cos(\tfrac{1}{2}\Omega\tau), \qquad (3.31a)$$

and $$\bar{M}_B = \bar{M}_{Bx} \sin(\tfrac{1}{2}\Omega\tau) + \bar{M}_{By} \cos(\tfrac{1}{2}\Omega\tau)$$

$$= \bar{M}_{Ax} e^{\mu_x} \sin(\tfrac{1}{2}\Omega\tau) + \bar{M}_{Ay} e^{\mu_y} \cos(\tfrac{1}{2}\Omega\tau), \qquad (3.31b)$$

where θ and $\bar{M}$ represent the slope and the bending moment (non-dimensional) with subscripts A and B referring to the ends A and B and subscripts x and y referring to the contribution of the sine and the cosine components, respectively. μ_x and μ_y are the propagation constants associated with the sine and the cosine waves respectively.

As explained in Chapter 2, to determine the natural frequencies of an N-span pipe, any dynamic disturbance is considered in terms of two opposite going waves.

Let

$$\bar{M}_+ = \bar{M}_{x^+} \sin(\tfrac{1}{2}\Omega\tau) + \bar{M}_{y^+} \cos(\tfrac{1}{2}\Omega\tau), \qquad (3.32a)$$

and $$\bar{M}_- = \bar{M}_{x^-} \sin(\tfrac{1}{2}\Omega\tau) + \bar{M}_{y^-} \cos(\tfrac{1}{2}\Omega\tau), \qquad (3.32b)$$

be the bending moments at the first support due to the positive going and the negative going waves respectively. The respective bending moments due to these waves at the last support will be

$$\bar{M}_{N^+} = \bar{M}_{x^+} e^{N\mu_x^+} \sin(\tfrac{1}{2}\Omega\tau) + \bar{M}_{y^+} e^{N\mu_y^+} \cos(\tfrac{1}{2}\Omega\tau) \qquad (3.33a)$$

$$\bar{M}_{N^-} = \bar{M}_{x^-} e^{N\mu_x^-} \sin(\tfrac{1}{2}\Omega\tau) + \bar{M}_{y^-} e^{N\mu_y^-} \cos(\tfrac{1}{2}\Omega\tau) \qquad (3.33b)$$

Since the total bending moments at the end supports must vanish (for these are simple supports), one gets

$$\bar{M}_{+} + \bar{M}_{-} = 0 \qquad (3.34a)$$

$$\bar{M}_{N^+} + \bar{M}_{N^-} = 0 \qquad (3.34b)$$

Substituting equations (3.32) and (3.33) into equations (3.3.4) and equating the coefficients of the terms $\sin(\frac{1}{2}\Omega\tau)$ and $\cos(\frac{1}{2}\Omega\tau)$ from both sides, one gets

$$\bar{M}_{x^+} + \bar{M}_{x^-} = 0 \qquad (3.35a)$$

$$\bar{M}_{y^+} + \bar{M}_{y^-} = 0 \qquad (3.35b)$$

$$\bar{M}_{x^+} e^{N\mu_x^+} + \bar{M}_{x^-} e^{N\mu_x^-} = 0 \qquad (3.35c)$$

$$\bar{M}_{y^+} e^{N\mu_y^+} + \bar{M}_{y^-} e^{N\mu_y^-} = 0 \qquad (3.35d)$$

Equations (3.35) are satisfied by either of the following conditions

$$(e^{N\mu_x^+} - e^{N\mu_x^-}) = 0 \quad \text{with} \quad \bar{M}_{y^+} = \bar{M}_{y^-} = 0 \,, \qquad (3.36a)$$

$$(e^{N\mu_y^+} - e^{N\mu_y^-}) = 0 \quad \text{with} \quad \bar{M}_{x^+} = \bar{M}_{x^-} = 0 \,. \qquad (3.36b)$$

Sen Gupta [51] has shown that for the determination of natural frequencies, only propagating waves (with $\mu_r = 0$) need to be considered. So equations (3.36) reduce to

$$(e^{iN\mu^+_{ix}} - e^{iN\mu^-_{ix}}) = 0 \quad \text{with} \quad \bar{M}_{y^+} = \bar{M}_{y^-} = 0 \tag{3.37a}$$

$$(e^{iN\mu^+_{iy}} - e^{iN\mu^-_{iy}}) = 0 \quad \text{with} \quad \bar{M}_{x^+} = \bar{M}_{x^-} = 0 \tag{3.37b}$$

As usual, the values of $|\mu^+_{ix} - \mu^-_{ix}|$ and $|\mu^+_{iy} - \mu^-_{iy}|$ in propagation bands will vary between 0 and 2π. Hence, equations (3.37) can be simplified to

$$\mu^*_x = |\mu^+_{ix} - \mu^-_{ix}| = \frac{2j\pi}{N}, \; j=0, 1,2,\ldots,N \text{ with } \bar{M}_{y^+} = \bar{M}_{y^-} = 0 \tag{3.38a}$$

and $$\mu^*_y = |\mu^+_{iy} - \mu^-_{iy}| = \frac{2j\pi}{N}, \; j=0,1,2,\ldots, N \text{ with } \bar{M}_{x^+} = \bar{M}_{x^-} = 0 \tag{3.38b}$$

Now the graphical approach presented in section 2.3 can be used to find out the natural frequencies. First the curves of μ^*_x (with $\bar{M}_{y^+} = \bar{M}_{y^-} = 0$) versus Ω and μ^*_y (with $\bar{M}_{x^+} = \bar{M}_{x^-} = 0$) versus Ω are to be drawn. Then, by dividing the range of μ^* in the propagation bands into N equal divisions, one gets N natural frequencies after deleting the highest frequency in each propagation band. The two sets of frequencies obtained in this manner give the boundaries of the primary instability regions.

The propagation constants μ_x with $\bar{M}_{y^+} = \bar{M}_{y^-} = 0$ (i.e., $\bar{M}_y = 0$) and μ_y with $\bar{M}_{x^+} = \bar{M}_{x^-} = 0$ (i.e., $\bar{M}_x = 0$) can be determined as discussed in the following section.

3.6.1 Determination of Propagation Constants

To determine the propagation constants, receptance method is used. In case of the propagation constant μ_x with $\bar{M}_y = 0$, equation (3.31b) reduces to

$$\bar{M}_B = \bar{M}_{Bx} \sin(\tfrac{1}{2}\Omega\tau) = \bar{M}_{Ax} e^{\mu_x} \sin(\tfrac{1}{2}\Omega\tau) \qquad (3.39)$$

It should be noted that due to coupled differential equations (3.15), receptance β_{ij}, in general, will be of form

$$\beta_{ij} = \beta^x_{ij} \sin(\tfrac{1}{2}\Omega\tau) + \beta^y_{ij} \cos(\tfrac{1}{2}\Omega\tau)$$

where β^x_{ij} and $\beta_{ij}{}^y$ are the sine and the cosine components of the slope at end i due to a non-dimensional unit harmonic moment $\sin(\frac{1}{2}\Omega\tau)$ at end j.

Expressing slopes in equation (3.31a) in terms of the moments $\bar{M}_{Ax}$ and $\bar{M}_{Bx}$ through the receptances, one gets

$$(\beta^x_{BA}\,\bar{M}_{Ax} + \beta^x_{BB}\,\bar{M}_{Bx}) \sin(\tfrac{1}{2}\Omega\tau) + (\beta^y_{BA}\,\bar{M}_{Ax} + \beta^y_{BB}\,\bar{M}_{Bx}) \cos(\tfrac{1}{2}\Omega\tau)$$

$$= e^{\mu_x} \{\beta^x_{AA}\,\bar{M}_{Ax} + \beta^x_{AB}\,\bar{M}_{Bx}) \sin(\tfrac{1}{2}\Omega\tau) + e^{\mu_y} (\beta^y_{AA}\,\bar{M}_{Ax} + \beta^y_{AB}\,\bar{M}_{Bx}) \cos(\tfrac{1}{2}\Omega\tau) \qquad (3.40)$$

Substituting equation (3.39) into equation (3.40) and equating the coefficients of the terms $\sin(\frac{1}{2}\Omega\tau)$ and $\cos(\frac{1}{2}\Omega\tau)$ from both sides of the resulting equation, one gets

$$\beta^x_{AB} e^{2\mu_x} + (\beta^x_{AA} - \beta^x_{BB}) e^{\mu_x} - \beta^x_{BA} = 0 \qquad (3.41a)$$

$$\beta^{y}_{AB}\, e^{\mu_x + \mu_y} + (\beta^{y}_{AA}\, e^{\mu_y} - \beta^{y}_{BB}\, e^{\mu_x}) - \beta^{y}_{BA} = 0 \qquad (3.41b)$$

From equation (3.41a), two values of μ_x (with $\bar{M}_y = 0$) are obtained, one for the positive going wave and the other for the negative going wave. Equation (3.41b) gives the value of μ_y which is of no use for the present computation, as we need to calculate the values of μ_y with $\bar{M}_x = 0$. The receptances to be used in equations (3.41) are determined in the manner discussed below.

To determine the receptances β_{AA} and β_{BA}, apply a non-dimensional unit harmonic moment $\sin(\frac{1}{2}\Omega\tau)$ at the end A of the span AB (Figure A-1.1). Solutions for equations (3.15) are now given by equations (3.19), with the following boundary conditions:

$$\begin{aligned}
&\bar{X}_1(0) = 0, && \bar{Y}_1(0) = 0 \quad , \\
&\bar{X}_1(1) = 0, && \bar{Y}_1(1) = 0 \quad , \\
&-X_1''(0) = 1, && -\bar{Y}_1''(0) = 0 \quad , \\
&-X_1''(1) = 0, && -Y_1''(1) = 0 \quad .
\end{aligned} \qquad (3.42)$$

Use of equation (3.19) into equations (3.42) yields the following system of equations

$$ZC = T_1 \qquad (3.43)$$

where $Z=$

$$\begin{vmatrix} 1 & 1 & 1 & \cdots & 1 \\ e^{\lambda_1} & e^{\lambda_2} & e^{\lambda_3} & \cdots & e^{\lambda_8} \\ -\lambda_1^2 & -\lambda_2^2 & -\lambda_3^2 & \cdots & -\lambda_8^2 \\ -\lambda_1^2 e^{\lambda_1} & -\lambda_2^2 e^{\lambda_2} & -\lambda_3^2 e^{\lambda_3} & \cdots & -\lambda_8^2 e^{\lambda_8} \\ t_1 & t_2 & t_3 & \cdots & t_8 \\ t_1 e^{\lambda_1} & t_e e^{\lambda_2} & t_3 e^{\lambda_3} & & t_8 e^{\lambda_8} \\ -\lambda_1^2 t_1 & -\lambda_2^2 t_2 & -\lambda_3^2 t_3 & \cdots & -\lambda_8^2 t_8 \\ -\lambda_1^2 t_1 e^{\lambda_1} & -\lambda_2^2 t_2 e^{\lambda_2} & -\lambda_3^2 t_3 e^{\lambda_3} & \cdots & -\lambda_8^2 t_8 e^{\lambda_8} \end{vmatrix},$$

$$t_n = \frac{\lambda_n^4 + (u_o^2 + \gamma + \frac{u_o^2\delta^2}{2} - u_o^2\delta)\,\lambda_n^2 - \frac{\Omega^2}{4}}{\beta u_o \Omega \lambda_n}, \quad n=1,2,\ldots 8,$$

$$C = \{C_{11} \quad C_{12} \quad C_{13} \quad C_{14} \quad C_{15} \quad C_{16} \quad C_{17} \quad C_{18}\}^t,$$

$$T_1 = \{0 \quad 0 \quad 1 \quad 0 \quad 0 \quad 0 \quad 0 \quad 0\}^t,$$

and t denotes the transpose

Knowing C_{1n}'s from equation (3.43), C_{2n}'s can be determined using equation (3.22). The receptances β_{AA} and β_{BA} can be expressed as

$$\beta_{AA} = \beta_{AA}^x \sin(\tfrac{1}{2}\Omega\tau) + \beta_{AA}^y \cos(\tfrac{1}{2}\Omega\tau), \tag{3.44a}$$

and

$$\beta_{BA} = \beta_{BA}^x \sin(\tfrac{1}{2}\Omega\tau) + \beta_{BA}^y \cos(\tfrac{1}{2}\Omega\tau), \tag{3.44b}$$

where $\beta^{x}_{AA} = \bar{X}'_1(0) = \sum_{n=1}^{8} C_{1n}\lambda_n$,

$\beta^{y}_{AA} = \bar{Y}'_1(0) = \sum_{n=1}^{8} C_{2n}\lambda_n$,

$\beta^{x}_{BA} = \bar{X}'_1(1) = \sum_{n=1}^{8} C_{1n}\lambda_n e^{\lambda_n}$,

and $\beta^{y}_{BA} = \bar{Y}'_1(1) = \sum_{n=1}^{8} C_{2n}\lambda_n e^{\lambda_n}$.

To calculate the receptances β_{AB} and β_{BB}, apply a non-dimensional unit harmonic moment $\sin(\frac{1}{2}\Omega\tau)$ at the end B of the span AB. The system of equations obtained in this case is

$$ZC = T'_1 , \tag{3.45}$$

where $T'_1 = \{0 \quad 0 \quad 0 \quad 1 \quad 0 \quad 0 \quad 0 \quad 0\}^{t}$,

and t denotes the transponse.

The receptances β_{AB} and β_{BA} can be written as

$$\beta_{AB} = \beta^{x}_{AB}\sin(\tfrac{1}{2}\Omega\tau) + \beta^{y}_{AB}\cos(\tfrac{1}{2}\Omega\tau), \tag{3.46a}$$

$$\beta_{BB} = \beta^{x}_{BB}\sin(\tfrac{1}{2}\Omega\tau) + \beta^{y}_{BB}\cos(\tfrac{1}{2}\Omega\tau), \tag{3.46b}$$

where $\beta^{x}_{AB} = \bar{X}'_1(0) = \sum_{n=1}^{8} C_{1n}\lambda_n$,

$\beta^{y}_{AB} = \bar{Y}'_1(0) = \sum_{n=1}^{8} C_{2n}\lambda_n$,

$\beta^{x}_{BB} = \bar{X}'_1(1) = \sum_{n=1}^{8} C_{1n}\lambda_n e^{\lambda_n}$,

$\beta^{y}_{BB} = \bar{Y}'_1(1) = \sum_{n=1}^{8} C_{2n}\lambda_n e^{\lambda_n}$,

and the C_{1n}'s are solutions of equation (3.45) with the C_{2n}'s obtained by using equation (3.22).

In case of determining μ_y with $\bar{M}_x = 0$, equation (3.31b) reduces to

$$\bar{M}_B = \bar{M}_{By} \cos(\tfrac{1}{2}\Omega\tau) = \bar{M}_{Ay} e^{\mu_y} \cos(\tfrac{1}{2}\Omega\tau) \qquad (3.47)$$

The slopes in equation (3.31a) are expressed in term of the moments $\bar{M}_{By}$ and $\bar{M}_{Ay}$ through the receptances (now to be obtained with a non-dimensional unit harmonic moment $\cos(\frac{1}{2}\Omega\tau)$). Then, equation analogous to equation (3.41a) is obtained as

$$\beta^y_{AB} e^{2\mu_y} + (\beta^y_{AA} - \beta^y_{BB}) e^{\mu_y} - \beta^y_{BA} = 0 \qquad (3.48)$$

While calculating the receptances with a non-dimensional unit harmonic moment $\cos(\frac{1}{2}\Omega\tau)$, vector T_1 in equation (3.43) and T_1' in equation (3.45) will be

$$T_1 = \{0 \quad 0 \quad 0 \quad 0 \quad 0 \quad 1 \quad 0 \quad 0\}^t ,$$

and $$T_1' = \{0 \quad 0 \quad 0 \quad 0 \quad 0 \quad 0 \quad 0 \quad 1\}^t ,$$

respectively.

Now, to determine the regions of secondary instability, using equation (3.23), the displacement of the pipe in any bay, $\bar{y}_1$, is written as

$$\bar{y}_1 = \bar{Y}_o + \bar{X}_2 \sin(\Omega\tau) + \bar{Y}_2 \cos(\Omega\tau) \qquad (3.49)$$

Proceeding similarly as in the case of primary instabilities, equations analogous to equations (3.41a) and (3.48) can again be obtained for propagation constants. The unit harmonic moments to be used, for calculating the receptances, in this case will be $\sin(\Omega\tau)$ and $\cos(\Omega\tau)$ instead of $\sin(\frac{1}{2}\Omega\tau)$ and $\cos(\frac{1}{2}\Omega\tau)$, respectively.

3.7 Effect of Neglecting Mass Ratio Parameter

If the terms with mass ratio parameter, β, are neglected in equation (3.2), all the methods for determining the instability regions are simplified considerably. The modified equations, when the terms with β are neglected, can be obtained by letting $\beta = 0$ in the analyses presented. It should be noted, however, that $m_r = 0$ is not implied by letting β equal to zero.

In the analysis of the first method, if β is set to zero, then for $K = 1$ approximation, equation (3.10) reduces to the following form

$$D_{11}\, D_{22} = 0$$

Hence, the boundaries of the primary instability regions can be determined from the equations

$$D_{11} = -\frac{\Omega^2}{4}[I] + [S] + (u_o^2 + \gamma + \frac{u_o^2\delta^2}{2} - u_o^2\,\delta)[R] = 0, \qquad (3.50a)$$

and

$$D_{22} = -\frac{\Omega^2}{4}[I] + [S] + (u_o^2 + \gamma + \frac{u_o^2\delta^2}{2} + u_o^2\,\delta)[R] = 0. \qquad (3.50b)$$

Equation (3.12), giving the secondary instability regions for $K = 2$ approximation, reduces to

$$D_{22} \begin{vmatrix} D_{11} & D_{13} \\ D_{31} & D_{33} \end{vmatrix} = 0$$

Hence, $D_{22} = 0$, and

$$\begin{vmatrix} D_{11} & D_{13} \\ D_{31} & D_{33} \end{vmatrix} = 0 \ ,$$

give the boundaries of the secondary instability regions.

In the analysis of the second method, discussed in section (3.5), if β is neglected, then equations (3.15) reduce to the following forms:

$$\frac{d^4\bar{X}_1}{d\xi^4} + (u_o^2 + \gamma + \frac{u_o^2\delta^2}{2} - u_o^2\delta) \frac{d^2\bar{X}_1}{d\xi^2} - \frac{\Omega^2}{4} = 0 \qquad (3.51a)$$

$$\frac{d^4\bar{Y}_1}{d\xi^4} + (u_o^2 + \gamma + \frac{u_o^2\delta^2}{2} + u_o^2\delta) \frac{d^2\bar{Y}_1}{d\xi^2} - \frac{\Omega^2}{4} = 0 \qquad (3.51b)$$

Thus, we get uncoupled differential equations for $\bar{X}_1$ and $\bar{Y}_1$. The solutions for equation (3.51) can be written as

$$\bar{X}_1 = \sum_{n=1}^{4} C_{1n} e^{\lambda_{1n}\xi} \ , \qquad (3.52a)$$

$$\bar{Y}_1 = \sum_{n=1}^{4} C_{2n} e^{\lambda_{2n}\xi} \ , \qquad (3.52b)$$

where λ_{1n}'s and λ_{2n}'s are the roots of the polynomial

$$\lambda^4 + (u_o^2 + \gamma + \frac{u_o^2\delta^2}{2} - u_o^2\delta)\,\lambda^2 - \frac{\Omega^2}{4} = 0 \quad ,$$

$$\lambda^4 + (u_o^2 + \gamma + \frac{u_o^2\delta^2}{2} + u_o^2\delta)\,\lambda^2 - \frac{\Omega^2}{4} = 0 \quad ,$$

respectively. The constants C_{1n} and C_{2n} can be determined using the boundary conditions given by equations (3.21). Substitution of equations (3.52) in the boundary conditions and for non-trivial solution of C_{1n}'s (and C_{2n}'s), the determinant of the coefficients of the resulting equation is equated to zero. In this case, we get two determinants, each of size 4N, zeros of which give the boundaries of the primary instability regions.

For the secondary instabilities, if β is neglected, equations (3.24) reduce to the following forms:

$$\frac{d^4\bar{X}_2}{d\xi^4} + (u_o^2 + \gamma + \frac{u_o^2\delta^2}{2})\,\frac{d^2\bar{X}_2}{d\xi^2} - \Omega^2\bar{X}_2 = 0 \qquad (3.53a)$$

$$\frac{d^4\bar{Y}_o}{d\xi^4} + (u_o^2 + \gamma + \frac{u_o^2\delta^2}{2})\,\frac{d^2\bar{Y}_o}{d\xi^2} + u_o^2\delta\,\frac{d\bar{Y}_2}{d\xi} = 0 \qquad (3.53b)$$

$$\frac{d^4\bar{Y}_2}{d\xi^4} + (u_o^2 + \gamma + \frac{u_o^2\delta^2}{2})\,\frac{d^2\bar{Y}_2}{d\xi^2} - \Omega^2\bar{Y}_2 + 2u_o^2\delta\,\frac{d\bar{Y}_o}{d\xi} = 0 \qquad (3.53c)$$

One boundary of the instability regions is obtained from the solution of equation (3.53a) and the other from the solution of coupled differential equations (3.53b) and (3.53c). Solutions for equations (3.53) can be written as

$$\bar{X}_2 = \sum_{j=1}^{4} C_{1n} \, e^{\lambda_{1j}\xi} \, ,$$

$$\bar{Y}_o = \sum_{j=1}^{6} C_{oj} \, e^{\lambda_{2j}\xi} + C_{o7} + C_{o8}\,\xi \, ,$$

and $$\bar{Y}_2 = \sum_{j=1}^{6} C_{2j} \, e^{\lambda_{2j}\xi} \, ,$$

where λ_{1n}'s are the roots of the polynomial

$$\lambda^4 + (u_o^2 + \gamma + \frac{u_o^2\delta^2}{2}) \; \lambda^2 - \Omega^2 = 0$$

and λ_{2j}'s are the roots of the polynomial

$$\begin{vmatrix} \lambda^2 + (u^2 + \gamma + \frac{u_o^2\delta^2}{2}) & u_o^2\delta \\ 2u_o^2\delta & \lambda^4 + (u_o^2 + \gamma + \frac{u_o^2\delta^2}{2}) \; \lambda^2 - \Omega^2 \end{vmatrix} = 0$$

Coefficients C_{1n}'s, C_{on}'s and C_{2n}'s can be determined using the boundary conditions of an N-span pipe. Proceeding similarly as in section 3.5, two determinants are obtained in this case. The zeros of these determinants give the boundaries of the secondary instability regions.

If β is neglected, the wave approach for the determination of natural frequencies developed in section 2.3 can be used directly. With $\beta = 0$, one gets uncoupled differential equations for $\bar{X}_1$ and $\bar{Y}_1$. One boundary of the instability regions is obtained by solving

for $\bar{X}_1$ and the other is obtained from the solution of $\bar{Y}_1$. As in Chapter 2, assume the solutions for $\bar{X}_1$ and $\bar{Y}_1$ of the form:

$$\bar{X}_1 = \sum_{n=1}^{4} C_{1n} e^{i\lambda_{1n}\xi} ,$$

$$\bar{Y}_1 = \sum_{n=1}^{4} C_{2n} e^{i\lambda_{2n}\xi} ,$$

where the λ_{1n}'s and the λ_{2n}'s are the roots of the polynomial

$$\lambda^4 - (u_o^2 + \gamma + \frac{u_o^2\delta^2}{2} - u_o^2\delta)\lambda^2 - \frac{\Omega^2}{4} = 0 , \qquad (3.54a)$$

and $$\lambda^4 - (u_o^2 + \gamma + \frac{u_o^2\delta^2}{2} + u_o^2\delta)\lambda^2 - \frac{\Omega^2}{4} = 0 , \qquad (3.54b)$$

respectively. Using equation (3.54a) instead of equation (A-1.5), propagation constants can be determined following the method outlined in section 2.2.1. From these propagation constants, natural frequencies can be obtained using the graphical method discussed in section 2.3. These frequencies give one of the boundaries of the instability region. Similarly, the other boundary can be obtained by using equation (3.54b) instead of equation (3.54a).

For the secondary instability also, one of the boundaries can be obtained in the manner described in the case of primary instability. only equation (3.53a) has to be used instead of equation (3.51). The other boundary is obtained from the solution of coupled differential equations (3.53b) and (3.53c). The method developed in section 3.6

has to be used to determine this boundary. It should be noted, however, that in the present case, the order of the characteristic polynomial equation for λ's is reduced to only 6 (from 10 in section 3.6). This reduces the computational time considerably.

3.8 Effect of Damping

If the damping in the pipe is included, equation (3.4) can be written as

$$(1+\alpha \frac{\partial}{\partial \tau}) \frac{\partial^4 \bar{y}}{\partial \xi^4} + \{u_o^2(1+\delta \cos\Omega\tau)^2+\gamma\}\frac{\partial^2 \bar{y}}{\partial \xi^2} + 2\beta u_o(1+\delta \cos\Omega\tau)\frac{\partial^2 \bar{y}}{\partial \xi \partial \tau}$$

$$- \beta\, u_o \delta\Omega \sin\Omega\tau \frac{\partial \bar{y}}{\partial \xi} + \eta_c \frac{\partial \bar{y}}{\partial \tau} + \frac{\partial^2 \bar{y}}{\partial \tau^2} = 0 \qquad (3.55)$$

where $\alpha = \{\frac{I}{E(m_f+m_p)}\}^{1/2} \frac{E^*}{\ell^2}$,

$$\eta_c = \frac{C_o \ell^2}{\{(m_f+m_p)EI\}^{1/2}} ,$$

E^* is the loss modulus of the pipe material, and C_o is the viscous damping on the motion of the pipe.

In the following analysis, hysteretic type damping has been considered, i.e., $\alpha\Omega = \frac{E^*\omega}{E}$ is replaced by η_b, where η_b is called the loss factor of the pipe material.

The regions of parametric instabilities of equation (3.55) can be found out by determining the periodic solutions of period 2T and T. All the three methods discussed earlier can be used to compute these regions. The changes necessary in the formulations described earlier for undamped case, are given below. Rest of the procedures remain same.

If the first method is used, then the terms D_{12} and D_{21} in equation (3.10), giving the regions of primary instability, become

$$D_{12} = -\frac{1}{2}\,\eta_b\,[S] - \frac{1}{2}\,\eta_c\Omega\,[I] - \beta\,u_o\,\Omega\,[P]\,,$$

and $$D_{21} = \frac{1}{2}\,\eta_b\,[S] + \frac{1}{2}\,\eta_c\Omega\,[I] + \beta\,u_o\,\Omega\,[P]\,,$$

respectively.

For the regions of secondary instability, inclusion of damping changes the terms in equation (3.12) as follows :

$$D_{23} = -\eta_b\,[S] - 2\beta\,u_o\,\delta\Omega\,[P] - \eta_c\,\Omega\,[I]\,,$$

$$D_{32} = \eta_b\,[S] + 2\beta\,u_o\,\delta\Omega\,[P] + \eta_c\,\Omega\,[I]\,,$$

and the other terms remaining same as defined after equation (3.12).

In the second method, inclusion of damping terms changes equations (3.15) (for the primary instability) as follows :

$$\frac{d^4\bar{X}_1}{d\xi^4} + \left(u_o^2 + \gamma + \frac{u_o^2\,\delta^2}{2} - u_o^2\,\delta\right)\frac{d^2\bar{X}_1}{d\xi^2} - \frac{\Omega^2}{4}\,\bar{X}_1 - \frac{1}{2}\,\eta_b\,\frac{d^4\bar{Y}_1}{d\xi^4} - \beta\,u_o\,\Omega\,\frac{d\bar{Y}_1}{d\xi}$$

$$- \frac{1}{2}\,\eta_c\,\Omega\,\bar{Y}_1 = 0 \qquad (3.56a)$$

$$\frac{d^4\bar{Y}_1}{d\xi^4} + \left(u_o^2 + \gamma + \frac{u_o^2\,\delta^2}{2} + u_o^2\,\delta\right)\frac{d^2\bar{Y}_1}{d\xi^2} - \frac{\Omega^2}{4}\,\bar{Y}_1 + \frac{1}{2}\,\eta_b\,\frac{d^4\bar{X}_1}{d\xi^4} + \beta\,u_o\,\Omega\,\frac{d\bar{X}_1}{d\xi}$$

$$+ \frac{1}{2}\,\eta_c\,\Omega\,\bar{X}_1 = 0 \qquad (3.56b)$$

Solutions for equations (3.56) can be determined as discussed in section 3.5 . The characteristic polynomial given by equation (3.18)

now becomes

$$\begin{vmatrix} \lambda^4+(u_o^2+\gamma+\frac{u_o^2\delta^2}{2}-u_o^2\delta)\lambda^2-\frac{\Omega^2}{4} & -\frac{1}{2}\eta_b\lambda^4-\beta u\Omega\lambda-\frac{1}{2}\eta_c\Omega \\ \frac{1}{2}\eta_b\lambda^4+\beta u\Omega\lambda+\frac{1}{2}\eta_c\Omega & \lambda^4+(u_o^2+\gamma+\frac{u_o^2\delta^2}{2}+u_o^2\delta)\lambda^2-\frac{\Omega^2}{4} \end{vmatrix} = 0 \qquad (3.57)$$

For the regions of the secondary instability, equations (3.24) reduce to the following forms :

$$\frac{d^4\bar{Y}_o}{d\xi^4}+(u_o^2+\gamma+\frac{u_o^2\delta^2}{2})\frac{d^2\bar{Y}_o}{d\xi^2}+u_o^2\delta\frac{d^2\bar{Y}_2}{d\xi^2}+\frac{1}{2}\beta u_o\delta\Omega\frac{d\bar{X}_2}{d\xi}=0\ , \qquad (3.58a)$$

$$\frac{d^4\bar{X}_2}{d\xi^4}+(u_o^2+\gamma+\frac{u_o^2\delta^2}{2})\frac{d^2\bar{X}_2}{d\xi^2}-\Omega^2\bar{X}_2-\eta_b\frac{d^4\bar{Y}_2}{d\xi^4}-2\beta u_o\Omega\frac{d\bar{Y}_2}{d\xi}-\eta_c\Omega\bar{Y}_2$$
$$-\beta u_o\delta\Omega\frac{d\bar{Y}_o}{d\xi}=0, \qquad (3.58b)$$

$$\frac{d^4\bar{Y}_2}{d\xi^4}+(u_o^2+\gamma+\frac{u_o^2\delta^2}{2})\frac{d^2\bar{Y}_2}{d\xi^2}-\Omega^2\bar{Y}_2+\eta_b\frac{d^4\bar{X}_2}{d\xi^4}+2\beta u_o\Omega\frac{d\bar{X}_2}{d\xi}+\eta_c\Omega\bar{X}_2$$
$$+2u_o^2\delta\frac{d\bar{Y}_o}{d\xi}=0. \qquad (3.58c)$$

Solutions for equations (3.58) can be obtained as discussed earlier by changing the characteristic polynomial, given by equation (3.27), to

$$\begin{vmatrix} \lambda^4+(u_o^2+\gamma+\frac{u_o^2\delta^2}{2})\lambda^2 & \frac{1}{2}\beta u_o\delta\Omega\lambda & u_o^2\delta\lambda^2 \\ -\beta u_o\delta\Omega\lambda & \lambda^4+(u_o^2+\gamma+\frac{u_o^2\delta^2}{2})\lambda^2-\Omega^2 & -\eta_b\lambda^4-2\beta u_o\Omega\lambda-\eta_c\Omega \\ 2u_o^2\delta\lambda & \eta_b\lambda^4+2\beta u_o\Omega\lambda+\eta_c\Omega & \lambda^4+(u_o^2+\gamma+\frac{u_o^2\delta^2}{2})\lambda^2-\Omega^2 \end{vmatrix} = 0 \quad (3.59)$$

The third method discussed in section 3.6 , can be used as such when damping is present. The only difference being that the λ's for the primary instabilities are to be calculated by using equation (3.57) and for the secondary instabilities by using equation (3.59).

3.9 Results and Discussions

3.9.1 Computations Performed

Using the analyses presented in the previous sections, the following computations have been performed. The regions of the primary and the secondary instabilities associated with the first two modes of a two span pipe are determined. The instability regions have been presented as plots of the non-dimensional frequency, Ω versus the excitation parameter, δ. Values of δ upto 0.5 have been considered in all the cases.

(i) The regions of instability have been obtained with $u_o = 2$, $\gamma = 2$ and $\beta = 0.5$. All the three methods have been used for the purpose of comparison and cross checking.

(ii) The effect of the mass ratio parameter, β , has been studied by taking various values of β like 0.2, 0.6, and 0.8. The other parameters being $u_o = 2$, and $\gamma = 2$.

(iii) Results have also been obtained by neglecting β altogether for $u_o = 2$, and $\gamma = 2$. These results are then compared with those obtained by taking $\beta = 0.5$, other parameters remaining the same.

(iv) To study the effect of the constant mean fluid velocity on the regions of instabilities, results have been computed with $u_o = 0.5$, 1.0, 2.0, and 2.5. The other parameters being $\gamma = 2$, and $\beta = 0.5$.

(v) The effect of the fluid pressure has been studied with values of $\gamma = 0, 1, 2$, and 4 while maintaining other parameters unchanged.

(vi) To study the effect of damping on the regions of instabilities, computations have been carried out by taking viscous damping parameter, $\eta_c = 0.2$, 0.5, and 0.75. The other parameters being $u_o = 2$, $\gamma = 2$, and $\beta = 0$. The results have also been obtained for various values of the hysteretic damping, η_b.

The results mentioned in paragraphs (ii) - (v) have been obtained by using the wave approach outlined in section 3.6. However, to study the effect of damping, numerical results have been obtained using all the three methods.

3.9.2 Comparison of the Methods

The regions of the primary and the secondary instabilities associated with the first two modes of a two span pipe have been computed using all the three methods discussed in section 3.4, 3.5, and 3.6, respectively.

For the first method, equation (3.10) has been used to obtain the regions of the primary instability. The comparison functions ϕ_r's used

to evaluate the matrices P, S, R are the normalised mode shapes of a two span beam. Regions of the secondary instability have been obtained by using equation (3.12). Six mode approximation was found to be sufficient for the instability regions associated with the first two modes.

To get the results by the second method, procedure discussed in section 3.5 has been used.

While using the third method, the propagation constant μ_x with $\bar{M}_y = 0$, is determined using equation (3.41a). Thereafter, natural frequencies are obtained by using the graphical approach. These frequencies give one of the boundaries of the instability regions. Similarly, the other boundary is obtained by determining the propagation constant μ_y with $\bar{M}_x = 0$. The regions of secondary instabilities have also been obtained as discussed in section 3.6. For a two span pipe, results for both the modes are obtained from the first propagation band.

It should be noted at this stage, that the natural frequencies of a two span pipe can be classified into two sets. Values in one set, consisting of the odd-numbered natural frequencies are given by the natural frequencies of a single span pinned-pinned pipe. The other set defining the even-numbered natural frequencies consists of the natural frequencies of a single span clamped-pinned pipe (see Section 2.5.3). The determination of the instability regions ultimately reduces to finding the natural frequencies. Hence, all the results for the instability regions of a two span pipe can be obtained from those of a single span pipe with appropriate end conditions. However, this

simple extension from the cases of single span pipes is not possible for all the modes if the number of spans is more than two.

Results obtained by all the three methods have been plotted in Figures 3.1a and 3.1b. The results for the primary instability have also been presented in Table 3.1. It is seen that the results obtained by all the three methods are in excellent agreement with each other.

The relative merits and demerits of each method are discussed below.

The first method, though simple to use, has certain drawbacks. For example, on evaluating the matrix $[P]$, one finds that the diagonal elements p_{11}, p_{22}, etc., are zero. Thus, for one mode approximation, the elements D_{12} and D_{21} in equation (3.10), and the elements D_{12}, D_{21}, D_{23}, and D_{32} in equation (3.12) become zero. This renders equation (3.10) and (3.12) independent of the value of β. Thus, the effect of the Coriolis acceleration in the equation of motion (3.4) is not accounted for. Moreover, it is obvious that parametric instabilities are obtained only in the modes used in approximating the pipe displacement. To use this method, the mode shapes of an N-span beam must be first obtained. Hence, it becomes unwieldy especially for large number of spans in the pipe.

As compared to the first method, the second method requires no previous knowledge of the mode shapes of an N-span beam. Moreover, the instability regions associated with all the modes are obtained simultaneously by determining the zeros of the same determinant. However, the order of this determinant increases with the number of spans in the pipe.

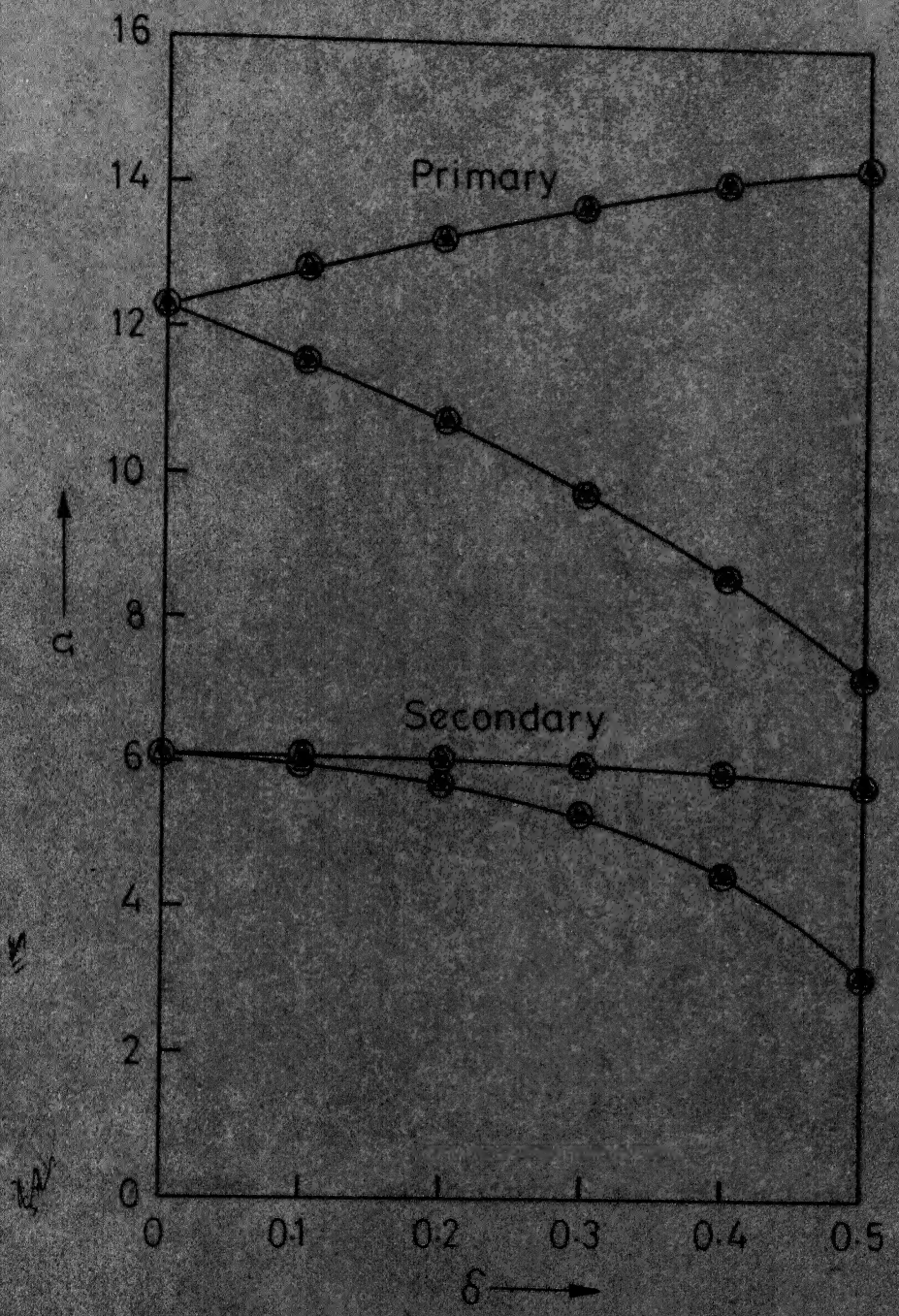

Figure 3.1a-The regions of instabilities associated with the first mode of a two span pipe for $u_0=2$, $\gamma=2$, $\beta=0.5$. Values obtained by the first method, O ; second method, Δ ; third method, .

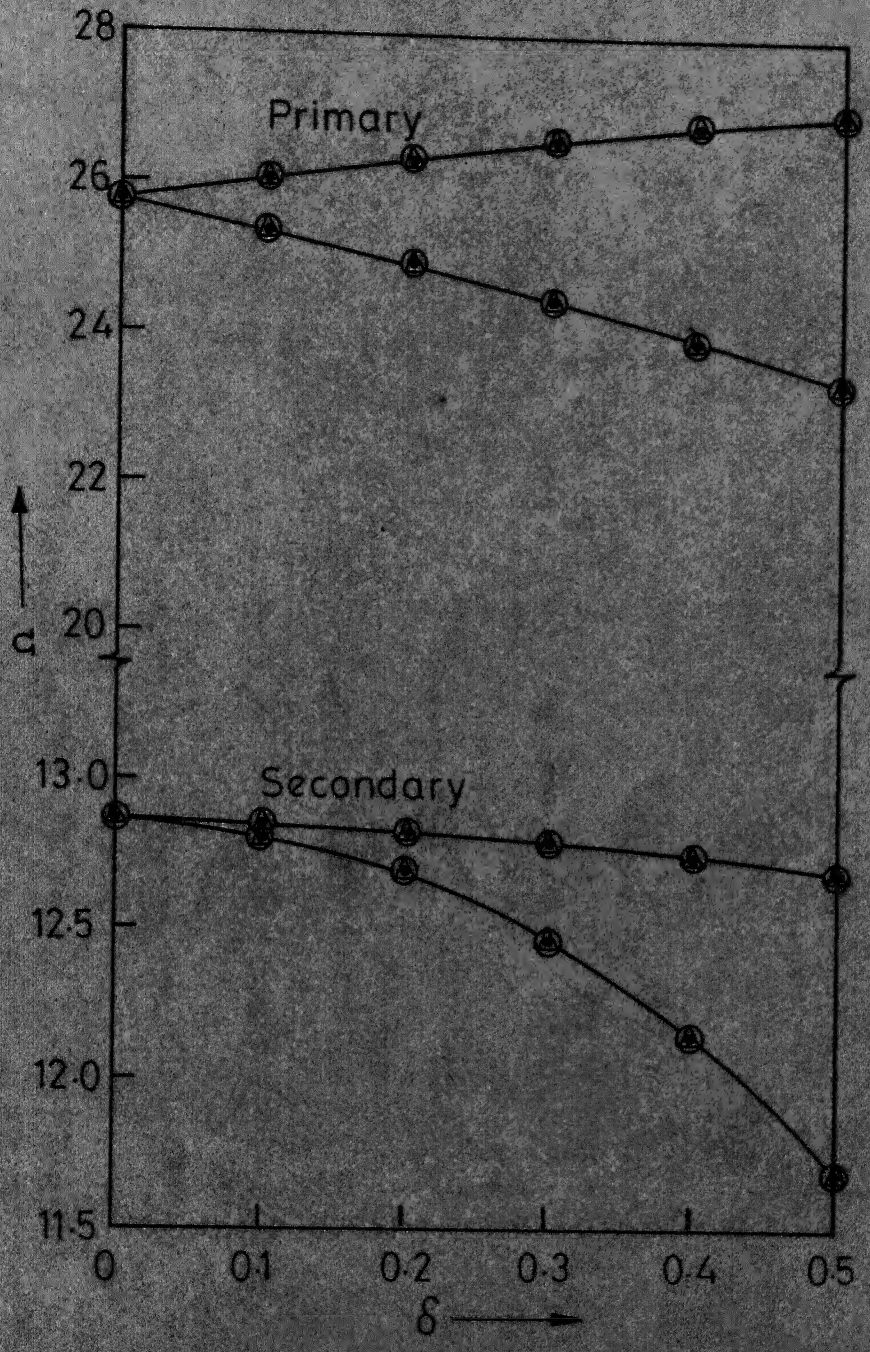

Figure 3.1b-The regions of instabilities associated with the second mode of a two span pipe for $u_0=2$, $\gamma=2$, $\beta=0.5$. Values obtained by the first method, O ; second method, Δ ; third method, • .

TABLE 3.1

Values of frequencies defining the boundaries of the primary instability regions associated with the first two modes of a two span pipe.

$u_o = 2$, $\gamma = 2$, and $\beta = 0.5$

FREQUENCIES Ω

Excitation parameter δ	First Mode						Second Mode					
	First Method		Second Method		Third Method		First Method		Second Method		Third Method	
	Lower	Upper	Lower	Upper	Lower	Upper	Lower	Upper	Lower	Upper	Lower	Upper
0.1	11.55	12.81	11.55	12.82	11.55	12.81	25.32	25.90	25.33	26.06	25.34	26.06
0.2	10.75	13.31	10.74	13.30	10.75	13.31	24.93	25.94	24.93	26.34	24.92	26.33
0.3	9.81	13.73	9.80	13.74	9.81	13.75	24.46	26.61	24.47	26.60	24.45	26.60
0.4	8.68	14.09	8.68	14.10	8.67	14.11	23.95	26.83	23.95	26.82	23.91	26.82
0.5	7.28	14.37	7.28	14.38	7.27	14.37	23.39	27.01	23.38	27.00	23.37	27.00

As compared to the other methods, the third method is most suitable for large number of spans in the pipe. Once the propagation constants are obtained, the instability regions for any number of spans can be obtained by dividing the ranges of μ_x^* and μ_y^* (in the propagation bands) into the same number of equal divisions as the number of spans in the pipe. Thus, in the third method, the amount of computation is independent of the number of spans in the pipe.

3.9.3 Effect of the Mass Ratio Parameter

Figures 3.2a and 3.2b show the regions of the primary instability associated with the first two modes of a two span pipe for various values of the mass ratio parameter, β. It is seen that increase in β slightly shifts the instability regions to lower frequencies. However, the shift reduces with increasing δ. The maximum shift in the regions is approximately within 3% over the range of β given by $0.2 \leq \beta \leq 0.8$.

Figures 3.3a and 3.3b show the regions of the secondary instability associated with the first two modes for various values of β. The effect of variation of β on these regions is same as that on the regions of the primary instability.

As stated in Chapter 2, the negligible effect of β should not, however, be interpreted as negligible effect of the mass of the fluid, m_f. This is because the non-dimensional frequency Ω also contains the term m_f. Thus, the marginal effect of the value of β only signifies that the terms containing β, like the Coriolis term, have little effect on the plots of Ω versus δ.

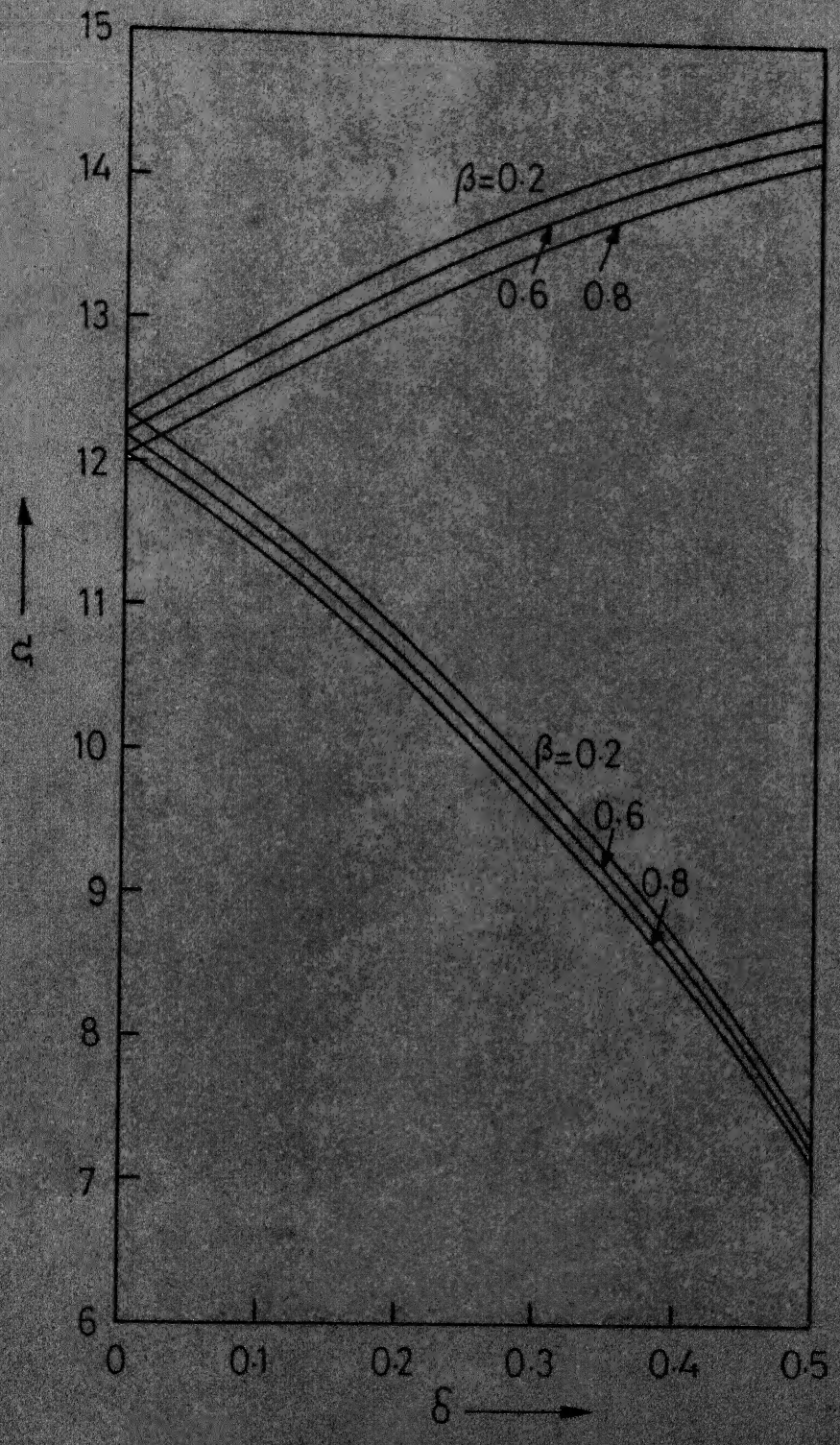

Figure 3·2a–The effect of β on the regions of the primary instability associated with the first mode of a two span pipe. $u_0=2$, $\gamma=2$.

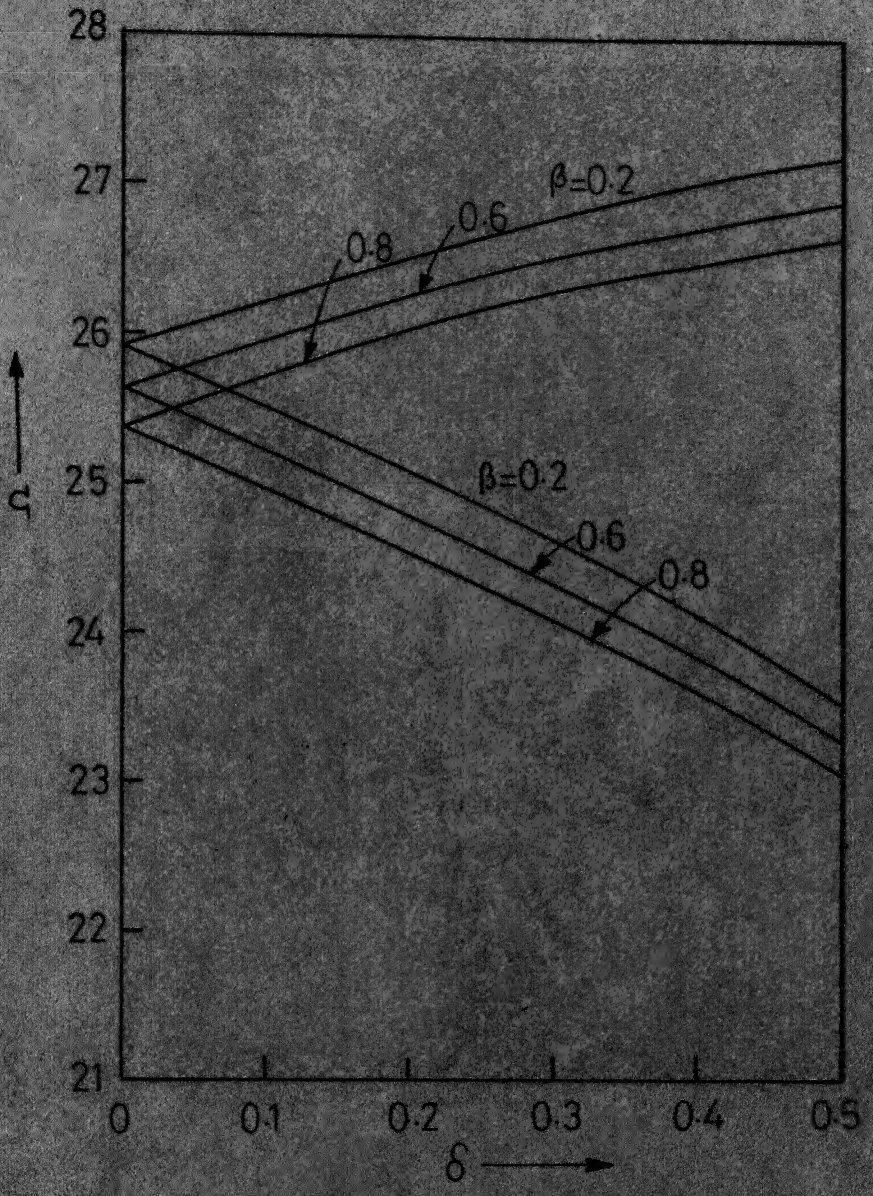

Figure 3.2 b-The effect of β on the regions of the primary instability associated with the second mode of a two span pipe.
$u_0 = 2$, $\gamma = 2$.

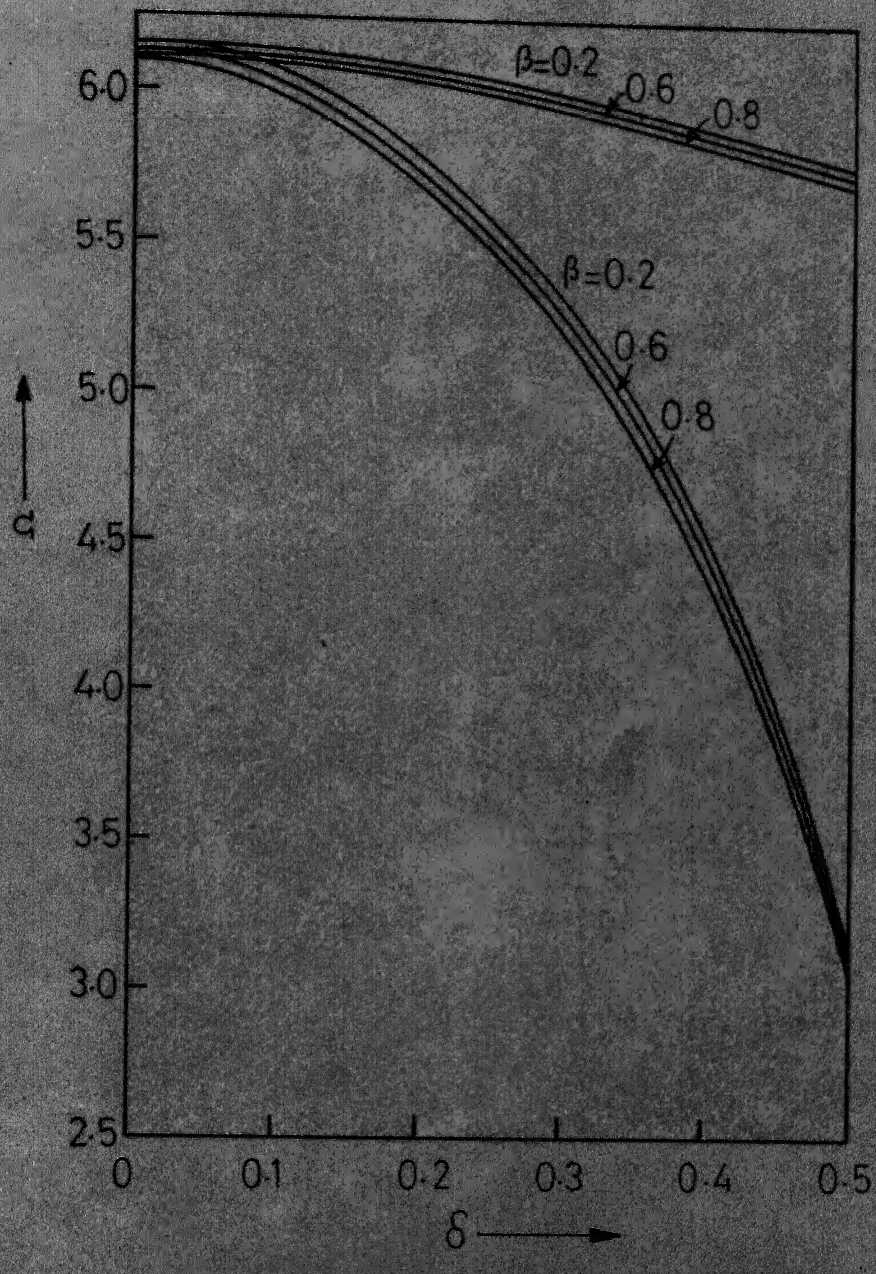

Figure 3.3a- The effect of β on the regions of the secondary instability associated with the first mode of a two span pipe.
$u_0 = 2$, $\gamma = 2$.

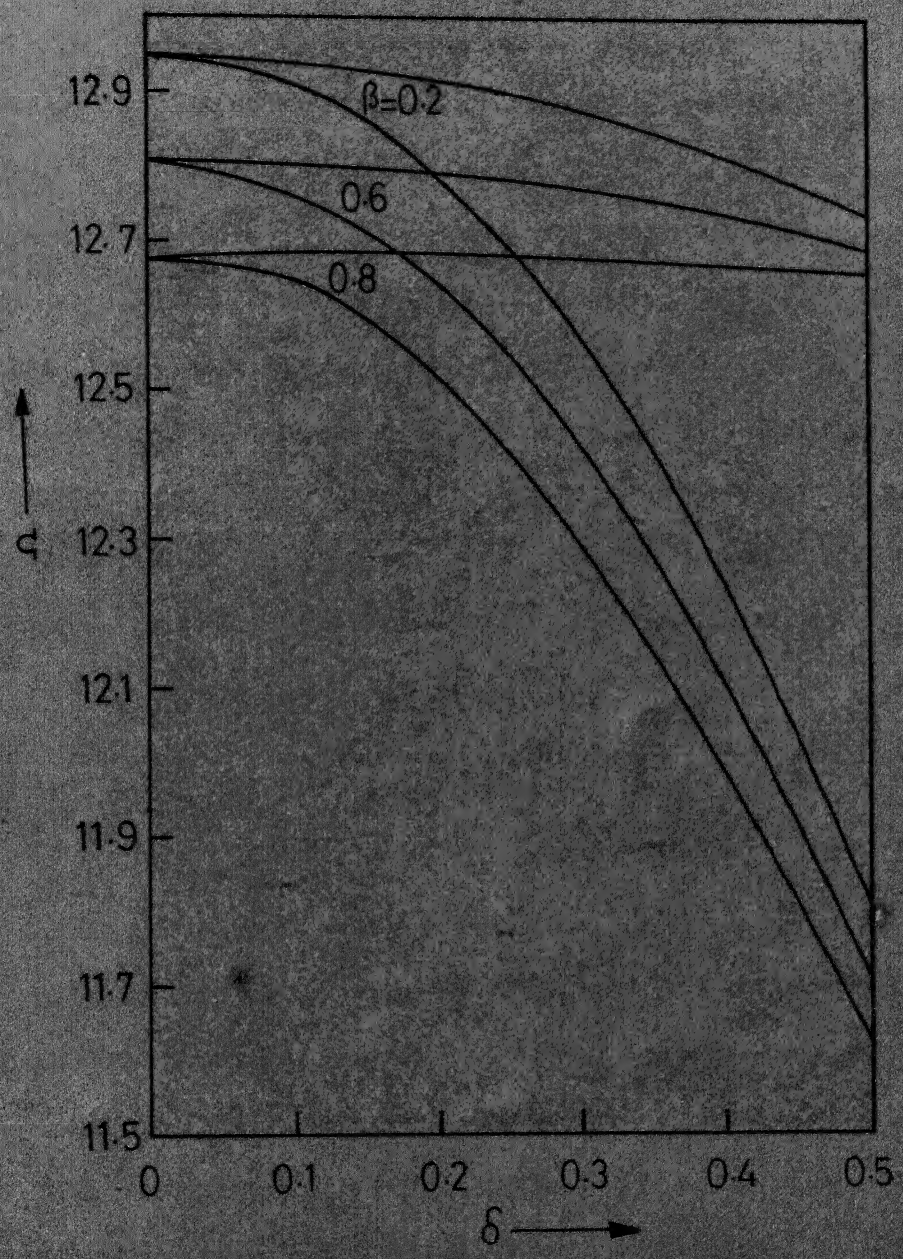

Figure 3.3b -The effect of β on the regions of the secondary instability associated with the second mode of a two span pipe. $u_0=2$, $\gamma=2$.

3.9.4 Effect of Neglecting the Mass Ratio Parameter

To study the effects neglecting β altogether, results have been obtained using the third method discussed in section 3.7. Figure 3.4 shows the regions of instability associated with the first mode of a two span pipe with $u_o = 2$, $\gamma = 2$, and $\beta = 0$. For the purpose of comparison, the same regions obtained with $u_o = 2$, $\gamma = 2$, and $\beta = 0.5$ are also shown in the same figure. It is seen that the results obtained by neglecting β altogether have an accuracy of the order of 98% for the primary instability region. The regions of the secondary instability are not distinguishable for $\beta = 0$ and $\beta = 0.5$. However, as stated already in section 3.7, the computational effort reduces considerably if β is neglected.

3.9.5 Effect of the Constant Mean Velocity

The method discussed in section 3.6 has been used to study the effect of the constant mean velocity, u_o, on the regions of instabilities.

Figure 3.5a shows the effect of u_o on the regions of primary instability associated with the first mode. It is seen that the regions become wider and are shifted to lower frequencies with increasing u_o. For large value of u_o, the instability region may even start with zero frequency if the excitation parameter is sufficiently high. This implies that with these combinations of u_o and δ, the equivalent axial load (represented by the coefficient of the term $\frac{d^2\bar{Y}_1}{d\xi^2}$ in equation (3.15b)) is more than the critical load required for buckling.

Figure 3.5b shows the effect of u_o on the regions of primary instability associated with the second mode. The effect is seen to be

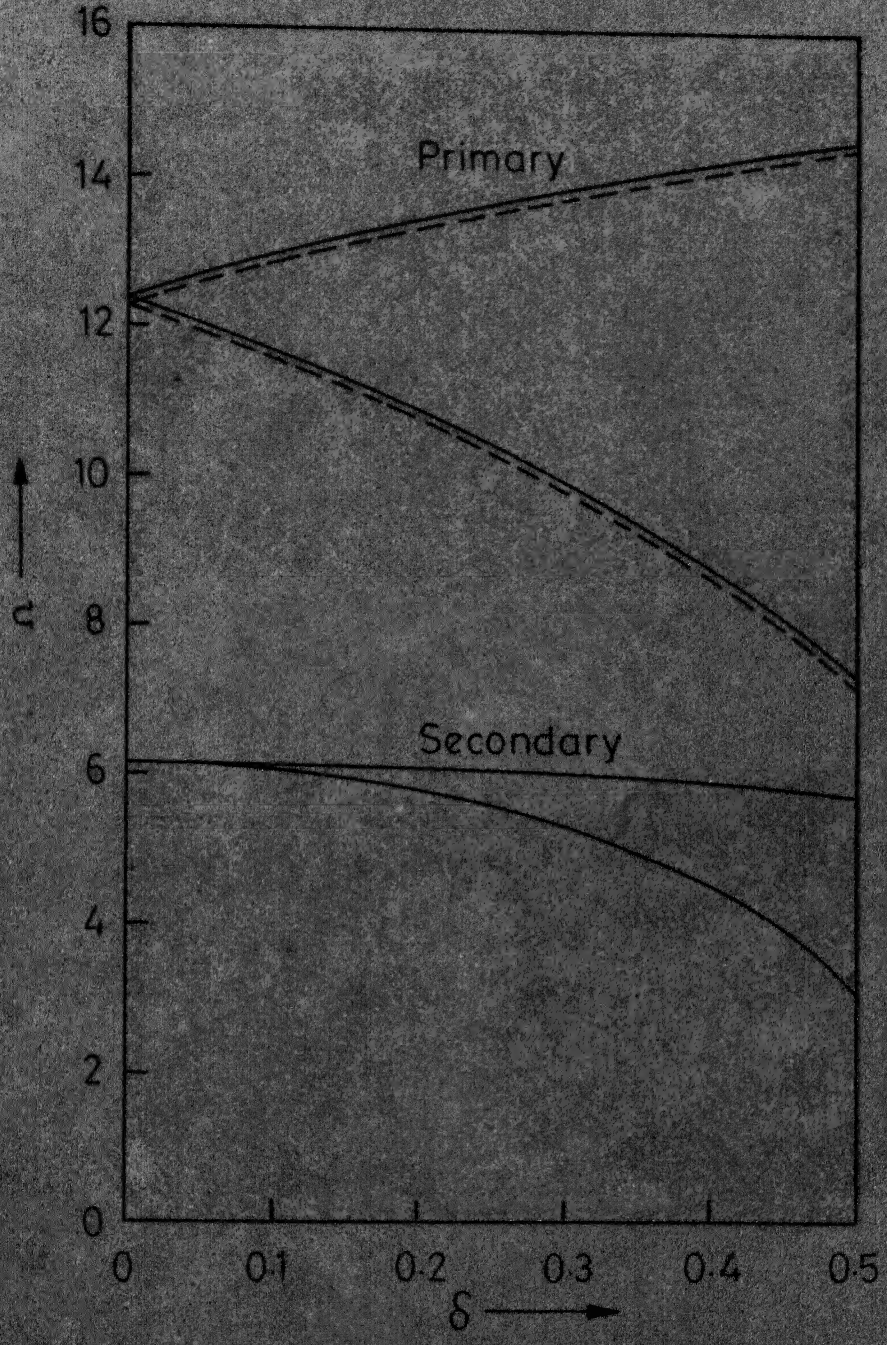

Figure 3.4 - The effect of neglecting β on the regions of instabilities associated with the first mode of a two span. ——, $\beta = 0$;
– – – –, $\beta = 0.5$.
$u_0 = 2$, $\gamma = 2.0$

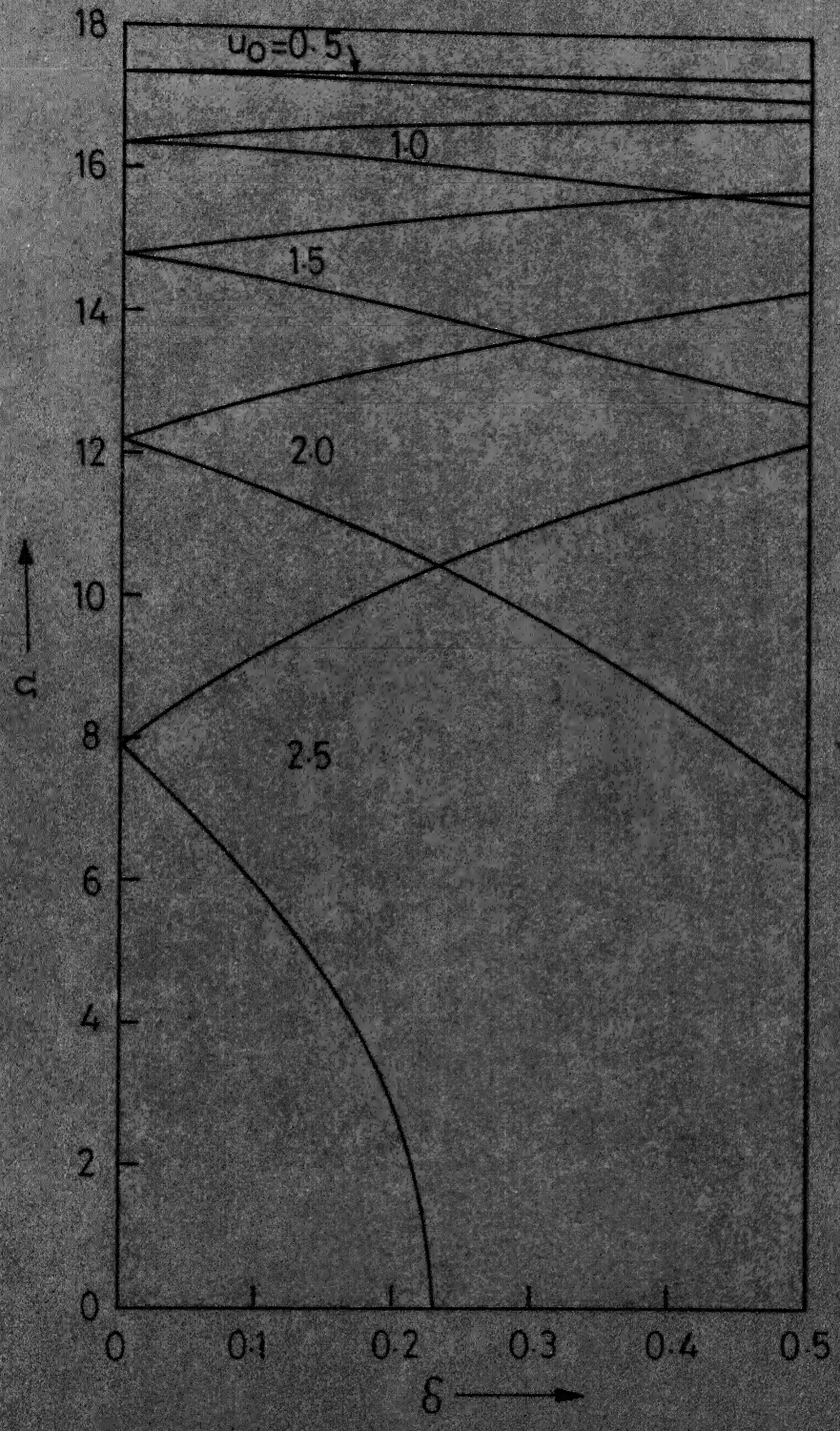

Figure 3.5a - The regions of the primary instability associated with the first mode of a two span pipe for various values of u_0. $\gamma = 2$, $\beta = 0.5$.

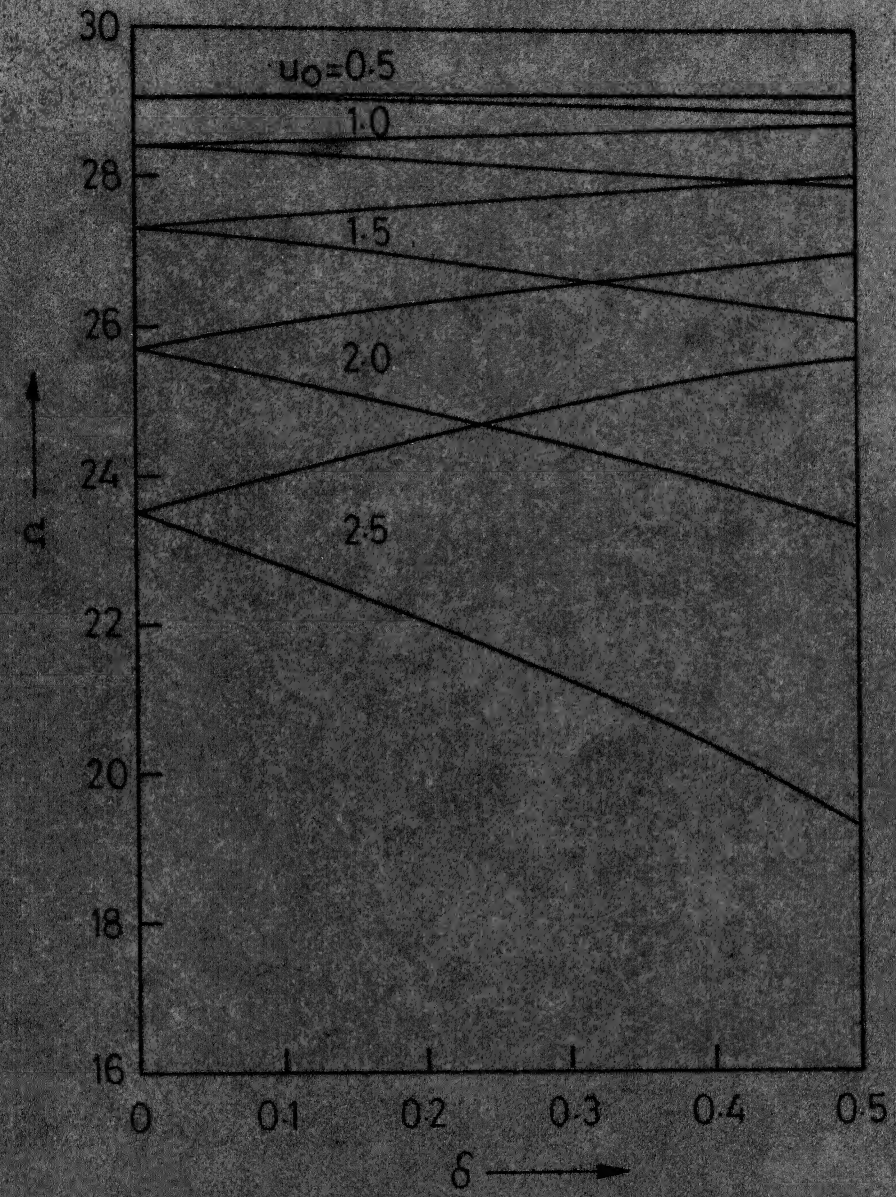

Figure 3.5b - The regions of the primary instability associated with the second mode of a two span pipe for various values of u_o. $\gamma = 2$, $\beta = 0.5$.

similar to that in the first mode. However, the regions do not become as wide as in the first mode, with increase in u_o.

Figures 3.6a and 3.6b show the effect of u_o on the regions of the secondary instabilities in the first two modes. In these cases also, the regions become wider and get shifted to lower frequencies with increasing u_o. It should be noted that the upper boundaries of the secondary instability regions not change much with increasing δ.

Comparing the regions of primary and the secondary instabilities, it is seen that the upper boundary of the primary instability shifts to higher frequency with increasing δ, whereas the upper boundary of the secondary instability regions shifts to lower frequency with increasing δ.

As seen in section 3.9.4, the regions of instability do not change significantly by letting $\beta = 0$. Thus, the changes in the instability regions described above can also be studied qualitatively from equations (3.51) and (3.53). The coefficients of the terms having second order derivatives (like $\frac{d^2\bar{X}_1}{d\xi^2}$, $\frac{d^2\bar{Y}_1}{d\xi^2}$, etc.) increase with increasing u_o. The coefficients of these terms represent the equivalent axial load on the system. Therefore, the natural frequencies of the systems governed by equations (3.51) and (3.53) shift to lower values.

In equations (3.51) which governs the regions of primary instabilities, the coefficient of the term $\frac{d^2\bar{X}_1}{d\xi^2}$ reduces with increasing δ. Thus the natural frequencies, i.e., one of the boundary of the instability region increases to higher value with increasing δ. On the other hand, the coefficient of the term $\frac{d^2\bar{Y}_1}{d\xi^2}$ increases with increasing δ. Hence, the

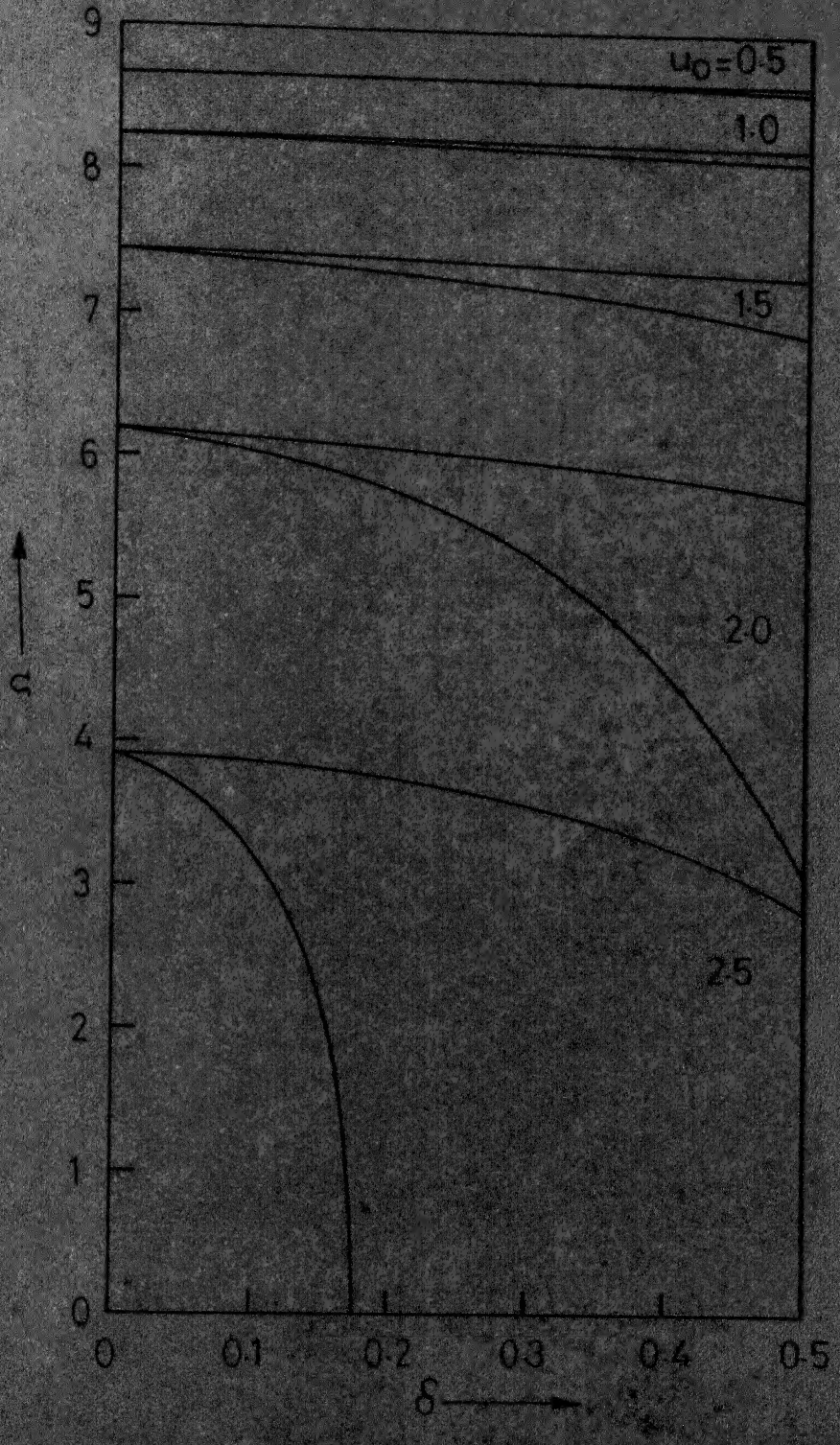

Figure 3.6a-The regions of the secondary instability associated with the first mode of a two span pipe for various values of u_0. $\gamma = 2$, $\beta = 0.5$.

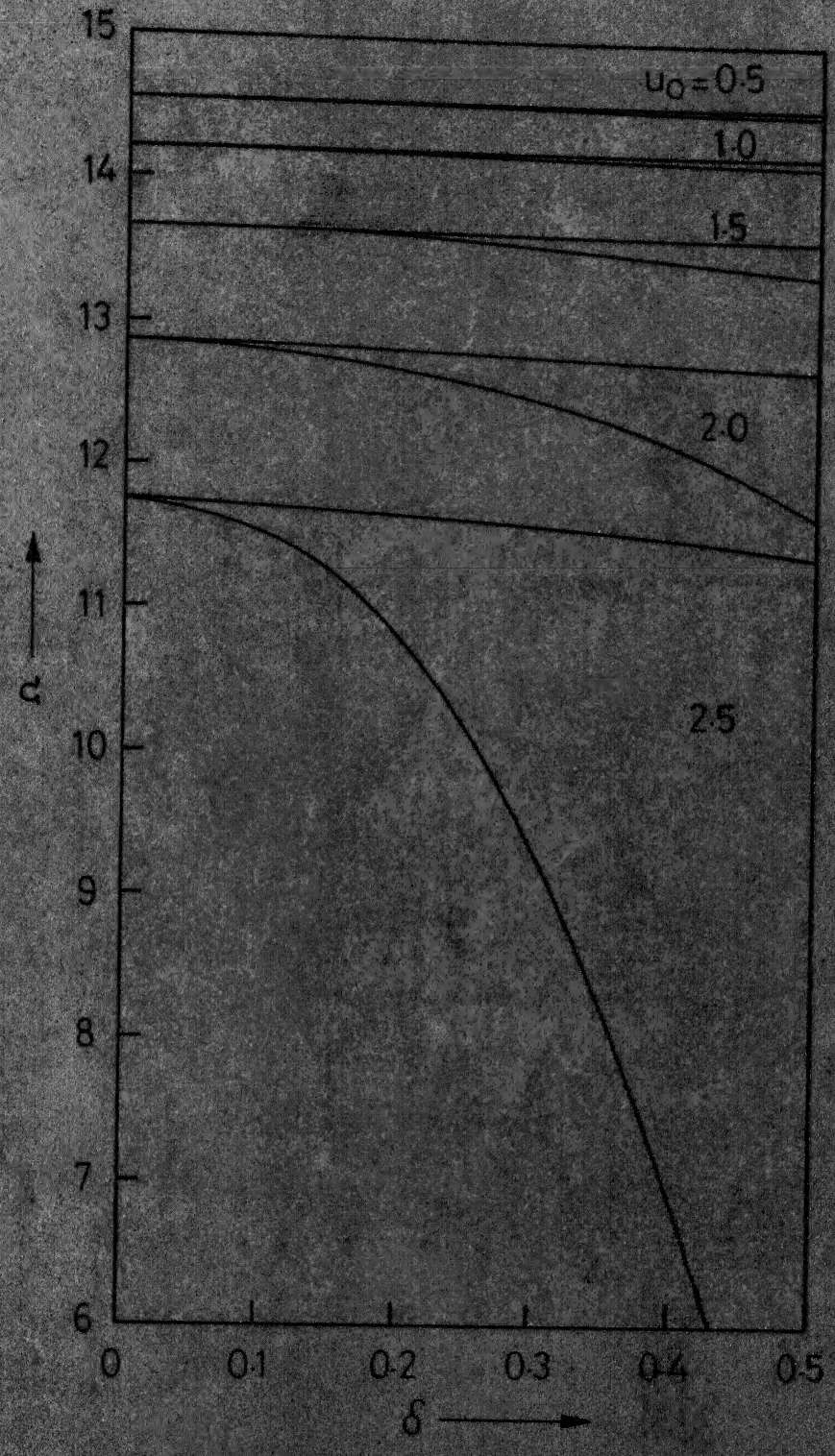

Figure 3·6 b - The regions of the secondary instability associated with the second mode of a two-span pipe for various values of u_0. $\gamma = 2$, $\beta = 0.5$.

natural frequencies reduce to lower values with increasing δ. The net outcome of these two opposite changes is the considerable increase in the width of the instability regions with increasing δ.

If we consider equation (3.53) governing the regions of the secondary instabilities, the coefficients of the terms with second order derivatives increase with increasing δ. Thus, both the boundaries of the instability regions shift to lower values with increasing δ. As a result, the width of these regions does not change as much as in the case of the primary regions. Moreover, with δ as a fraction, the terms signifying the equivalent axial load in equation (3.51) change more drastically with δ than those in equation (3.53). This explains the considerable change in the primary instability regions with the increasing value of δ.

3.9.6 Effect of the Fluid Pressure

Figures 3.7a and 3.7b show the regions of the primary instabilities associated with the first two modes of a two span pipe for various values of the fluid pressure, γ. It is seen that the instability regions associated with both the modes shift to lower frequencies with increasing γ.

Figure 3.8a and 3.8b show the regions of secondary instabilities for various values of γ. The effect of variation of γ on these regions is similar to that on the regions of the primary instabilities.

3.9.7 Effect of Damping

The effect of damping on the regions of instabilities, has been studied using the methods discussed in section 3.8. Both viscous and hysteretic types of damping have been considered.

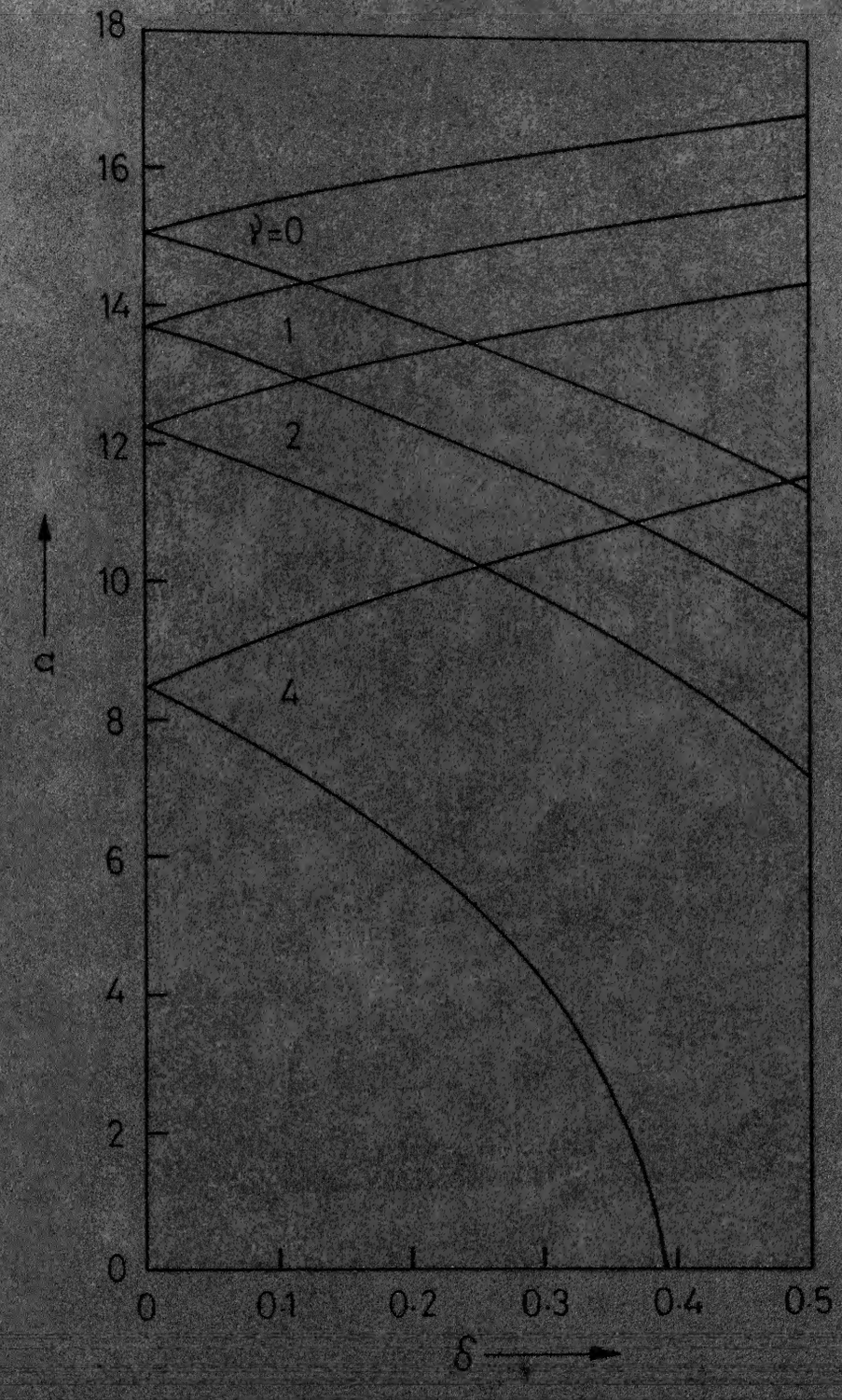

Figure 3.7a - The effect of γ on the regions of the primary instability associated with the first mode of a two span pipe. $u_0=2, \beta=0.5$

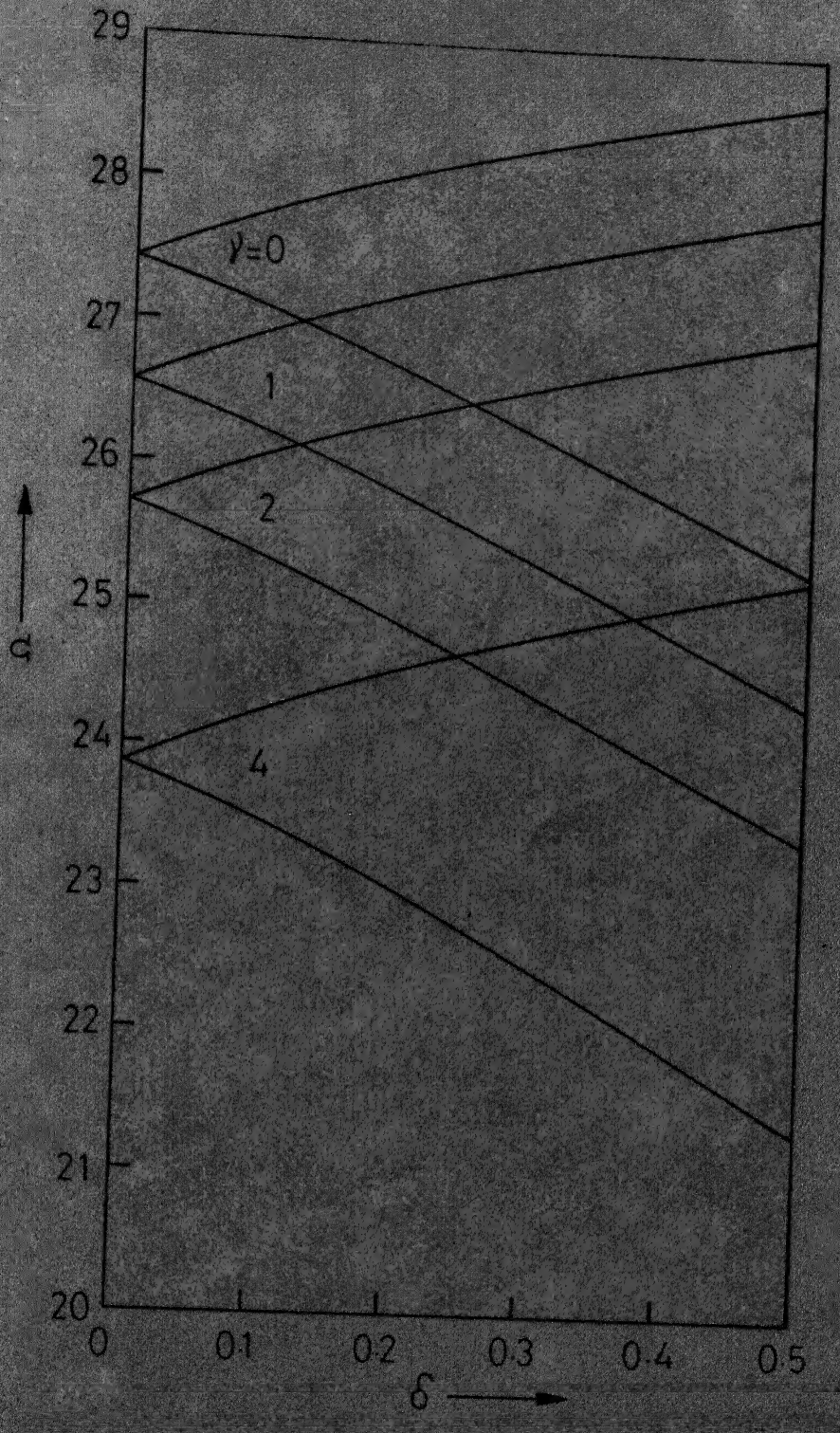

Figure 37b - The effect of γ on the regions of the primary instability associated with the second mode of a two span pipe. $u_0=2, \beta=0.5$

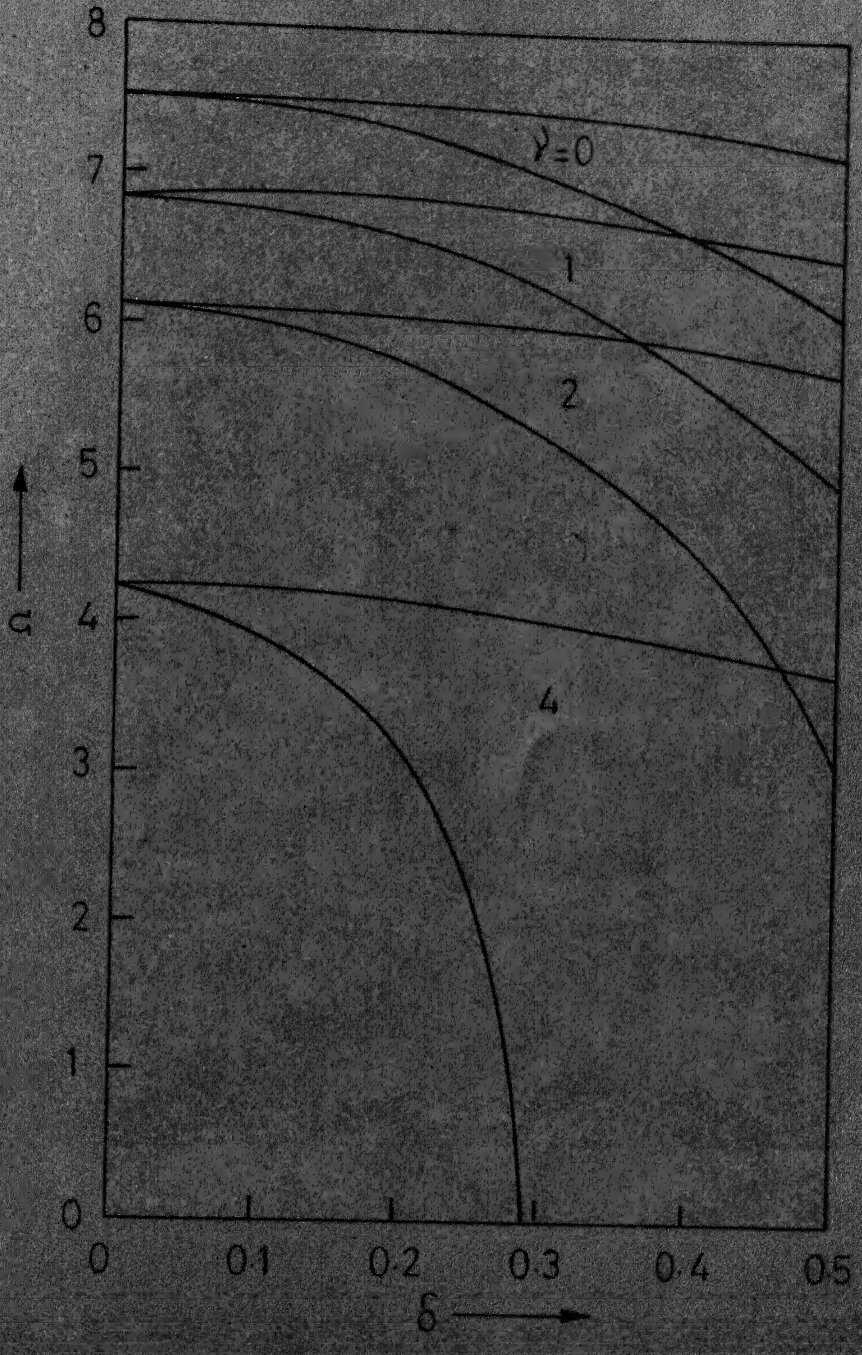

Figure 3.8a - The effect of γ on the regions of the secondary instability associated with the first mode of a two span pipe. $u_0 = 2$, $\beta = 0.5$.

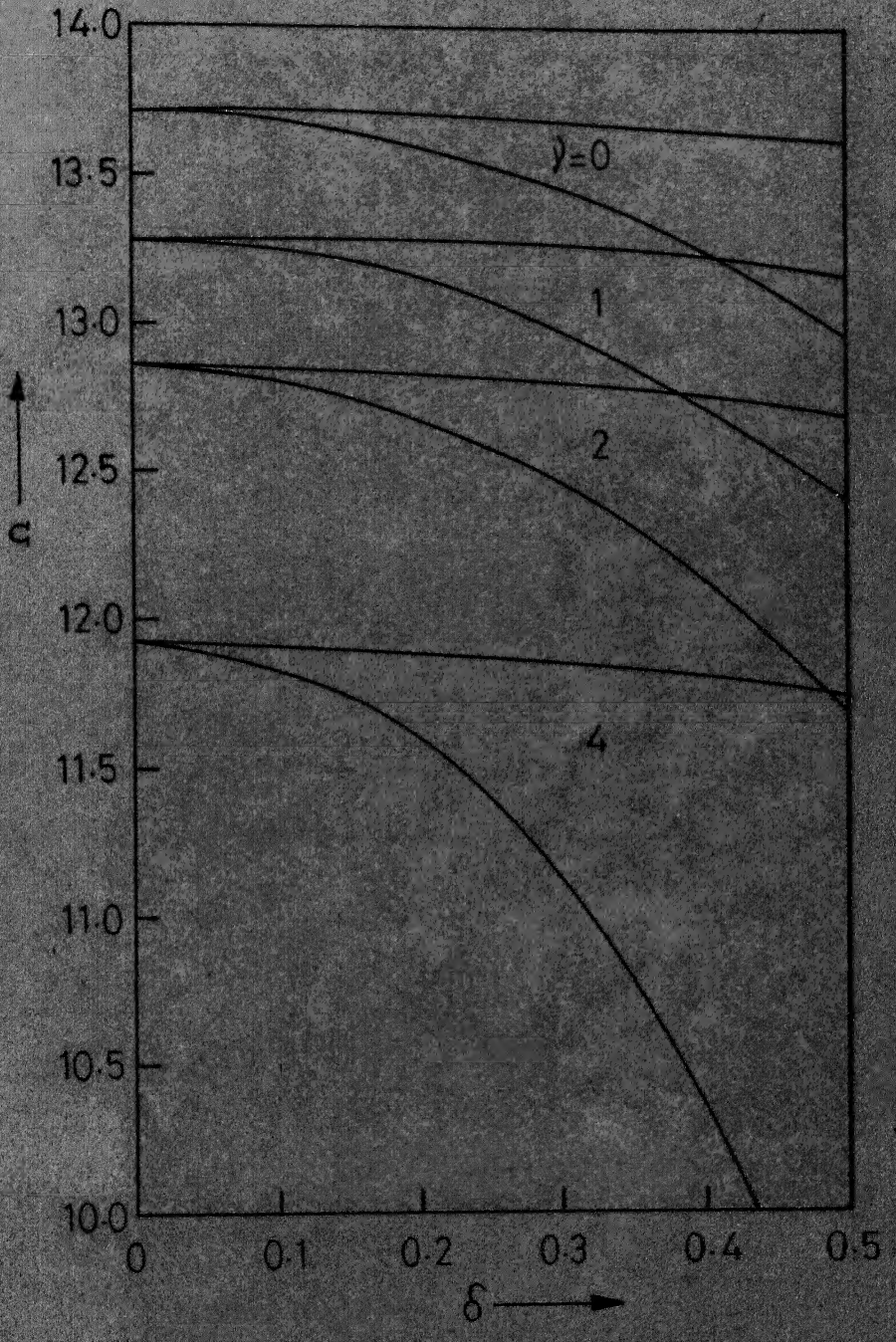

Figure 3.8b - The effect of γ on the regions of the secondary instability associated with the second mode of a two span pipe. $u_0 = 2$, $\beta = 0.5$

Figure 3.9a shows the regions of instabilities associated with the first mode of a two span pipe for three values of the viscous damping parameter η_c. It is seen that the presence of damping diminishes the extent of the instability regions. A finite critical value of δ is required to have the instabilities. If δ is less than the critical value then the pipe is not subjected to parametric instabilities. The critical value of δ increases with increasing η_c. In other words, large excitations are required to excite the instabilities if the damping is increased. The effect of η_c on the regions of the instabilities reduces with increasing δ.

It is also seen from Figure 3.9a that the damping has more pronounced effect on the regions of the secondary instability as compared to the primary instability. For a given value of η_c, the critical value of δ is much more as compared to that for the primary instability.

Figure 3.9b shows the effect of damping on the regions of instabilities associated with the second mode. As compared to its effect on the regions associated with the first mode, the damping is more effective and the regions become considerably narrower. For values of η_c just more than 0.2, the secondary instability may be totally eliminated for δ even upto 0.5.

Figure 3.10a and 3.10b show the effect of the hysteretic damping, η_b, on the regions of instabilities associated with the first two modes. As with viscous damping, η_c, three values are also used for η_b. In order to compare the effectiveness of the viscous and the hysteretic type of damping, equivalent values for η_b and η_c are used in the computation.

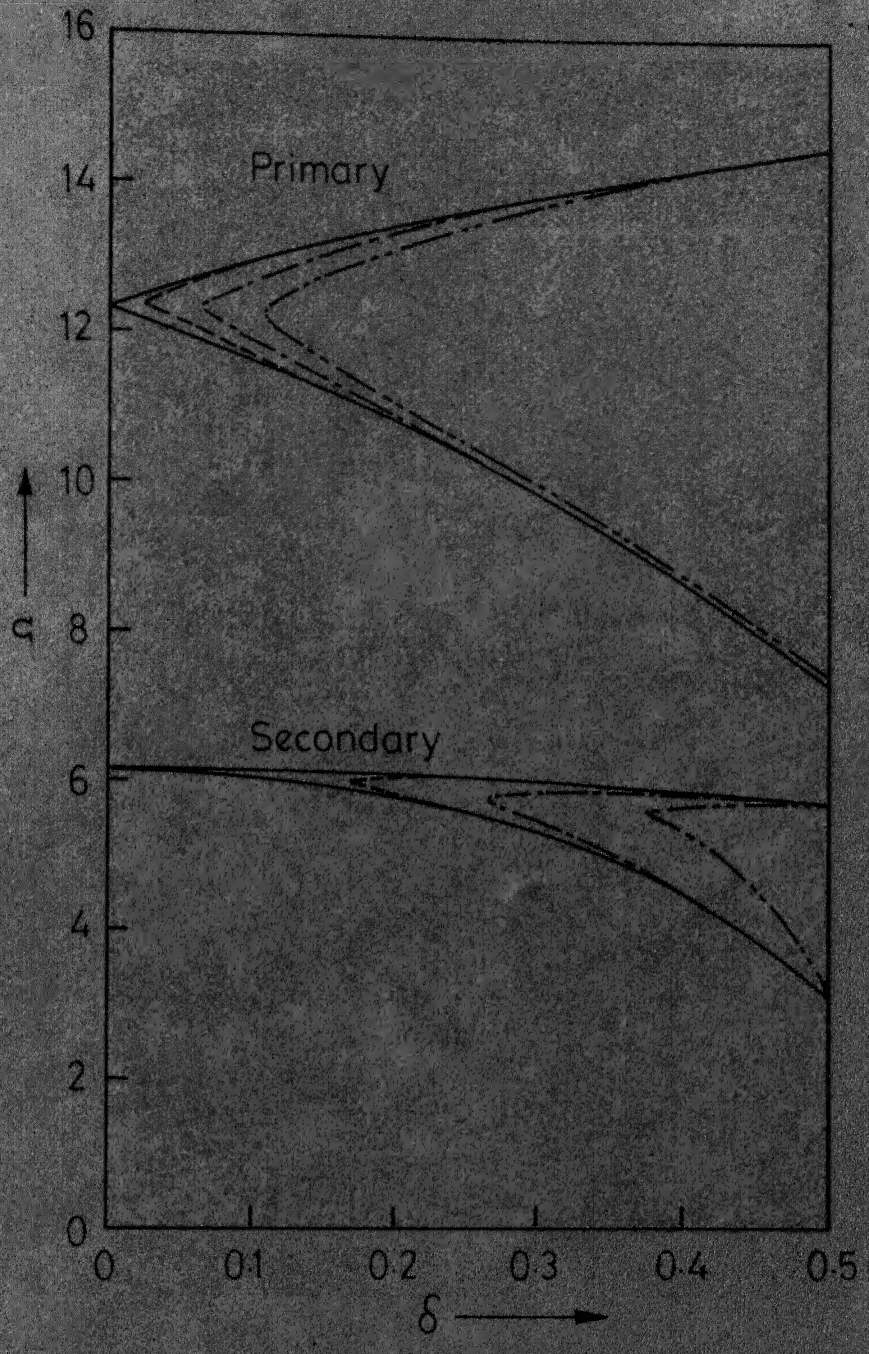

Figure 3·9a - The effect of η_c on the regions of instabilities associated with the first mode of a two span pipe for $u_0=2$, $\gamma=2$, $\beta=0$, and $\eta_b=0$; ——, $\eta_c=0$; - - - -, $\eta_c=0.2$; — — —, $\eta_c=0.5$; ———, $\eta_c=0.75$.

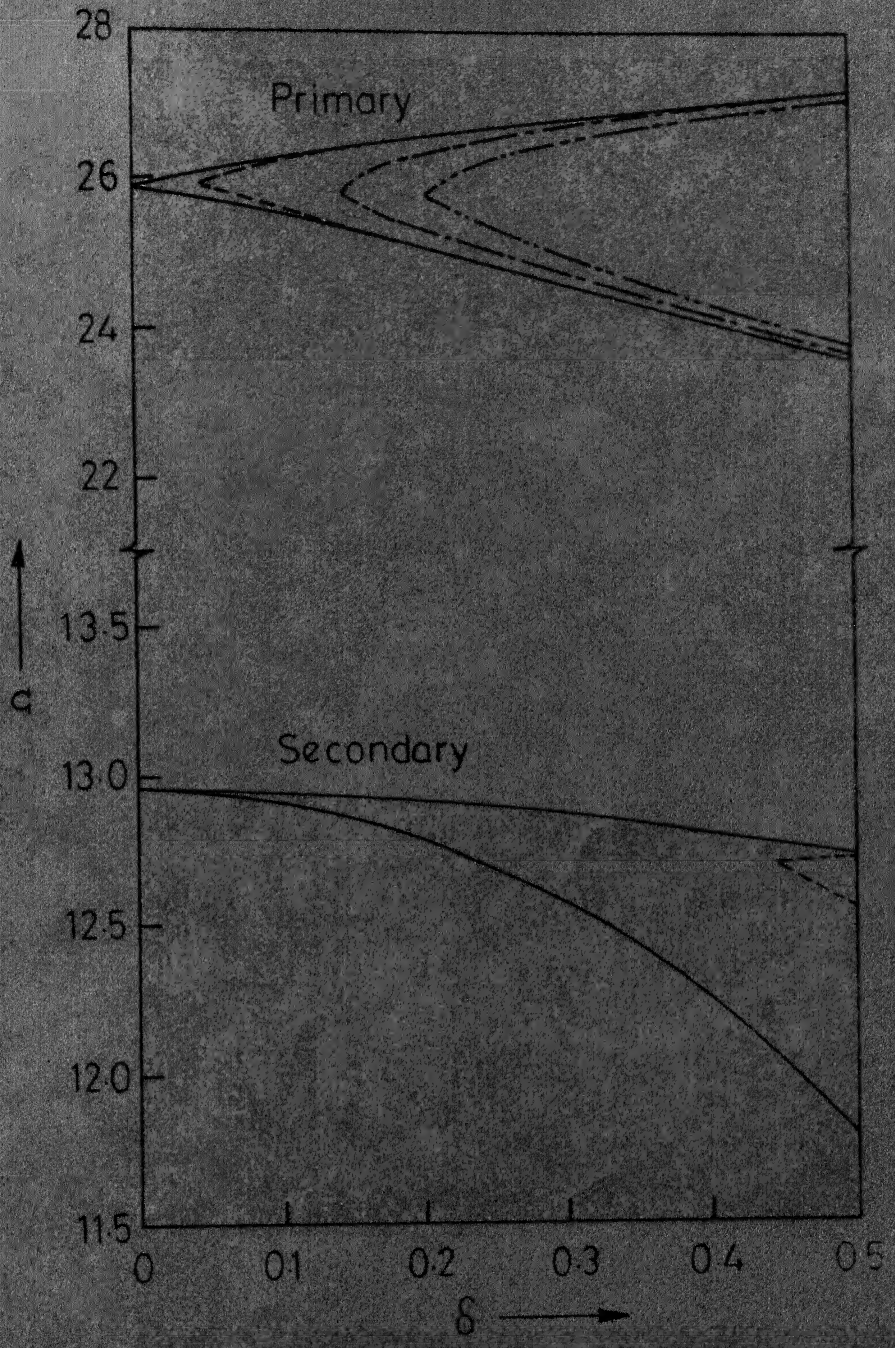

Figure 3·9b - The effect of η_c on the regions of instabilities associated with the second mode of a two span pipe for $u_0=2, \gamma=2, \beta=0$, and $\eta_b=0$; ——, $\eta_c=0$; - - - -, $\eta_c=0.2$; — · —, $\eta_c=0.5$; — · · —, $\eta_c=0.75$.

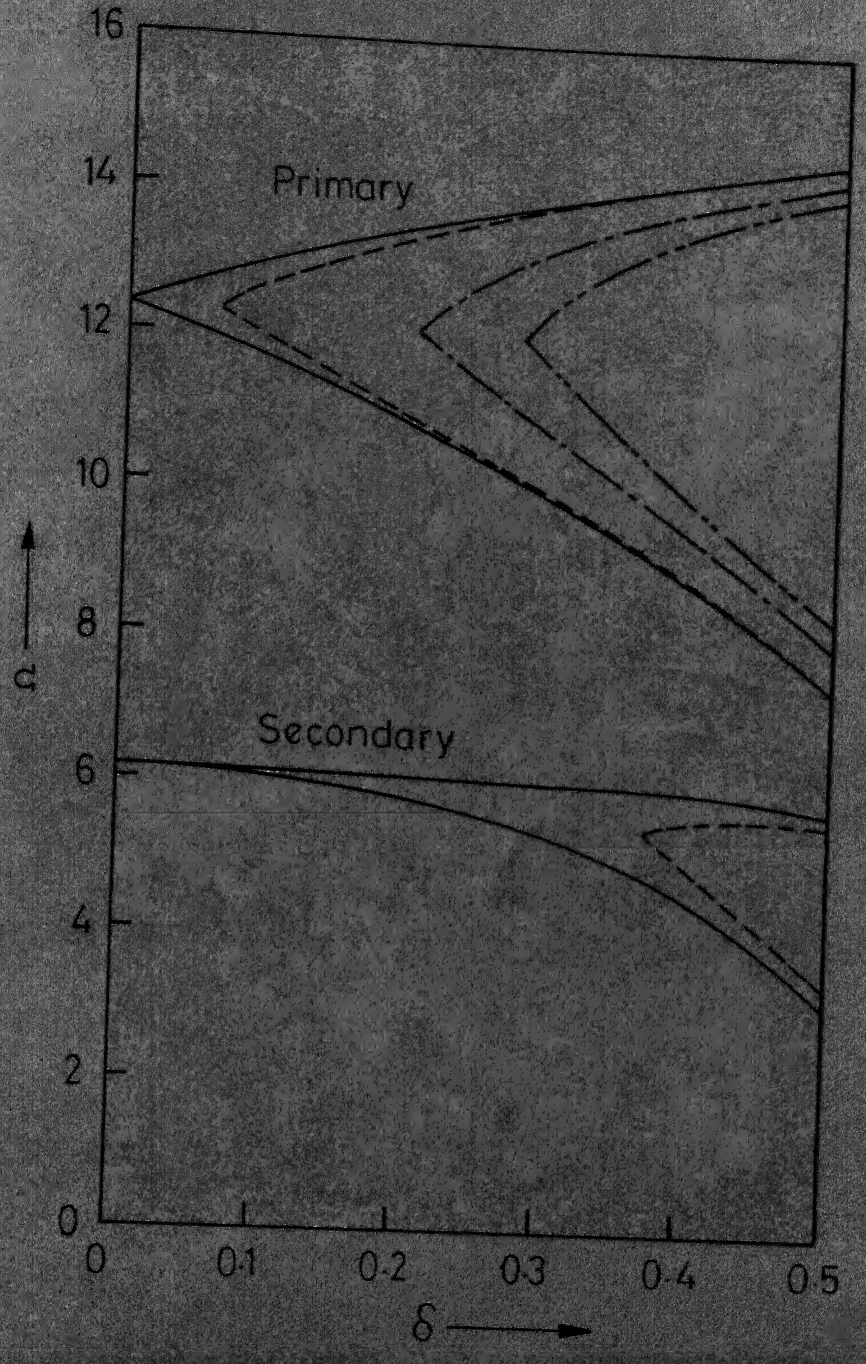

Figure 3·10 a - The effect of η_b on the regions of instabilities associated with the first mode of a two span pipe for $u_0=2$, $\gamma=2$, $\beta=0$, and $\eta_c=0$; ———, $\eta_b=0$; – – –, $\eta_b=0{\cdot}064$; —·—, $\eta_b=0{\cdot}191$; ———, $\eta_b=0{\cdot}234$.

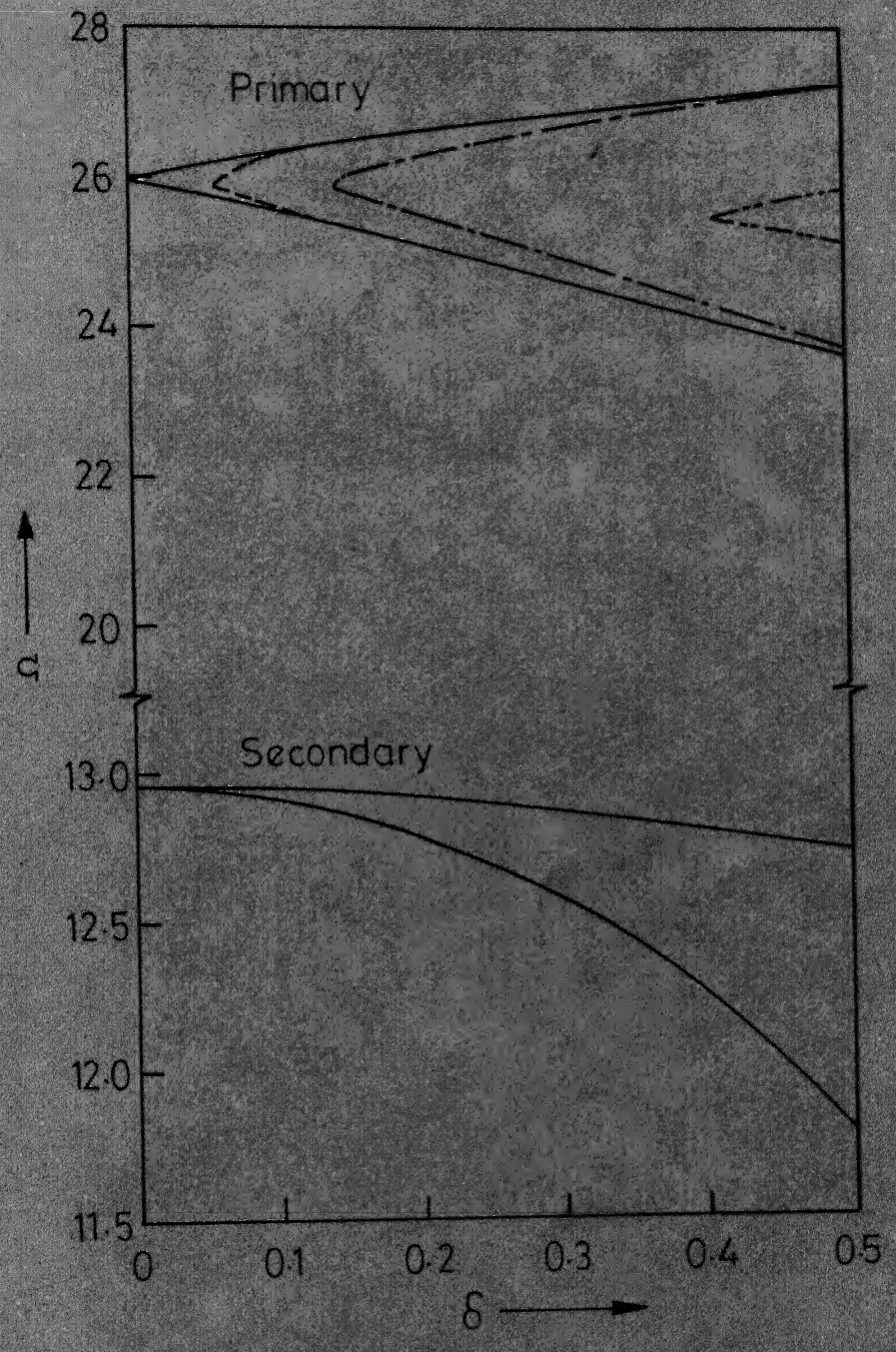

Figure 3.10b - The effect of η_b on the regions of instabilities associated with the second mode of a two span pipe for $u_0=2$, $\gamma=2$, $\beta=0.5$, and $\eta_c=0$; ——, $\eta_b=0$; - - -, $\eta_b=0.064$; — — —, $\eta_b=0.191$; — · — · —, $\eta_b=0.234$.

This equivalence is based on the same decay rate in the first mode of a simply supported pipe when both the fluid pressure and velocity are zero. The effect of η_b is seen to be more pronounced than the corresponding value of η_c. The secondary instability region associated with the first mode is eliminated totally for $\eta_b = 0.191$. The secondary instability region associated with the second mode is eliminated even for $\eta_b = 0.064$.

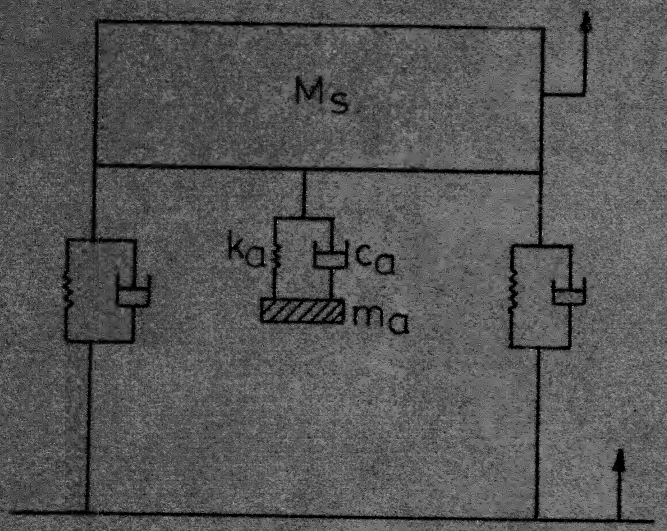

(a)

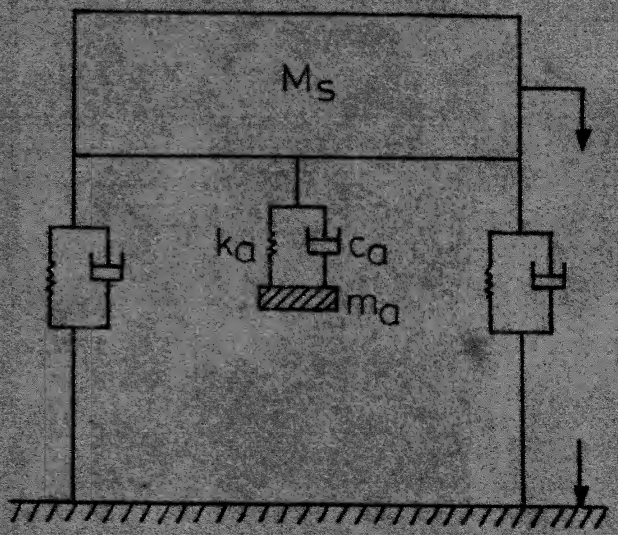

(b)

Figure 4.1 - Different applications of a dynamic absorber.

CHAPTER 4

INVESTIGATION OF THE EFFECT OF DYNAMIC ABSORBERS ON THE REGIONS OF THE PARAMETRIC INSTABILITIES OF A PIPE

4.1 Introduction

A dynamic absorber normally consists of a lumped mass that is attached by a damped resilient element to a vibrating system, the motion of which is found to be excessive. Frequently, the vibrating system of mass, M_s, is found to resonate on resilient supports as shown in Figure 4.1. The dynamic absorber is tuned to a frequency close to that of the vibrating system. The motion of M_s is then reduced because, in effect, the absorber mass, m_a, is greatly magnified in the neighbourhood of this frequency and controls the motion of M_s.

The dynamic absorbers have been used successfully to reduce undesired resonant vibrations of a system caused by "ground vibrations" as shown in Figure 4.1a. Dynamic absorbers may also be employed to reduce the force transmitted by a machine to the ideally rigid foundation as shown in Figure 4.1b. These absorbers also find applications in reducing the resonant motion of rods vibrating in their longitudinal modes or beams vibrating in their transverse modes [54].

In the present chapter, a viscously damped dynamic absorber has been tried for a different use from its conventional role of reducing the resonant motion. The aim of the present study is to determine whether the dynamic absorber can control effectively the regions of parametric

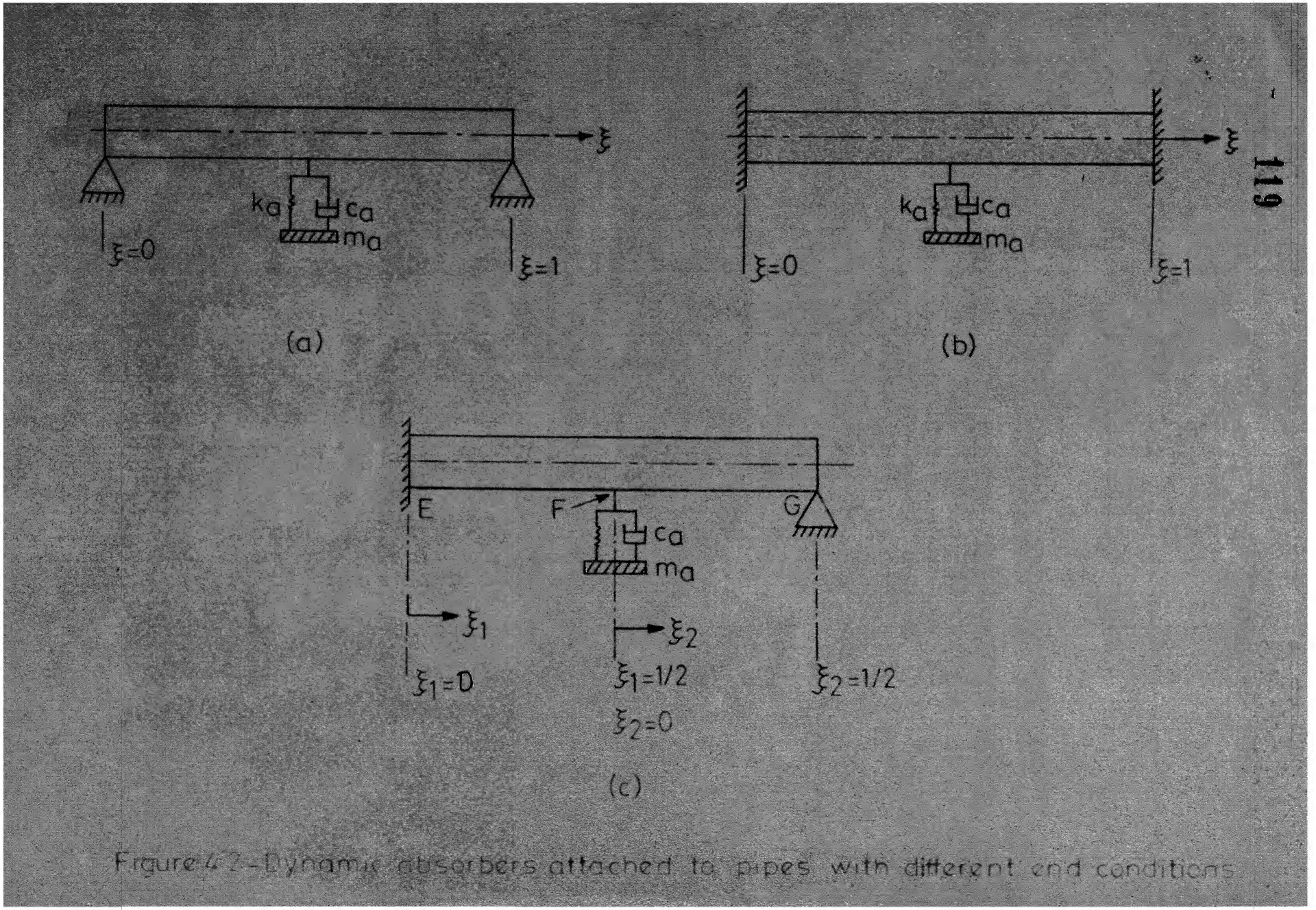

Figure 4.2-Dynamic absorbers attached to pipes with different end conditions

instabilities of a pipe. As stated in Chapter 3, in most of the practical cases, the principal region of instability is of primary importance. This is why, in the present work the effect of dynamic absorber on these regions only has been investigated. It has also been shown in Chapter 3 that the mass ratio parameter, β , has very insignificant effect on the regions of primary instability. Hence, in the present study this parameter has been neglected altogether. Moreover, damping in the pipe has also been omitted.

In this chapter, first we consider a viscously damped dynamic absorber attached at the mid-point of a single span pipe. Three different end conditions for the pipe, viz., pinned-pinned, clamped-clamped, and clamped-pinned, are considered separately. The effects of different absorber parameters, like the mass, the damping, and the spring constant, on the regions of instability have been studied. For computation of the instability regions, the second method discussed in section 3.5 has been used. This is followed by the analysis of a periodically supported pipe with a spring-mass type absorber attached at the centre of each span. The 'wave approach' developed in section 3.7 has been used.

4.2 Theoretical Formulation

Consider a pipe of length ℓ resting on transversely rigid supports. A viscously damped absorber of mass, m_a, spring constant, k_a, and viscous damping, c_a, is attached at the mid-point of the pipe (Figure 4.2). Let the velocity of the fluid flowing through the pipe, be

$$u = u_0 (1 + \delta \cos \Omega\tau),$$

where u_o is the non-dimensional constant mean velocity,

δ is the excitation parameter,

Ω is the non-dimensional frequency,

and τ is the non-dimensional time.

It was seen in Chapter 3 that the effect of neglecting mass ratio parameter, β, on the princtipal regions of instability was negligible, and the analysis becomes much simplified. So for the present study also, the effect of β has not been included. For the regions of primary instability corresponding to K = 1 approximation, the displacement of the pipe, $\bar{y}_1$, is given by equation (3.30)

$$\bar{y}_1(\xi,\tau) = \bar{X}_1(\xi) \sin(\tfrac{1}{2}\Omega\tau) + \bar{Y}_1(\xi) \cos(\tfrac{1}{2}\Omega\tau),$$

where $\bar{X}_1$ and $\bar{Y}_1$ satisfy equations (3.51)

$$\frac{d^4\bar{X}_1}{d\xi^4} + (u_o^2 + \gamma + \frac{u_o^2\delta^2}{2} - u_o^2\delta)\frac{d^2\bar{X}_1}{d\xi^2} - \frac{\Omega^2}{4}\bar{X}_1 = 0,$$

$$\frac{d^4\bar{Y}_1}{d\xi^4} + (u_o^2 + \gamma + \frac{u_o^2\delta^2}{2} + u_o^2\delta)\frac{d^2\bar{Y}_1}{d\xi^2} - \frac{\Omega^2}{4}\bar{Y}_1 = 0.$$

The solutions for equations (3.51) are given by equations (3.52)

$$\bar{X}_1(\xi) = \sum_{n=1}^{4} C_{1n} e^{\lambda_{1n}\xi},$$

$$\bar{Y}_1(\xi) = \sum_{n=1}^{4} C_{2n} e^{\lambda_{2n}\xi},$$

where the λ_{1n}'s and the λ_{2n}'s are the roots of the polynomials

$$\lambda^4 + (u_o^2 + \gamma + \frac{u_o^2\delta^2}{2} - u_o^2\delta)\lambda^2 - \frac{\Omega^2}{4} = 0,$$

and $\lambda^4 + (u_o^2 + \gamma + \frac{u_o^2 \delta^2}{2} + u_o^2 \delta)\lambda^2 - \frac{\Omega^2}{4} = 0,$

respectively. The C_{1n}'s and the C_{2n}'s are unknown coefficients to be determined from the boundary conditions.

4.2.1 Equation of Motion for the Absorber-Mass

Assume y_a be the displacement of the mass, m_a. The equation of motion for the mass m_a is

$$m_a \frac{d^2 y_a}{dt^2} + C_a \frac{dy_a}{dt} + k_a y_a = C_a \ell \left.\frac{d\bar{y}_1}{dt}\right|_{\xi=\frac{1}{2}} + k_a \ell \left.\bar{y}_1\right|_{\xi=\frac{1}{2}} \qquad (4.1)$$

Substituting the value of $\bar{y}_1$ from equation (3.30) into equation (4.1) and noting $\Omega\tau = \omega t$, one gets

$$m_a \frac{d^2 y_a}{dt^2} + C_a \frac{dy_a}{dt} + k_a y_a = \ell I_m \left[\{(k_a \bar{X}_1(\tfrac{1}{2}) - \frac{C_a \omega}{2} \bar{Y}_1(\tfrac{1}{2})) + i(k_a \bar{Y}_1(\tfrac{1}{2}) + \frac{C_a \omega}{2} \bar{X}_1(\tfrac{1}{2}))\} e^{i(\frac{1}{2}\Omega\tau)} \right], \qquad (4.2)$$

where I_m denotes the imaginary part of the bracketed quantity.

The steady state solution of equation (4.2) is

$$y_a = \ell I_m \left[\frac{\{\bar{X}_1(\frac{1}{2}) - \frac{1}{2}\frac{C_a \omega}{k_a} \bar{Y}_1(\frac{1}{2})\} + i\{\bar{Y}_1(\frac{1}{2}) + \frac{C_a \omega}{2k_a} \bar{X}_1(\frac{1}{2})\}}{(1 - \frac{m_a \omega^2}{4k_a}) + i \frac{C_a \omega}{2k_a}} e^{i(\frac{1}{2}\Omega\tau)} \right] \qquad (4.3)$$

Let us introduce the following notations :

ω_a = natural frequency of the undamped absorber

$$= (\frac{k_a}{m_a})^{\frac{1}{2}},$$

C_c = critical damping of the absorber

$= 2m_a \omega_a$,

ζ_a = damping ratio of the absorber

$= \frac{C_a}{C_c}$,

σ_a = tuning ratio of the absorber

$= \frac{\omega_a}{\omega_o}$,

where ω_o is some reference frequency. In the present study, ω_o has been taken as the first natural frequency of a pinned-pinned pipe with fluid velocity u_o and fluid pressure γ.

Using these notations, $\frac{C_a \omega}{k_a}$ can be written as

$$\frac{C_a \omega}{k_a} = 2\left(\frac{\omega}{\omega_a}\right) \frac{C_a}{C_c} = 2\left(\frac{\omega_o}{\omega_a}\right) \left(\frac{\omega}{\omega_o}\right) \frac{C_a}{C_c}$$

$$= \frac{2}{\sigma_a} \left(\frac{\Omega}{\Omega_o}\right) \zeta_a = \Delta \text{ (say)} \qquad (4.4)$$

Similarly, $\frac{m_a \omega^2}{k_a}$ can be written as

$$\frac{m_a \omega^2}{k} = \left(\frac{\omega}{\omega_a}\right)^2 = \left(\frac{\omega_o}{\omega_a}\right)^2 \left(\frac{\omega}{\omega_o}\right)^2$$

$$= \frac{1}{\sigma_a^2} \left(\frac{\Omega}{\Omega_o}\right)^2, \qquad (4.5)$$

where Ω_o is the non-dimensional reference frequency

$$= \left(\frac{m_f + m_p}{EI}\right)^{\frac{1}{2}} \omega_o \ell^2$$

Substituting equations (4.4) and (4.5) into equation (4.3), one gets

$$y_a = \ell I_m \left[\frac{\{\bar{X}_1(\frac{1}{2}) - \frac{\Delta}{2}\bar{Y}_1(\frac{1}{2})\} + i\{\bar{Y}_1(\frac{1}{2}) + \frac{\Delta}{2}\bar{X}_1(\frac{1}{2})\}}{\{1 - \frac{1}{4\sigma_a^2}(\frac{\Omega}{\Omega_o})^2\} + i\frac{\Delta}{2}} e^{i(\frac{1}{2}\Omega\tau)} \right] \quad (4.6)$$

On simplification equation (4.6) reduces to

$$y_a = \ell\{A_o \bar{X}_1(\tfrac{1}{2}) + B_o \bar{Y}_1(\tfrac{1}{2})\} \sin(\tfrac{1}{2}\Omega\tau) + \ell\{A_o \bar{Y}_1(\tfrac{1}{2}) - B_o \bar{X}_1(\tfrac{1}{2})\} \cos(\tfrac{1}{2}\Omega\tau), \quad (4.7)$$

where $$A_o = \frac{[1 - \frac{1}{4\sigma_a^2}(\frac{\Omega}{\Omega_o})^2 + (\frac{\Delta}{2})^2]}{[1 - \frac{1}{4\sigma_a^2}(\frac{\Omega}{\Omega_o})^2]^2 + (\frac{\Delta}{2})^2},$$

and $$B_o = \frac{[1 - \frac{1}{4\sigma_a^2}(\frac{\Omega}{\Omega_o})^2](\frac{\Delta}{2})}{[1 - \frac{1}{4\sigma_a^2}(\frac{\Omega}{\Omega_o})^2]^2 + (\frac{\Delta}{2})^2}.$$

4.2.2 Boundary Conditions

In the present study, the pipes with following end supports have been considered.

(a) Pinned-Pinned Pipe

When both the ends of the pipe are pinned (Figure 4.2a), because of symmetry, one needs to consider only half of the pipe and the boundary conditions are

(i) for zero deflection at the left support,

$$\bar{y}_1(0,\tau) = 0,$$

i.e., $\bar{X}_1(0) = 0$, (4.8a)

and $\bar{Y}_1(0) = 0$ (4.8b)

(ii) for zero moment at the left support,

$$\bar{y}_1''(0,\tau) = 0,$$

i.e., $\bar{X}_1''(0) = 0,$ (4.8c)

and $\bar{Y}_1''(0) = 0$, (4.8d)

where primes denote differentiation with respect to ξ .

(iii) Due to symmetry, slope at the mid-point of the span must be zero

$$\bar{y}_1'(\tfrac{1}{2}, \tau) = 0 ,$$

i.e., $\bar{X}_1'(\tfrac{1}{2}) = 0$, (4.8e)

and $\bar{Y}_1'(\tfrac{1}{2}) = 0$ (4.8f)

(iv) At the mid-point of the span, change in shear force must be equal to the inertia force of the absorber mass, m_a. Thus,

$$(\frac{EI}{\ell^2})\ \bar{y}_1'''(\tfrac{1}{2}) = \frac{1}{2} m_a \frac{d^2 y_a}{dt^2} \qquad (4.9)$$

Substituting y_a from equation (4.7) into equation (4.9), one obtains

$$\bar{X}_1''(\tfrac{1}{2}) \sin(\tfrac{1}{2}\Omega\tau) + \bar{Y}_1''(\tfrac{1}{2}) \cos(\tfrac{1}{2}\Omega\tau) = -\frac{1}{8} \Gamma_a \Omega^2 [\{A_o \bar{X}_1(\tfrac{1}{2}) + B_o \bar{Y}_1(\tfrac{1}{2})\} \sin(\tfrac{1}{2}\Omega\tau) + \{A_o \bar{Y}_1(\tfrac{1}{2}) - B_o \bar{X}_1(\tfrac{1}{2})\} \cos(\tfrac{1}{2}\Omega\tau)] , \qquad (4.10)$$

where Γ_a is known as the mass ratio of the absorber and defined as

$$\Gamma_a = \frac{m_a}{(m_f + m_p)\ell} .$$

Equating the coefficients of the terms $\sin(\frac{1}{2}\Omega\tau)$ and $\cos(\frac{1}{2}\Omega\tau)$ from both sides of equation (4.10), we get

$$X_1'''(\tfrac{1}{2}) + \tfrac{1}{8}\Gamma_a \Omega^2 \{A_o \bar{X}_1(\tfrac{1}{2}) + B_o \bar{Y}_1(\tfrac{1}{2})\} = 0 , \qquad (4.11a)$$

$$\bar{Y}_1'''(\tfrac{1}{2}) + \tfrac{1}{8}\Gamma_a \Omega^2 \{A_o \bar{Y}_1(\tfrac{1}{2}) - B_o \bar{X}_1(\tfrac{1}{2})\} = 0. \qquad (4.11b)$$

Substituting equations (3.52) into equations (4.8) and (4.11), one obtains a system of homogeneous equations

$$D_{pp}\, C = 0 ,$$

where D_{pp} is a matrix of size 8 × 8 and its elements are given in Appendix 4. The subscript pp refers to the pinned-pinned pipe. C is a column matrix $\{C_{11}\ C_{12}\ C_{13}\ C_{14}\ C_{21}\ C_{22}\ C_{23}\ C_{24}\}^t$, where t denotes the transpose. For non-trivial solution of C in the above equation, determinant of D_{pp} must be zero. Frequencies at which the determinant $|D_{pp}|$ vanishes, give the boundaries of the instability regions. It should be noted that even after neglecting the mass ratio parameter, β, though the governing equations of motions (given by equations (3.51)) are uncoupled, the boundary conditions (given by equations (4.8) and (4.11)) are coupled through the damping of the absorber.

(b) Clamped-Clamped Pipe

When both ends of the pipe are clamped (Figure 4.2b), then again because of symmetry, one needs to consider only one half of the pipe.

The boundary conditions are same as for the pinned-pinned pipe (given by equations (4.8) and (4.11)) except for equations (4.8c) and (4.8d). Since for the present case, slopes at the supports must be zero, equations (4.8c) and (4.8d) are modified as

$$\bar{y}_1'(0,\tau) = 0 \ ,$$

i.e., $$\bar{X}_1'(0) = 0 \ ,$$

and $$\bar{Y}_1'(0) = 0.$$

Proceeding similarly as in the case of a pinned-pinned pipe, instability regions are determined by the zeros of an eighth order determinant $|D_{cc}|$. The elements of the matrix D_{cc} are given in Appendix 4. The subscript cc refers to the clamped-clamped pipe.

(c) Clamped-Pinned pipe

Figure 4.2c shows a clamped-pinned pipe with a viscously damped dynamic absorber attached at the mid-point of the span. Using equation (3.30), the displacement of the pipe can be written as

$$\bar{y}_1^1 = \bar{X}_1^1(\xi_1) \sin(\tfrac{1}{2}\Omega\tau) + \bar{Y}_1^1(\xi_1) \cos(\tfrac{1}{2}\Omega\tau), \quad 0 \le \xi_1 \le \tfrac{1}{2} \qquad (4.12a)$$

$$\bar{y}_1^2 = \bar{X}_1^2(\xi_2) \sin(\tfrac{1}{2}\Omega\tau) + \bar{Y}_1^2(\xi_2) \cos(\tfrac{1}{2}\Omega\tau), \quad 0 \le \xi_2 \le \tfrac{1}{2} \qquad (4.12b)$$

where $$\bar{X}_1^1 = \sum_{n=1}^{4} C_{1n}^1 e^{\lambda_{1n}\xi_1} \ , \qquad (4.13a)$$

$$\bar{Y}_1^1 = \sum_{n=1}^{4} C_{2n}^1 e^{\lambda_{2n}\xi_1} \ , \qquad (4.13b)$$

$$\bar{X}_1^2 = \sum_{n=1}^{4} C_{1n}^2 e^{\lambda_{1n}\xi_2}, \qquad (4.13c)$$

$$\bar{Y}_1^2 = \sum_{n=1}^{4} C_{2n}^2 e^{\lambda_{2n}\xi_2}, \qquad (4.13d)$$

ξ_1 and ξ_2 are the non-dimensional co-ordinates along the length of the pipe as shown in Figure 4.2c. The constants C_{1n}^1's, ___C_{2n}^1's, C_{1n}^2's, and C_{2n}^2's can be determined from the following boundary conditions :

(i) for zero deflection at the supports E and G

$$\bar{y}_1^1(0,\tau) = 0 ,$$

$$\bar{y}_1^2(\tfrac{1}{2},\tau) = 0 ,$$

i.e., $$\bar{X}_1^1(0) = 0 , \qquad (4.14a)$$

$$\bar{Y}_1^1(0) = 0 , \qquad (4.14b)$$

$$\bar{X}_1^2(\tfrac{1}{2}) = 0 , \qquad (4.14c)$$

and $$\bar{Y}_1^2(\tfrac{1}{2}) = 0 \qquad (4.14d)$$

(ii) for zero slope at the support E

$$\bar{y}_1'^1(0,\tau) = 0 ,$$

i.e., $$\bar{X}_1'^1(0) = 0 , \qquad (4.15a)$$

and $$\bar{Y}_1'^1(0) = 0 . \qquad (4.15b)$$

(iii) for zero moment at the support G

$$\bar{y}_1''^2(\tfrac{1}{2},\tau) = 0 ,$$

i.e., $$\bar{X}_1''^2(\tfrac{1}{2}) = 0 , \qquad (4.16a)$$

and $$\bar{Y}_1''^2(\tfrac{1}{2}) = 0. \qquad (4.16b)$$

(iv) for continuity of displacement at the mid-point of the pipe, F

$$\bar{y}_1^1(\tfrac{1}{2},\tau) = \bar{y}_1^2(0,\tau),$$

i.e., $$\bar{X}_1^1(\tfrac{1}{2}) = \bar{X}_1^2(0), \qquad (4.17a)$$

and $$\bar{Y}_1^1(\tfrac{1}{2}) = \bar{Y}_1^2(0). \qquad (4.17b)$$

(v) for continuity of slope at the point F

$$\bar{y}_1'^1(\tfrac{1}{2},\tau) = \bar{y}_1'^2(0,\tau) ,$$

i.e., $$\bar{X}_1'^1(\tfrac{1}{2}) = \bar{X}_1'^2(0) , \qquad (4.18a)$$

and $$\bar{Y}_1'^1(\tfrac{1}{2}) = \bar{Y}_1'^2(0). \qquad (4.18b)$$

(vi) for continuity of moment at the point F

$$\bar{y}_1''^1(\tfrac{1}{2},\tau) = \bar{y}_1''^2(0,\tau),$$

i.e., $$\bar{X}_1''^1(\tfrac{1}{2}) = \bar{X}_1''^2(0) , \qquad (4.19a)$$

and $$\bar{Y}_1''^1(\tfrac{1}{2}) = \bar{Y}_1''^2(0) \qquad (4.19b)$$

(vii) again at the point F, change in shear force must be equal to the inertia force of the absorber mass, m_a. This results in

$$\left(\frac{EI}{\ell^2}\right)\{-\bar{y}_1'''^1(\tfrac{1}{2}) + \bar{y}_1'''^2(0)\} = -m_a \frac{d^2 y_a}{dt^2} \tag{4.20}$$

On simplification, equation (4.20) gives

$$\bar{X}_1'''^1(\tfrac{1}{2}) - \bar{X}_1'''^2(0) + \tfrac{1}{4} r_a \Omega^2 \{A_o \bar{X}_1^1(\tfrac{1}{2}) + B_o \bar{Y}_1^1(\tfrac{1}{2})\} = 0 \tag{4.21a}$$

$$\bar{Y}_1'''^1(\tfrac{1}{2}) - \bar{Y}_1'''^2(0) + \tfrac{1}{4} r_a \Omega^2 \{A_o \bar{Y}_1^1(\tfrac{1}{2}) - B_o \bar{X}_1^1(\tfrac{1}{2})\} = 0 \tag{4.21b}$$

Using equations (4.13) in equations (4.14) - (4.19) and (4.21), one gets a system of equations given by

$$D_{cp}\, C = 0 \,, \tag{4.22}$$

where D_{cp} is a matrix of order 16 x 16, and its elements are given in Appendix 4; the subscript cp refers to the clamped-pinned pipe. C is column matrix with elements $\{C_{11}^1\ C_{12}^1\ C_{13}^1\ C_{14}^1\ C_{21}^1\ C_{22}^1\ C_{23}^1\ C_{24}^1\ C_{11}^2\ C_{12}^2\ C_{13}^2\ C_{14}^2\ C_{21}^2\ C_{22}^2\ C_{23}^2\ C_{24}^2\}^t$, where t denotes the transpose. It should be noted that the order of the matrix D_{cp} is twice the order of D_{pp} and D_{cc}. This is obviously due to the loss of symmetry of the structure about its mid-point.

For non-trivial solutions of C's in equation (4.22), we get

$$|D_{cp}| = 0 \tag{4.23}$$

Thus, the zeros of the determinant of the matrix D_{cp} give the boundaries of the instability regions.

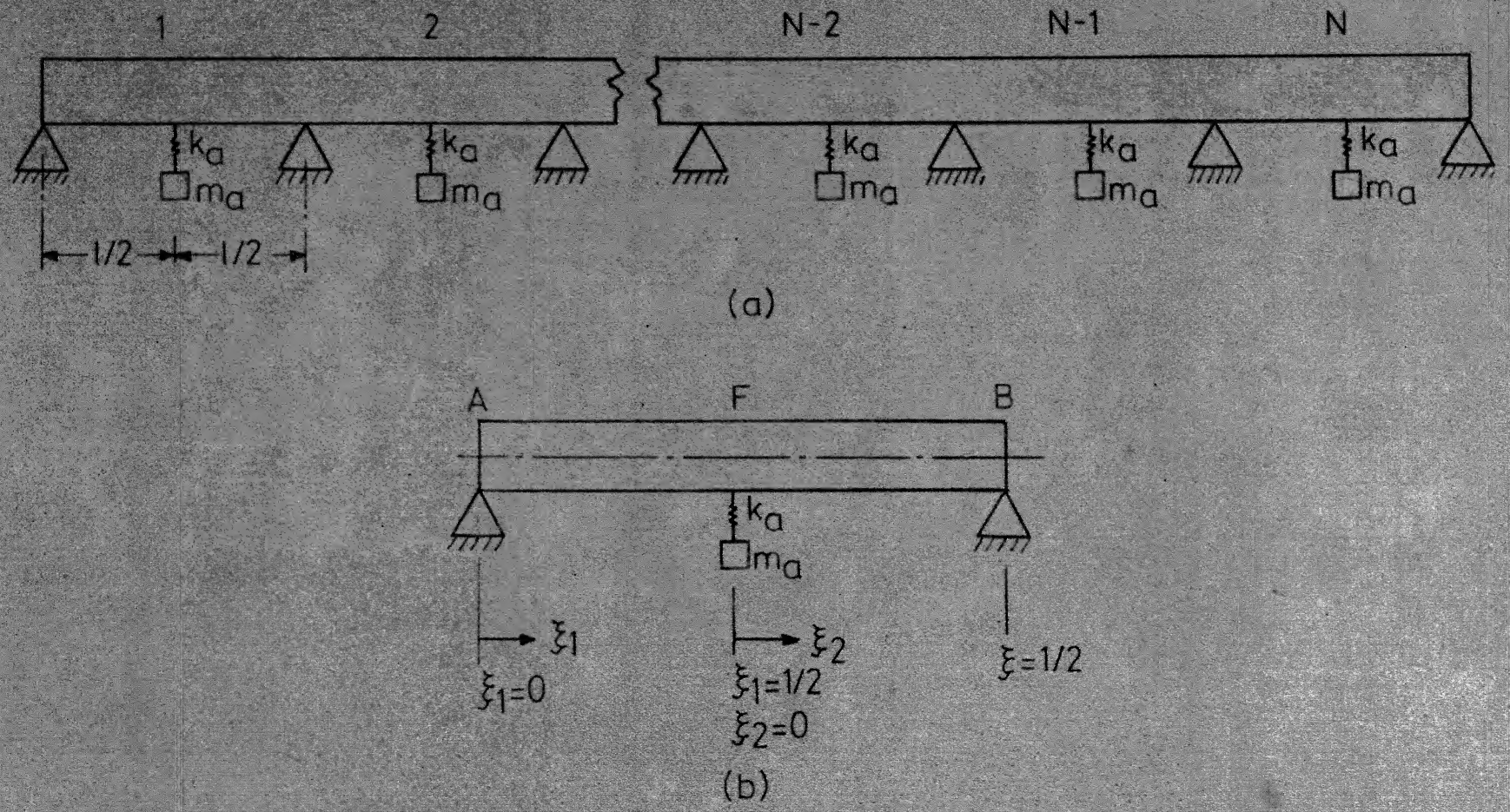

Figure 4.3 - (a) Undamped dynamic absorbers attached to a periodically supported N-span pipe, (b) Periodic element of the system shown above.

4.3 Undamped Dynamic Absorber Attached at the Mid-Point of Each Bay of a Periodically Supported Finite Pipe

Figure 4.3a shows a periodically supported N-span pipe. Identical undamped dynamic absorbers are attached at the mid-point of each span. The effect of attaching these absorbers on the regions of instabilities of the pipe is investigated in this section.

If the absorber is undamped, i.e., $\Delta = 0$, equation (4.7) describing the motion of the absorber mass, m_a, in any bay, reduces to

$$y_a = \ell A_o \{\bar{X}_1(\tfrac{1}{2}) \sin(\tfrac{1}{2}\Omega\tau) + \bar{Y}_1(\tfrac{1}{2}) \cos(\tfrac{1}{2}\Omega\tau)\} , \qquad (4.24)$$

where $$A_o = \frac{1}{1 - \frac{1}{4\sigma_a^2}(\frac{\Omega}{\Omega_o})^2} .$$

Let us consider any span of the pipe, say AB shown in Figure 4.3b. The displacement of the pipe, $\bar{y}_1$, in this span is given by equations (4.12). At the mid-point of the span, the change in shear force must be equal to the inertia force of the absorber mass, m_a. This result in

$$(\frac{EI}{\ell^2}) [- \bar{y}_1'''^1 (\tfrac{1}{2}) + \bar{y}_1'''^2(0)] = - m_a \frac{d^2 y_a}{dt^2} \qquad (4.25)$$

Substituting y_a from equation (4.24) into equation (4.25), we get

$$\{\bar{X}_1'''^1(\tfrac{1}{2}) - \bar{X}_1'''^2(0) + \tfrac{1}{4} \Gamma_a \Omega^2 A_o \bar{X}_1^1(\tfrac{1}{2})\} \sin(\tfrac{1}{2}\Omega\tau)$$

$$+ \{\bar{Y}_1'''^1(\tfrac{1}{2}) - \bar{Y}_1'''^2(0) + \tfrac{1}{4} \Gamma_a \Omega^2 A_o \bar{Y}_1^1(\tfrac{1}{2})\} \cos(\tfrac{1}{2}\Omega\tau) = 0 \qquad (4.26)$$

Since this equation holds good for all values of τ, one gets

$$\bar{X}_1'''^1(\tfrac{1}{2}) - \bar{X}_1'''^2(0) + \frac{1}{4} r_a \Omega^2 A_o \bar{X}_1^1(\tfrac{1}{2}) = 0 \qquad (4.27a)$$

$$\bar{Y}_1'''^1(\tfrac{1}{2}) - \bar{Y}_1'''^2(0) + \frac{1}{4} r_a \Omega^2 A_o \bar{Y}_1^1(\tfrac{1}{2}) = 0 \qquad (4.27b)$$

If we examine the boundary conditions for the pipes dealt in section 4.2.2, it is found that the boundary conditions relating the change in shear force at point F, are coupled in $\bar{X}_1$ and $\bar{Y}_1$. However, for the present case with an undamped absorber, we get uncoupled equations (4.27) in $\bar{X}_1$ and $\bar{Y}_1$. Thus, one boundary of the instability regions can be obtained by solving equation (3.51a) with the corresponding boundary conditions. Similarly, the other boundary of the instability regions is obtained by solving equation (3.51b) with the corresponding boundary conditions.

To find the natural frequencies of the system governed by equation (3.51a), the 'wave approach' outlined in section 2.3 can be used. The propagation constants are obtained by using equation (2.3). The receptances to be used in this equation are obtained in the manner discussed below.

To calculate the receptances β_{AA} and β_{BB}, apply a non-dimensional unit harmonic moment $\sin(\frac{1}{2}\Omega\tau)$ at the end A of the span AB. The boundary conditions are :

$$\bar{X}_1^1(0) = 0 , \qquad -\bar{X}_1''^1(0) = 1 ,$$

$$\bar{X}_1^2(\tfrac{1}{2}) = 0 , \qquad -\bar{X}_1''^2(\tfrac{1}{2}) = 0 , \tag{4.28}$$

$$\bar{X}_1^1(\tfrac{1}{2}) = \bar{X}_1^2(0) , \qquad \bar{X}_1'^1(\tfrac{1}{2}) = \bar{X}_1'^2(0) ,$$

$$\bar{X}_1''^1(\tfrac{1}{2}) = \bar{X}_1'^2(0) , \qquad \bar{X}_1''^1(\tfrac{1}{2}) - \bar{X}_1''^2(0) + \tfrac{1}{4}\Gamma_a \Omega^2 A_o \bar{X}_1^1(\tfrac{1}{2}) = 0$$

Use of equations (4.13a) and (4.13c) in equations (4.28), results in the following system of equations.

$$Z_a C = T_1 , \tag{4.29}$$

where Z_a is a matrix (of order 8 x 8) and its elements are given in Appendix 4.

$$C = \{C_{11}^1 \; C_{12}^1 \; C_{13}^1 \; C_{14}^1 \; C_{11}^2 \; C_{12}^2 \; C_{13}^2 \; C_{14}^2\}^t ,$$

and $$T_1 = \{0 \;\; 1 \;\; 0 \;\; 0 \;\; 0 \;\; 0 \;\; 0 \;\; 0\}^t ,$$

with t denoting the transpose.

The receptances β_{AA} and β_{BA} are given as

$$\beta_{AA} = \bar{X}_1'^1(0) = \sum_{n=1}^{4} C_{1n}^1 \lambda_{1n} ,$$

$$\beta_{BA} = \bar{X}_1'^2(\tfrac{1}{2}) = \sum_{n=1}^{4} C_{1n}^2 \lambda_{1n} e^{\lambda_{1n}/2} ,$$

where the C_{1n}^1's and the C_{1n}^2's are solutions of equation (4.29).

To calculate the receptances β_{AB} and β_{BB}, apply a non-dimensional unit harmonic moment $\sin(\frac{1}{2}\Omega\tau)$ at the end B of the span AB. The system of equations obtained in this case is

$$Z_a \; C = T_1', \tag{4.30}$$

where $T_1' = \{0 \quad 0 \quad 0 \quad 1 \quad 0 \quad 0 \quad 0 \quad 0\}^t$.

The receptances β_{AB} and β_{BB} can be written as

$$\beta_{AB} = \bar{X}_1'^1(0) = \sum_{n=1}^{4} C_{1n}^1 \lambda_{1n},$$

$$\beta_{BB} = \bar{X}_1'^2(\tfrac{1}{2}) = \sum_{n=1}^{4} C_{1n}^2 \lambda_{1n} e^{\lambda_{1n}/2},$$

where the C_{1n}^1's and C_{1n}^2's are solutions of equation (4.30).

The other boundary of the instability regions is obtained by solving equation (3.51b) in the similiar manner as discussed above for the solution of equation (3.51a). In this case, the receptances are to be calculated with a non-dimensional harmonic moment $\cos(\frac{1}{2}\Omega\tau)$.

Once the propagation constants have been determined, natural frequencies can be found out by using the graphical approach developed in section 2.3.

4.4 Results and Discussions

4.4.1 Computations Performed

Using the analyses presented in previous sections, numerical results, listed below, have been obtained. As in Chapter 3, the instability regions have been presented as plots of frequency versus the excitation parameter. The value of the excitation parameter upto 0.5 has been considered.

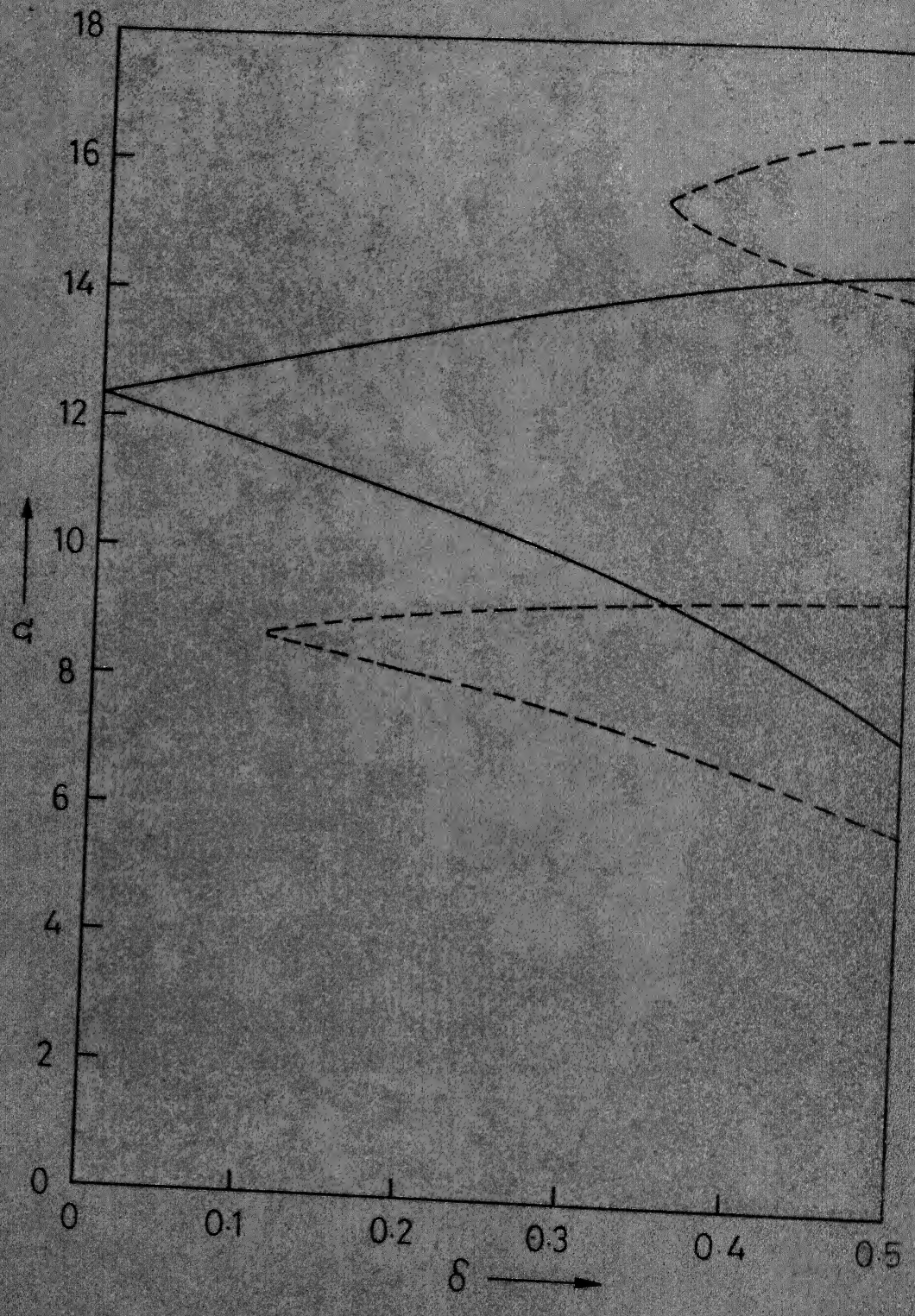

Figure 4.4 - Instability regions of a pinned-pinned pipe with and without the absorber. $u_0=2$, $\gamma=2$, $\sigma_a=0.9$, $\mathcal{J}_a=0.1$, and $\Gamma_a=0.2$; ——, without absorber; – – – –, with absorber.

(i) The instability regions of a pinned-pinned pipe with and without the absorber have been obtained.

(ii) The effects of various parameters of the absorber have been studied by obtaining the instability regions of a pinned-pinned pipe with various combinations of these parameters.

(iii) Results have been obtained to study the effect of u_o and γ on the instability regions of a pinned-pinned pipe when an absorber is attached to it.

(iv) The instability regions of clamped-clamped, and clamped-pinned pipes with absorbers attached at their mid-points have also been computed.

(v) The analysis presented in section 4.3 has been checked by determining the instability regions of a two span pipe with identical undamped absorbers at the mid-point of each bay.

Only a limited range of frequency covering the principal instability region without the absorber has been investigated in all the cases.

4.4.2 Effect of an Absorber on the Instability Regions

To study the effect of a dynamic absorber on the instability regions, ___ results have been obtained for a pinned-pinned pipe with and without the absorber. The method presented in section 3.7 has been used for the pipe without an absorber. Using the method outlined in section 4.2.2, instability regions of a pipe with an absorber have been obtained. For the purpose of comparison, both the results have been shown in Figure 4.4.

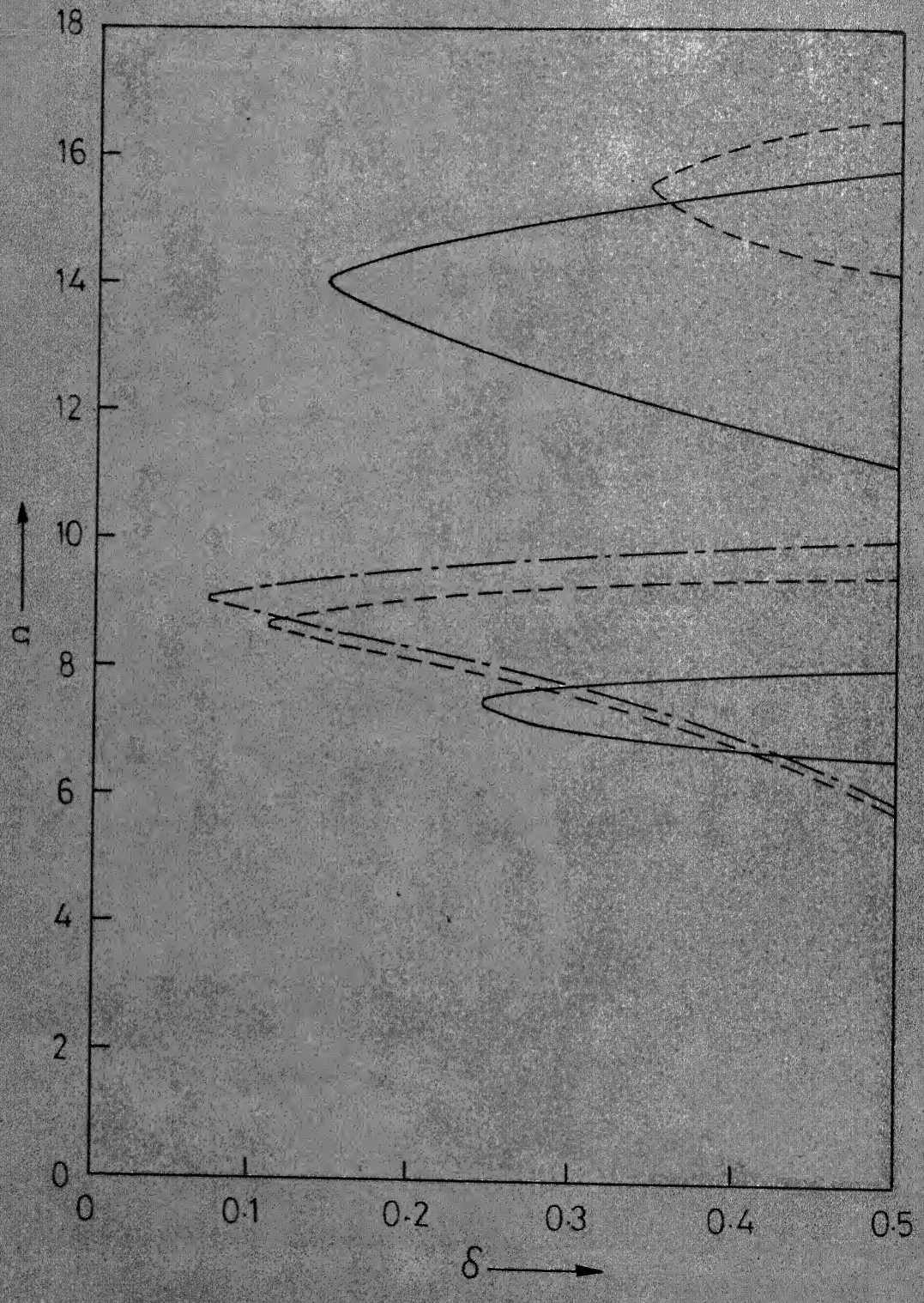

Figure 4.5 - The effect of tuning ratio of the absorber on the regions of instability of a pinned-pinned pipe. $u_0=2$, $\gamma=2$, $\zeta_a=0.1$ and $r_a=0.2$; ——, $\sigma_a=0.7$; – – –, $\sigma_a=0.9$; —·—, $\sigma_a=1.0$.

It is seen from Figure 4.4 that the attachment of an absorber has marked effect on the regions of instability. Without the absorber, only one region of instability is obtained, while with the absorber there are two regions of instabilities over the same range of frequencies. However, the widths of these two regions are quite small as compared to the original one. It is also seen that the instability regions obtained with the absorber are distinctly separated from each other. Moreover, approximately the entire instability region without the absorber has been converted to a region of stability when the absorber is attached to the pipe.

4.4.3 Effect of the Absorber Parameters

Effects of various parameters of the absorber on the regions of instability of a pinned-pinned pipe have been shown in Figures 4.5 - 4.8.

Figure 4.5 shows the instability regions for various values of the tuning ratio, σ_a, of the absorber. It is seen that with low tuning ratio, the first region is quite narrow and the critical value of δ, required for this region to start, is very large. On the other hand, the second region with this tuning ratio is quite wide and critical value of δ is rather small. With increase in σ_a, the first region shifts to higher frequencies and becomes wider. The critical value of the δ is also reduced. Whereas, the second region becomes narrower and the critical value of δ increases considerably. It is also seen that the second region is totally eliminated upto $\delta = 0.5$ for $\sigma_a \geq 1.0$. Thus, the effect of the tuning ratio on the two regions (obtained with the

absorber) is of opposite nature.

Figure 4.6 shows the effect of the damping ratio, on the regions of instability. The effect is seen to be quite significant. The second region of the instability is much affected by the damping of the absorber. It is totally eliminated for damping ratios higher than 0.05.

The effect of the damping ratio, ζ_a, on the first region of instability can be summarised as follows. Upto a certain value, the damping diminishes the extent of the instability regions, but beyond that critical value, the regions become quite wide and the critical value of δ starts reducing. This behaviour of damping shows that there is an optimum value of ζ_a. This optimum value of ζ_a can be determined only for given objectives like, critical value of δ should be maximum or the width of the region should be minimum, etc.

Figure 4.7 shows the instability regions for a pinned-pinned pipe with different mass ratios when an undamped dynamic absorber is attached to it. It is seen that with the decrease in the mass ratio, Γ_a, both the regions of instability get closer to each other. Eventually, with zero mass ratio, i.e., without the absorber, only one region of instability is obtained. Figure 4.8 shows the effect of the mass ratio, Γ_a, when damping in the absorber is also considered. It is seen that the effect is similar to that of an undamped absorber. But with a damped absorber, a critical value of δ is required to cause instability. It is also seen from Figure 4.8 that for low values of the mass ratio of the absorber, Γ_a, only one region is obtained. For large values of δ, the width of this region is comparable with the region obtained without

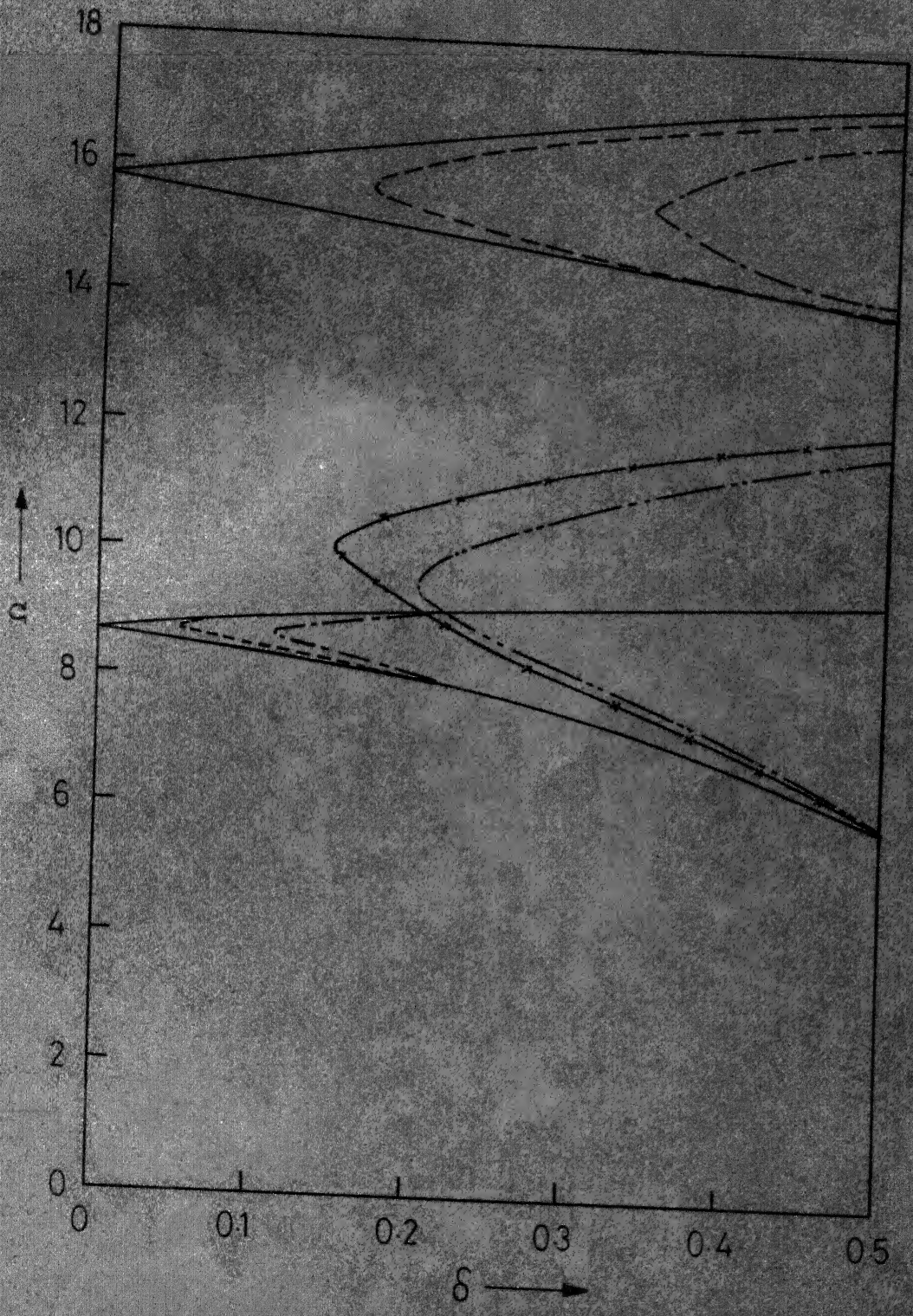

e 4·6 - The effect of damping ratio of the absorber on the regions
t instability of a pinned-pinned pipe $u_0=2$, $\gamma=2$, $\sigma_a=0.9$, and
$\Gamma_a=0.2$; ——, $\zeta_a=0$; - - - -, $\zeta_a=0.05$; — — —, $\zeta_a=0.1$ —··—··—, $\zeta_a=0.5$;
—×—, $\zeta_a=0.8$.

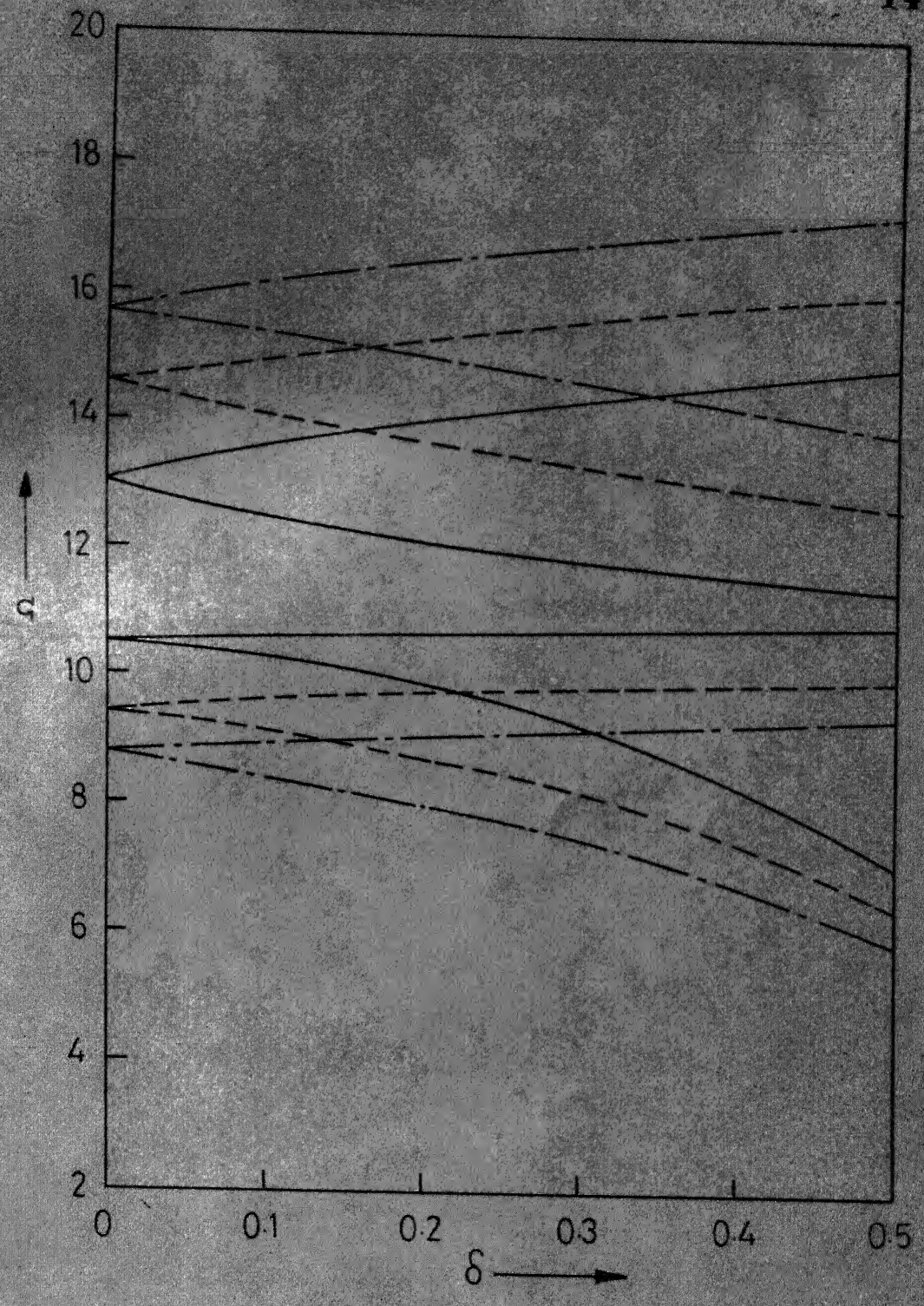

Figure 4.7 - The effect of mass ratio of an undamped absorber on the regions of instability of a pinned-pinned pipe. $u_0=2$, $\gamma=2$, $\sigma_a=0.9$, $\zeta_a=0$; ———, $\Gamma_a=0.02$; – – – –, $\Gamma_a=0.1$; —·—·—, $\Gamma_a=0.2$.

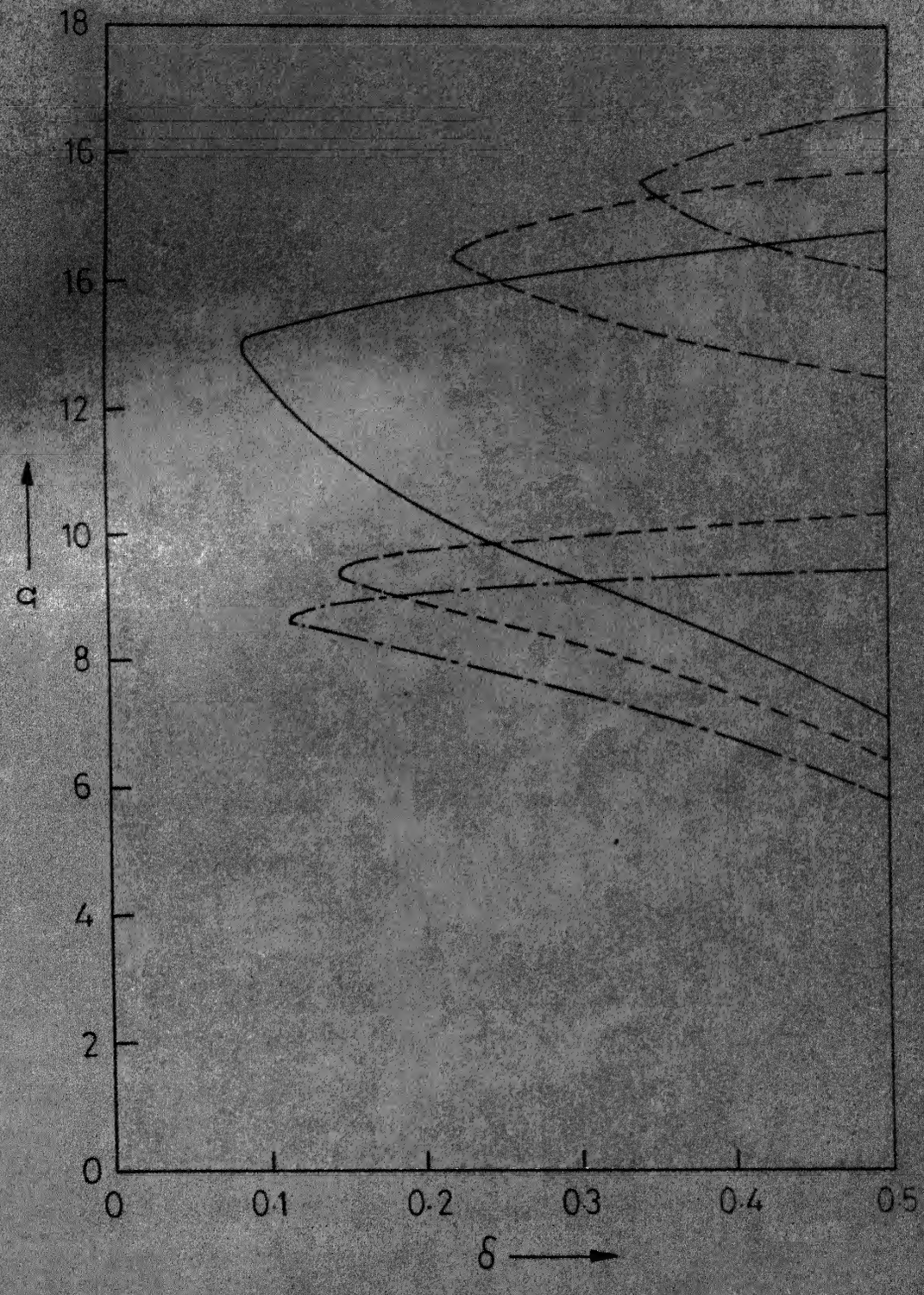

Figure 4.8 – The effect of mass ratio of a damped absorber on the regions of instability of a pinned-pinned pipe. $u_0=2$, $\gamma=2$, $\sigma_a=0.9$, $\zeta_a=0.1$; ———, $\Gamma_a=0.02$; – – –, $\Gamma_a=0.1$; ——·——, $\Gamma_a=0.2$.

the absorber (Figure 4.4). For large values of Γ_a, two instability regions are obtained and the widths of these regions are small in comparison to the region obtained without the absorber (Figure 4.4). This behaviour of Γ_a indicates that there exists a critical value of Γ_a to have two regions of instability. Furthermore, examining Figures 4.7 and 4.8, it is concluded that the damping has more pronounced effect on the second region (in case it is there) than the first region of instability.

4.4.4 Effect of the Pressure and the Constant Mean Velocity of the Fluid

Figure 4.9 shows the effect of the fluid pressure, γ, on the regions of instability of a pinned-pinned pipe with an absorber ($\sigma_a = 0.9$, $\zeta_a = 0.1$ and $\Gamma_a = 0.2$) attached to it. It is seen that with increase in γ, the instability region becomes wider and the critical value of δ reduces. For sufficiently large value of γ, there may be even two regions of instability. Examining Figures 4.4 and 4.9 together, it is seen that the second region (in case it is there) experiences similar effect of γ as the first region discussed above.

Figure 4.10 shows the effect of the constant mean velocity, u_o, on the regions of instability of a pinned-pinned pipe with an absorber ($\sigma_a = 0.9$, $\zeta_a = 0.05$, $\Gamma_a = 0.2$) attached to it. It is seen that increase in u_o reduces the critical value of δ. There may be two regions of instability for large values of u_o. It is also seen from Figure 4.10 that there is no unstable region for u_o less than 1.0. If the damping in the absorber is increased to $\zeta_a = 0.1$ from 0.05, the instability region associated with $u_o = 1$ has been found to be eliminated upto

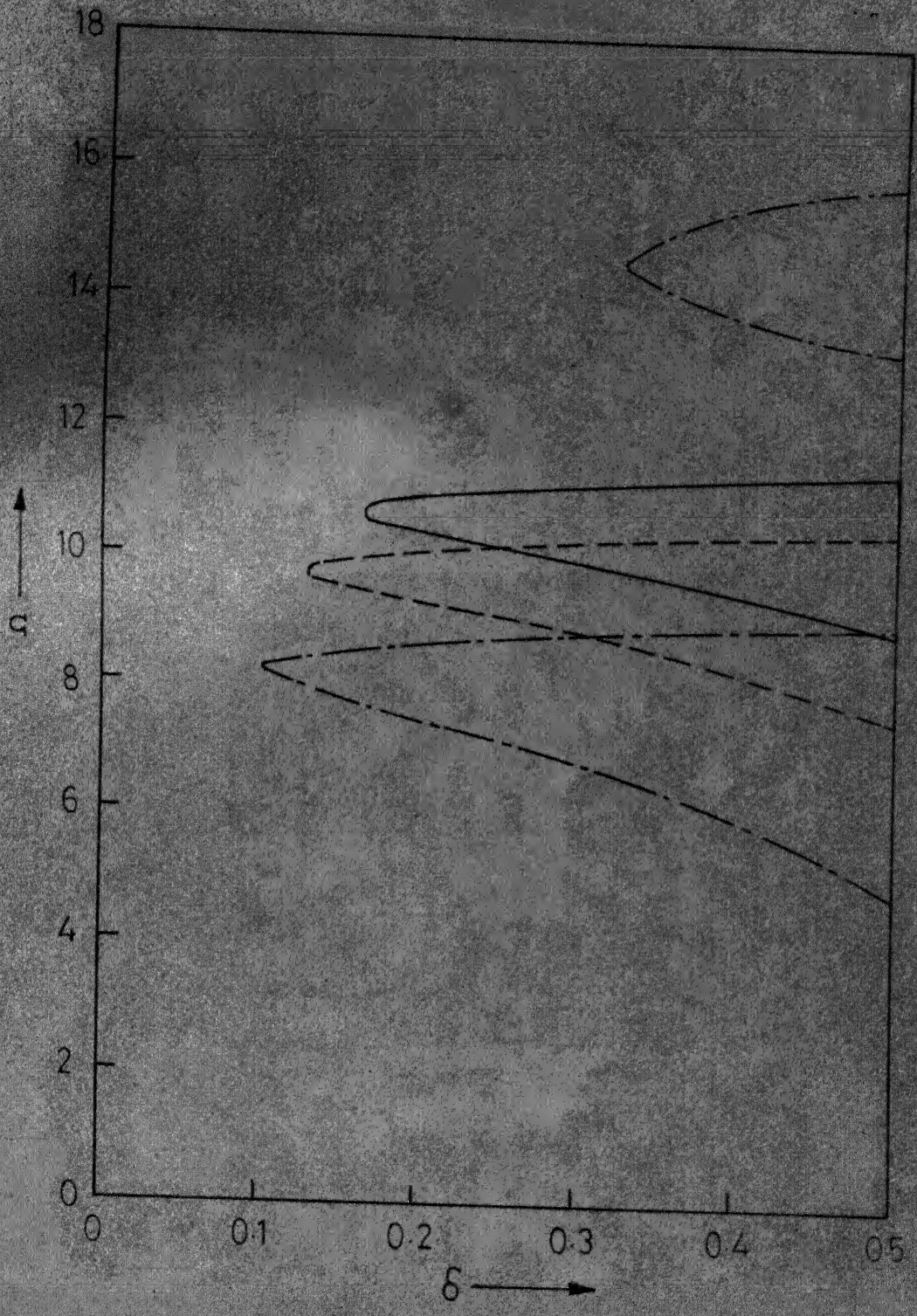

Figure 4·9 - The effect of the fluid pressure on the regions of instability of a pinned-pinned pipe with an absorber attached to it. $u_0 = 2$, $\sigma_a = 0.9$, $\Im_a = 0.1$, $\Gamma_a = 0.2$; ———, $\gamma = 0$; – – – –, $\gamma = 1$; —·—, $\gamma = 2.5$.

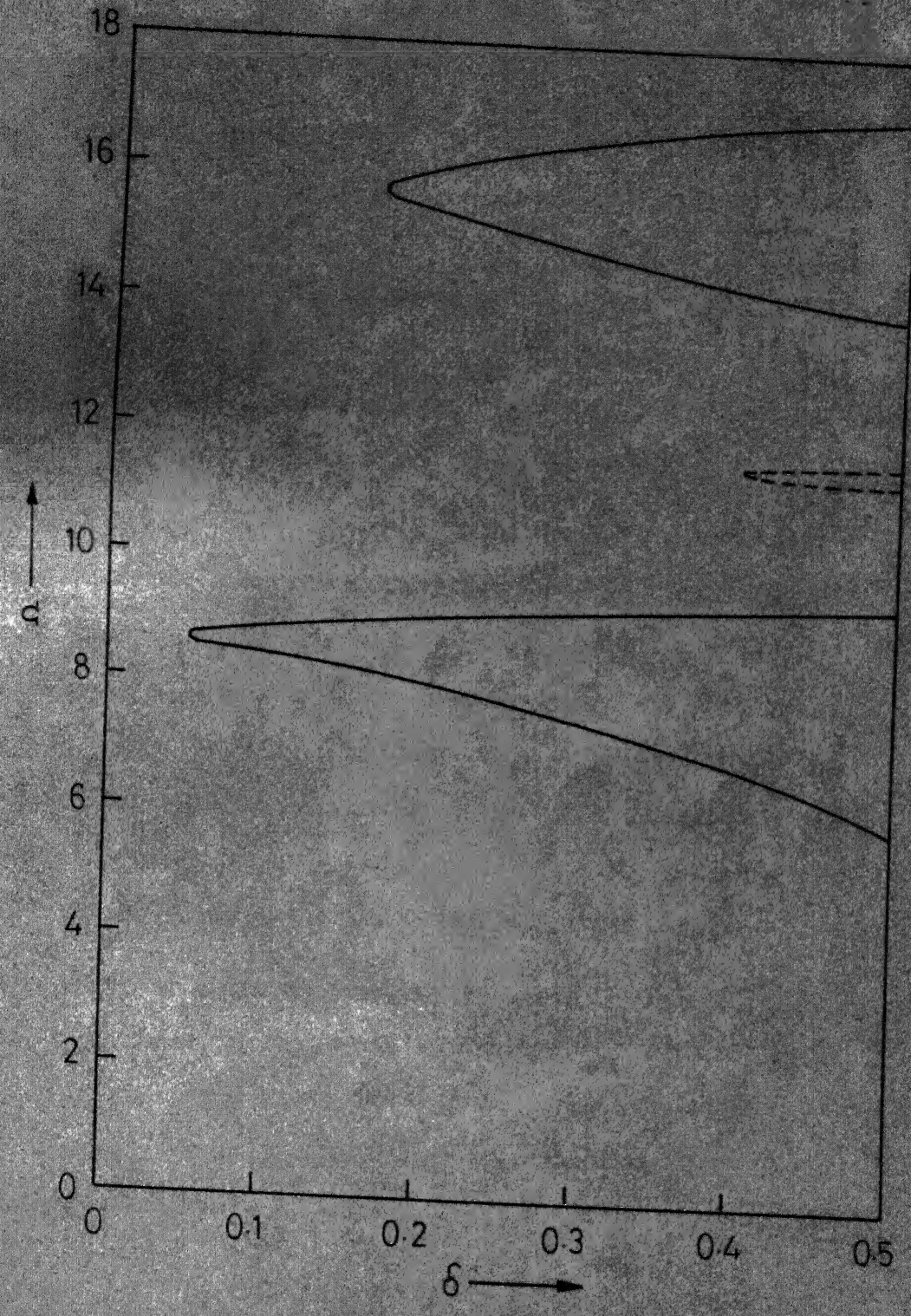

Figure 4.10 - The effect of the constant mean velocity of the fluid on the regions of instability of a pinned-pinned pipe with an absorber attached to it. $\gamma = 2, \sigma_a = 0.9, \zeta_a = 0.05; \Gamma_a = 0.2$; ----, $u_0 = 1$; ——, $u_0 = 2$.

$\delta = 0.5$. The instability region for $u_o = 2$ has already been shown in Figure 4.4.

4.4.5 Pipes with Other End Conditions

Results with other end conditions indicated very similar trends of effects of various parameters as observed in the pinned-pinned case. Hence, only representative curves are discussed below, one each for a clamped-pinned pipe and a clamped-clamped pipe.

Figure 4.11 shows the regions of instability of a clamped-pinned pipe with the absorber attached at its mid-point. It is seen that with an undamped absorber, two regions of instability are obtained. These regions are greatly affected by the damping present in the absorber. The effect is similar to that on the instability regions of pinned-pinned pipes. The first region of instability is totally eliminated upto $\delta = 0.5$ when the damping in the absorber is taken as $\zeta_a = 0.1$. The critical value of δ for second region becomes approximately 0.36 with $\zeta_a = 0.1$.

Figure 4.12 shows the instability regions of a clamped-clamped pipe with the absorber attached to it. It is seen that like in other cases, with an undamped absorber, two regions of instability are obtained. The damping has more pronounced effect on the instability regions of the pipe under consideration in comparison to its effect on the instability regions of the pipe with other end conditions. No unstable region is obtained if the damping in the absorber is taken as $\zeta_a = 0.1$ with other parameters being same as shown in Figure 4.12.

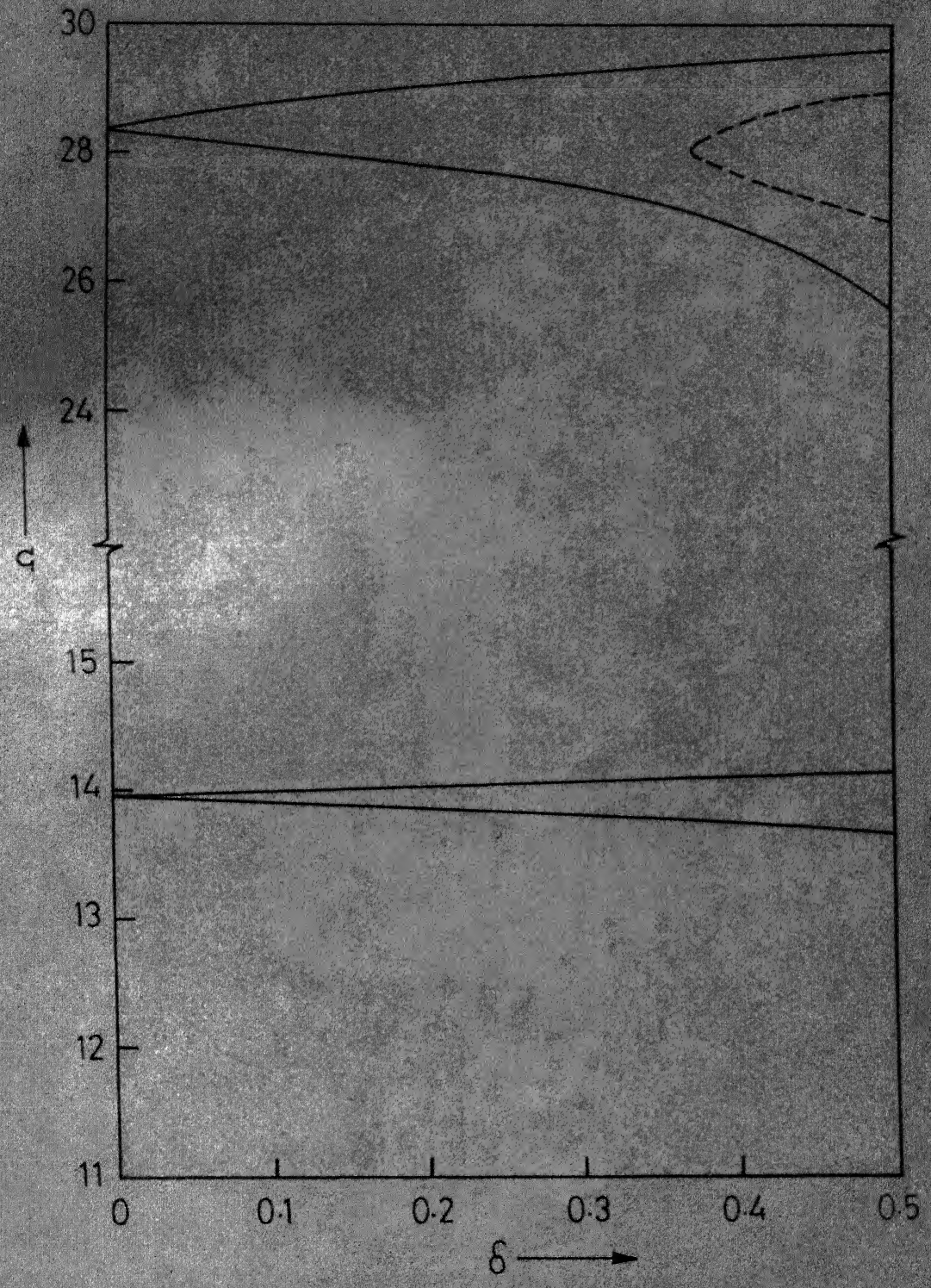

Figure 4·11 - The instability regions of a clamped-pinned pipe with an absorber attached to it. $u_0=2$, $\gamma=2$, $\sigma_a=1{\cdot}25$, $\Gamma_a=0{\cdot}2$; ——, $\zeta_a=0$; – – – –, $\zeta_a=0{\cdot}1$.

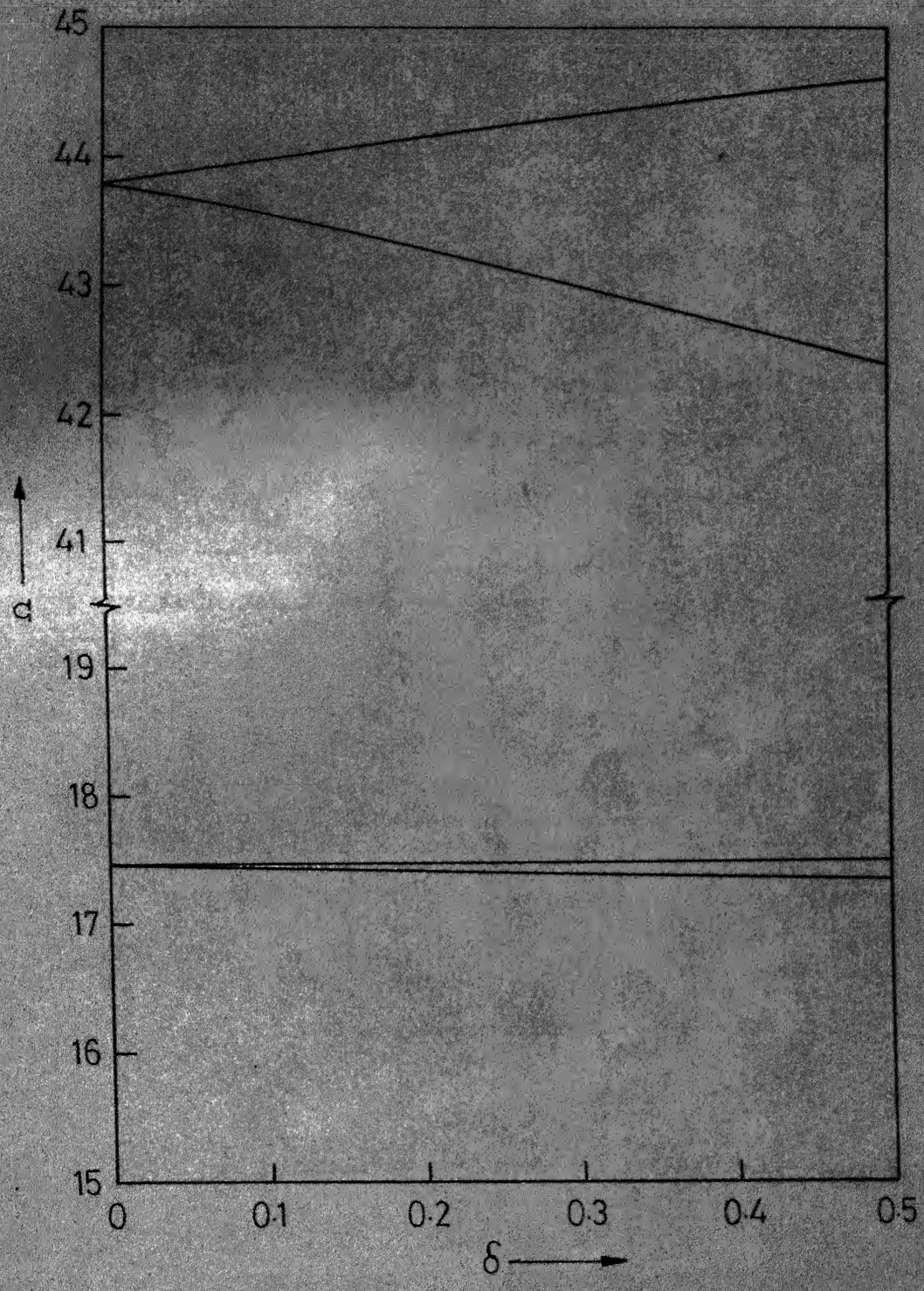

Figure 4.12 - The instability regions of a clamped-clamped pipe with an absorber attached to it. $u_0 = 2, \gamma = 2, \sigma_a = 1.5, \zeta_a = 0, \Gamma_a = 0.2$.

4.4.6 Instability Regions of a Periodically Supported Pipe

The regions of instability of a two span pipe, with identical, undamped absorbers attached at the mid-point of each bay have been determined. The wave approach outlined in section 4.3 has been used to compute the regions of instability.

It has already been stated in Chapter 3 that the instability regions of a periodically supported two span pipe consist of those of a pinned-pinned and a clamped-pinned pipe. Likewise, the instability regions for such two span pipes with absorbers can also be obtained from the results presented above for the pinned-pinned and the clamped-pinned cases. These results have been found to be in excellent agreement with those obtained by using the wave approach.

However for number of spans more than two, the results cannot be extrapolated from the results of single span pipes. In such cases, all the regions of instability can be obtained by using the method discussed in section 4.3.

CHAPTER 5

CONCLUSIONS

5.1 Conclusions

From the results presented in Chapters 2,3, and 4, the following conclusions are drawn.

The dynamics of a periodically supported pipe, conveying fluid at constant velocity and pressure, can be conveniently analysed by studying the free harmonic wave propagation in a similar infinite structure. There exist alternate frequency bands of attenuation and propagation of free harmonic waves.

The effect of rotational stiffnesses at the supports is to shift the start of the propagation bands to higher frequencies, whereas the ends of the propagation bands are independent of the rotational stiffness. Both the ends of the propagation bands shift to lower frequencies with increasing pressure and velocity of the fluid.

Free harmonic waves travel with different velocities in the positive and the negative directions. This is due to the presence of the Coriolis acceleration term in the equation of motion of the pipe. Natural frequencies of a periodically supported pipe can be easily determined from the curves of propagation constant. Propagation constant values can also be used to determine the natural frequencies of a pipe resting on identical supports (with rotational constraints) at regular intervals. In both the above cases, the amount of computation

is independent of the number of spans of the pipe. Furthermore, the static buckling of periodically supported pipes can also be studied from the values of the propagation constants.

The response of a periodically supported infinite pipe to a convected harmonic pressure field can be determined using the wave approach. The 'coincidence' occurs at a higher frequency with increasing convection velocity of the pressure field. Moreover, the 'coincidence' frequency depends on the direction of the convected pressure field, i.e., whether in the same or in the opposite direction of the fluid flow. The damping in the pipe is more effective in controlling the response than the damping in the supports.

When the velocity of the fluid is not constant and is having a harmonic fluctuation over and above a constant mean value, the pipe experiences parametric instabilities.

Out of the three methods presented for determination of these instabilities, the first method requires prior knowledge of the mode shapes of a periodically supported beam. This method also becomes unwieldy for large number of spans in the pipe. The number of modes to be considered depends on various factors, such as desired accuracy of the results, number of instability regions to be determined, etc.

The second method does not require any mode shape approximation and the instability regions associated with all the modes are obtained from the zeros of a determinant. The order of this determinant, however, increases drastically with the number of spans of the pipe.

The third method using the wave approach is most suitable if the number of spans are more than two. A simple graphical approach can be used to determine all the regions of instability. In this method, the amount of computation is independent of the number of spans of the pipe.

The mass ratio parameter (β) does not have any significant effect on the regions of the instability. Thus, neglecting this parameter the analysis can be made considerably simpler without any sacrifice in the accuracy.

With increase in the pressure and the velocity of the fluid the instability regions become wider and are shifted to lower frequencies.

Damping in the pipe reduces the extent of the instability regions and a finite value of the excitation parameter is required to start the instability. Damping has more pronounced effect on the instability regions associated with the higher modes. Hysteretic damping is more effective, as compared to viscous damping, in controlling the instability regions.

The instability regions of a pipe are markedly affected by attachment of dynamic absorbers. The wave approach can also be used to determine the instability regions of a periodically supported pipe with absorbers attached to each bay.

In the same range of frequency, the number of instability regions with an absorber are generally more than those without it. However, the widths of these regions are much smaller than the original regions. The regions can also be effectively controlled by varying parameters like

the mass ratio, the tuning ratio and the damping ratio of the absorber. The trends of the effects of these parameters suggest the existence of their optimum values. Hence, depending upon specific requirements, the optimum values of these parameters can be determined.

5.2 Recommendations for Future Work

In view of the results obtained in the present thesis, following recommendations can be made regarding future work in the area.

(i) Effect of axial tension and contraction of the pipe, neglected in the present work, can be accounted for.

(ii) Regions of combinational resonances for a periodically supported pipe can be investigated.

(iii) The problem of parametric instabilities of pipes with random fluctuations in the fluid velocity can be studied.

(iv) With a suitable choice of an objective function, optimisation of the absorber parameters for the best control of the parametric instabilities of pipes can be attempted.

REFERENCES

1. Archibald, F.R. and Emslie, A.S. 1958 Journal of Applied Mechanics 25, 347-348. The vibration of a string having a uniform motion along its length.

2. Ashley, H. and Haviland, G. 1950 Journal of Applied Mechanics 17, 229-232. Bending vibrations of a pipe line containing flowing fluid.

3. Benjamin, T.B. 1961 Proceedings of the Royal Society (London) A, 261, 457-486. Dynamics of a system of articulated pipes conveying fluid. I. Theory.

4. Benjamin, T.B. 1961 Proceedings of the Royal Society (London) A, 261, 487-499. Dynamics of a system of articulated pipes conveying fluid. II. Experiments.

5. Bishop, R.E.D. and Johnson, D.C. 1960 The Mechanics of Vibration. Cambridge : Cambridge University Press.

6. Bolotin, V.V. 1963 Nonconservative Problems of the Theory of Elastic Stability. Oxford : Pergamon Press.

7. Bolotin, V.V. 1964 The Dynamic Stability of Elastic Systems. San Francisco : Holden Day Inc.

8. Brillouin, L. 1946 Wave Propagation in Periodic Structures. New York : Dover Publications.

9. Chen, S.S. 1971 American Society of Mechanical Engineers, Paper 71-Vibr-39. Flow-induced instability of an elastic tube.

10. Chen, S.S. 1971 Journal of the Engineering Mechanics Division, Proceedings of the American Society of Civil Engineers 97, 1469-1485. Dynamic stability of a tube conveying fluid.

11. Chen, S.S. 1975 Journal of Engineering for Industry, Transcations of the American Society of Mechanical Engineers 97, 1212-1218. Vibrations of a row of circular cylinders in a liquid.

12. Chen, S.S. and Rosenberg, G.S. 1974 Journal of Engineering for Industry, Transactions of the American Society of Mechanical Engineers 96, 420-426. Free vibrations of fluid conveying cylindrical shells.

13. Chubachi, T. 1958 Bulletin of the Japan Society of Mechanical Engineers 1, 24-29. Lateral vibration of axially moving wires or belt form materials.

14. Dodds, H.L. Jr. and Runyan, H.L. 1965 NASA Technical Note D-2870. Effect of high velocity fluid flow on the bending vibrations and static divergence of a simply supported pipe.

15. Feodos'ev , V.P. 1951 Inzhenernyi Sbornik 10, 169-170. Vibrations and stability of a pipe when liquid flows through it.

16. Ginsberg, J.H. 1973 International Journal of Engineering Science 11, 1013-1024. The dynamic stability of a pipe conveying a pulsatile flow.

17. Gregory, R.W. and Païdoussis, M.P. 1966 Proceedings of the Royal Society (London) A, 293, 512-527. Unstable oscillation of tubular contilevers conveying fluid. I. Theory.

18. Gregory, R.W. and Païdoussis, M.P. 1966 Proceedings of the Royal Society (London) A, 293, 528-542. Unstable oscillation of tubular cantilevers conveying fluid. II. Experiments.

19. Handelman, G.H. 1955 Quarterly of Applied Mathematics 13, 326-330. A note on the transverse vibration of a tube containing flow fluid.

20. Heckl, M. 1964 Journal of the Acoustical Society of America 36, 1335-1343. Investigations on the vibrations of grillages and other simple beam structures.

21. Herrmann, G. 1967 Applied Mechanics Reviews 20, 103-108. Stability of equilibrium of elastic systems subjected to non-conservative forces.

22. Hermann, G. and Nemat-Nasser, S. 1967 International Journal of Solids and Structures 3, 39-52. Instability modes of cantilevered bars induced by fluid flow through attached pipes.

23. Housner, G.W. 1952 Journal of Applied Mechanics 19, 205-208. Bending vibrations of a pipeline containing flowing fluid.

24. Lee, L.S.S. 1975 Journal of Engineering for Industry, Transactions of the American Society of Mechanical Engineers 97, 23-32. Vibrations of an intermediately supported U-bendtube.

25. Lin, Y.K. 1962 Journal of Aero Space Sciences 29, 67-86. Stresses in continuous skin stiffener panels under random loading.

26. Lin, Y.K. and McDaniel, T.J. 1969 American Society of Mechanical Engineers, Paper 69-Vibr-17. Dynamics a beam-type periodic structures.

27. Liu, H.S. and Monte, C.D. Jr. 1973 American Society of Mechanical Engineers, Paper 73-DET-118. Dynamic response of pipes transporting fluids.

28. Long, R.H. Jr. 1955 Journal of Applied Mechanics 22, 65-68. Experimental and theoretical study of transverse vibration of a tube containing flowing fluid.

29. Mahalingam, S. 1957 British Journal of Applied Physics 8, 145-148. Transverse vibration of power transmission chains.

30. Mead, D.J. 1970 Journal of Sound and Vibration 11, 181-187. Free wave propagation in periodically-supported, infinite beams.

31. Mead, D.J. 1971 Journal of Engineering for Industry, Transactions of American Society of Mechanical Engineers, 93, 783-792. Vibration response and wave propagation in periodic structures.

32. Mead, D.J. 1973 Journal of Sound and Vibration 27, 253-260. A general theory of harmonic wave propagation in linear periodic systems with multiple coupling.

33. Mead, D.J. 1975 Journal of Sound and Vibration 40, 1-18. Wave propagation and natural modes in periodic systems. I. Mono-coupled systems.

34. Mead, D.J. 1975 Journal of Sound and Vibration 40, 19-39. Wave propagation and natural modes in periodic systems. II. Multi-coupled systems, with and without damping.

35. Mead, D.J. and Mallik, A.K. 1976 Journal of Sound and Vibration 47, 457-471. An approximate method of predicting the response of periodically supported beams subjected to random convected loading.

36. Mead, D.J. and Bujara, K.K. 1971 Journal of Sound and Vibration 14, 525-541. Space-harmonic analysis of periodically supported beams : response to convected random loading.

37. Meirovitch, L. 1967 Analytical Methods in Vibrations. New York : The Macmillan Company.

38. Movchan, A.A. 1965 Journal of Applied Mathematics and Mechanics 29, 760-762. On the problem of stability of a pipe with fluid flowing through it.

39. Naguleswaran, S. and Williams, C.J.H. 1968 The Journal of Mechanical Engineering Science 10, 228-238. Lateral vibration of a pipe conveying fluid.

40. Niordson, F.I. 1953 Transactions of the Royal Institute of Technology, Sweden, No. 73. Vibrations of a cylindrical tube containing flowing fluid.

41. Nemat-Nasser, S., Prasad, S.N. and Herrmann, G. 1966 American Institute of Aeronautics and Astronautics Journal 4, 1276-1280. Destabilizing effect of velocity-dependent forces in non-conservative continuous systems.

42. Orris, R.M. and Petyt, M. 1974 Journal of Sound and Vibration 33, 223-236. A finite element study of harmonic wave propagation in periodic structures.

43. Plaut, R.H. and Huseyin, K. 1975 Journal of Applied Mechanics 42, 889-890. Instability of fluid-conveying pipes under axial load.

44. Paidoussis, M.P. 1970 The Journal of Mechanical Engineering Science 12, 85-103, Dynamics of tubular cantilevers conveying fluid.

45. Paidoussis, M.P. and Deksnis, E.B. 1970 The Journal of Mechanical Engineering Science 12, 288-300. Articulated models of cantilevers conveying fluid : the study of a paradox.

46. Paidoussis, M.P. and Denise, J.-P. 1971 Journal of Sound and Vibration 16, 459-461. Flutter of cylindrical shells conveying fluid.

47. Paidoussis, M.P. and Denise, J.-P. 1972 Journal of Sound and Vibration 20, 9-26. Flutter of thin cylindrical shells conveying fluid.

48. Paidoussis, M.P. and Issid, N.T. 1974 Journal of Sound and Vibration 33, 267-294. Dynamic stability of pipes conveying fluid.

49. Paidoussis, M.P. and Sundararajan, C. 1975 Journal of Applied Mechanics 42, 780-784. Parametric and combination resonances of a pipe conveying pulsating fluid.

50. Rao, U.N. and Mallik, A.K. (accepted for publication in Journal of Sound and Vibration) Response of finite periodic beams to convected loading - an approximate method.

51. SenGupta, G. 1970 Journal of Sound and Vibration 13, 89-101. Natural flexural waves and the normal modes of periodically supported beams and plates.

52. Shimoyama, T. 1958 Transactions of the Japan Society of Mechanical Engineers 1, 24-29. Vibration of running belt.

53. Singh, K. and Mallik, A.K. 1977 Journal of Sound and Vibration 54, 55-66 . Wave propagation and vibration response of a periodically supported pipe conveying fluid.

54. Snowdon, J.C. 1968 Vibration and Shock in Damped Mechanical Systems. New York : John Wiley & Sons, Inc.

55. Srinivasan, P. and Kamath, M.P. 1970 Journal of Institution of Engineers (India), Mechanical Engineering Division 50, 149-154. Natural frequencies of vibrations of a tubular cantilever pipe conveying flowing fluid.

56. Srinivasan, P. and Lakshminarayanan, V. 1970 Transport Engineering Journal, Proceedings of the American Society of Civil Engineers 96, 165-174. Vibration of pipe carrying flowing fluid.

57. Stein, R.A. and Torbiner, M.W. 1970 Journal of Applied Mechanics 92, 906-916. Vibration of pipes containing flowing fluid.

58. Swope, R.D. and Ames, W.F. 1963 Journal of the Franklin Institute 275, 36-55. Vibrations of a moving threadline.

59. Thurman, A.L. and Monte, C.D. Jr. 1969 Journal of Engineering for Industry, Transactions of the American Society of Mechanical Engineers 91, 1147-1155. Non-linear oscillation of a cylinder containing flowing fluid.

60. Volkov, A.N. 1957 Moscow Inzhenierno Stroitelnyi Institut, No. 27, 3-11. Vibration of a cylindrical shell in the flow of a perfect fluid.

61. Weaver, D.S. and Unny, T.E. 1973 Journal of Applied Mechanics 40, 48-52. Dynamic stability of fluid-conveying pipes.

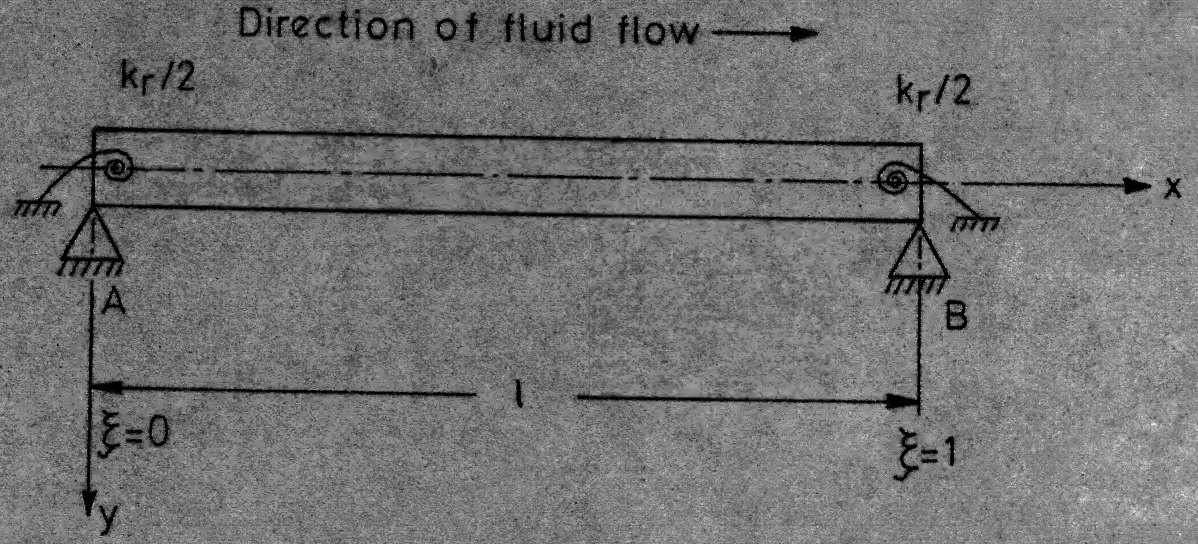

Figure A-1.1 - Pipe representing a periodic element of the system shown in Figure 2.1.

APPENDIX 1

CALCULATION OF RECEPTANCES FOR A PIPE CONVEYING FLUID

Consider a pipe of length ℓ, resting on transversely rigid supports and let the rotational stiffness at each end be $k_r/2$ (Figure A-1.1). This forms a periodic element of the infinite pipeline shown in Figure 2.1. The equation for transverse motion of the pipe, in absence of any external loading, is [57]

$$EI \frac{\partial^4 y}{\partial x^4} + (m_f V^2 + p_f A_p) \frac{\partial^2 y}{\partial x^2} + 2m_f V \frac{\partial^2 y}{\partial x \partial t} + m_f \frac{\partial V}{\partial t} \frac{\partial y}{\partial x} + (m_f + m_p) \frac{\partial^2 y}{\partial t^2} = 0 \qquad (A\text{-}1.1)$$

where EI is the flexural stiffness of the pipe,

y is the displacement of the pipe in the transverse direction,

x is the co-ordinate along the length of the pipe,

m_f is the mass of the fluid per unit length of the pipe,

V is the velocity of the fluid,

p_f is the pressure of the fluid,

A_p is the cross sectional area of the pipe,

and m_p is the mass of the pipe per unit length.

Equation (A-1.1) was derived with the following assumptions:

(i) The pipe behaves like a Euler beam-type structure.

(ii) The supports are such that they produce no axial force in the pipe.

(iii) The axial contraction of the pipe is negligible.

The significance of various terms in equation (A-1.1) can be explained as follows:

The leading term in equation (A-1.1) arises due to the bending of the pipe. The term $m_p \frac{\partial^2 y}{\partial t^2}$ represents the inertia force of the pipe and $pA \frac{\partial^2 y}{\partial x^2}$ is due to the pressure of the fluid. The terms $m_f V^2 \frac{\partial^2 y}{\partial x^2}$ and $2m_f V \frac{\partial^2 y}{\partial x \partial t}$ are due to the centrifugal and the Coriolis acceleration of the fluid (moving in a curved path), respectively. The acceleration due to unsteady flow of the fluid is accounted for by the term $m_f \frac{\partial V}{\partial t} \frac{\partial y}{\partial x}$. Finally, the term $m_f \frac{\partial^2 y}{\partial t^2}$ is the inertia force due to the displacement of the fluid in the transverse direction.

If the velocity and pressure of the fluid are assumed to be constant everywhere, then $\frac{\partial V}{\partial t} = 0$, and equation (A-1.1) reduces to

$$EI \frac{\partial^4 y}{\partial x^4} + (m_f V^2 + p_f A_p) \frac{\partial^2 y}{\partial x^2} + 2m_f V \frac{\partial^2 y}{\partial x \partial t} + (m_f + m_p) \frac{\partial^2 y}{\partial t^2} = 0 \qquad \text{(A-1.2)}$$

For harmonic solutions, by substituting $y = \bar{y} e^{i\omega t}$ in equation (A-1.2), one gets the following equation in terms of the non-dimensional quantities.

$$\frac{d^4 \bar{y}}{d\xi^4} + (u^2 + \gamma) \frac{d^2 \bar{y}}{d\xi^2} + i\, 2\beta u \Omega \frac{d\bar{y}}{d\xi} - \Omega^2 \bar{y} = 0 \,, \qquad \text{(A-1.3)}$$

where $\xi = \frac{x}{\ell}$, $u = \left(\frac{m_f}{EI}\right)^{1/2} V\ell$, $\gamma = \frac{p_f A_p \ell^2}{EI}$,

$$\beta = \left(\frac{m_f}{m_f + m_p}\right)^{1/2}, \quad \Omega = \left(\frac{m_f + m_p}{EI}\right)^{1/2} \omega \ell^2 .$$

The solution of equation (A-1.3) can be written as

$$\bar{y}(\xi) = \sum_{n=1}^{4} C_n e^{i\lambda_n \xi} , \qquad \text{(A-1.4)}$$

where the λ_n's are the roots of the polynomial

$$\lambda^4 - (u^2+\gamma)\lambda^2 - 2\beta u\Omega\lambda - \Omega^2 = 0 \qquad \text{(A-1.5)}$$

To determine the receptances β_{AA} and β_{BA}, used in section 2.2.1, apply a non-dimensional unit harmonic moment at end A, when the boundary conditions are

$$\bar{y}(0) = 0, \qquad \text{(A-1.6a)}$$

$$\bar{y}(1) = 0, \qquad \text{(A-1.6b)}$$

$$-\bar{y}''(0) = 1 - \frac{1}{2}\kappa_r \bar{y}'(0), \qquad \text{(A-1.6c)}$$

$$-\bar{y}''(1) = \frac{1}{2}\kappa_r \bar{y}'(1) , \qquad \text{(A-1.6d)}$$

where $\kappa_r = \dfrac{k_r \ell}{EI}$.

Upon using equation (A-1.4), equations (A-1.6) yield a system of equations

$$QC = R , \qquad \text{(A-1.7)}$$

where

$$Q = \begin{bmatrix} 1 & 1 & 1 & 1 \\ e^{i\lambda_1} & e^{i\lambda_2} & e^{i\lambda_3} & e^{i\lambda_4} \\ \lambda_1^2 + i\lambda_1 \frac{\kappa_r}{2} & \lambda_2^2 + i\lambda_2 \frac{\kappa_r}{2} & \lambda_3^2 + i\lambda_3 \frac{\kappa_r}{2} & \lambda_4^2 + i\lambda_4 \frac{\kappa_r}{2} \\ (\lambda_1^2 - i\lambda_1 \frac{\kappa_r}{2}) e^{i\lambda_1} & (\lambda_2^2 - i\lambda_2 \frac{\kappa_r}{2}) e^{i\lambda_2} & (\lambda_3^2 - i\lambda_3 \frac{\kappa_r}{2}) e^{i\lambda_3} & (\lambda_4^2 - i\lambda_4 \frac{\kappa_r}{2}) e^{i\lambda_4} \end{bmatrix}$$

$$C = \begin{Bmatrix} C_1 \\ C_2 \\ C_3 \\ C_4 \end{Bmatrix} \quad \text{and} \quad R = \begin{Bmatrix} 0 \\ 0 \\ 1 \\ 0 \end{Bmatrix}$$

Now, the receptances β_{AA} and β_{BA} are given as

$$\beta_{AA} = \bar{y}'(0) = \sum_{n=1}^{4} C_n(i\lambda_n), \qquad \text{(A-1.8a)}$$

$$\beta_{BA} = \bar{y}'(1) = \sum_{n=1}^{4} C_n(i\lambda_n)e^{i\lambda_n}, \qquad \text{(A-1.8b)}$$

where the C_n's are solutions of equation (A-1.7).

To calculate the receptances β_{AB} and β_{BB}, apply a non-dimensional unit harmonic moment at end B. Upon using the proper boundary conditions, the system of equation obtained in this case is

$$QC = R', \qquad \text{(A-1.9)}$$

where

$$R' = \begin{Bmatrix} 0 \\ 0 \\ 0 \\ 1 \end{Bmatrix}$$

The receptances β_{AB} and β_{BB} are then given as

$$\beta_{AB} = \sum_{n=1}^{4} C_n(i\lambda_n), \qquad \text{(A-1.10a)}$$

$$\beta_{BB} = \sum_{n=1}^{4} C_n(i\lambda_n)\, e^{i\lambda_n}, \qquad \text{(A-1.10b)}$$

where the C_n's are solutions of equation (A-1.9).

For a uniform beam, the receptances are related as $\beta_{AA} = -\beta_{BB}$ and $\beta_{BA} = -\beta_{AB}$ [5]. Due to the presence of the Coriolis acceleration, this symmetry of the receptances no longer holds good in case of a pipe. It is found that for a pipe conveying fluid, $\beta_{AA} = -\beta_{BB}$ and $\beta^*_{BA} = -\beta_{AB}$, where $*$ denotes the complex conjugate.

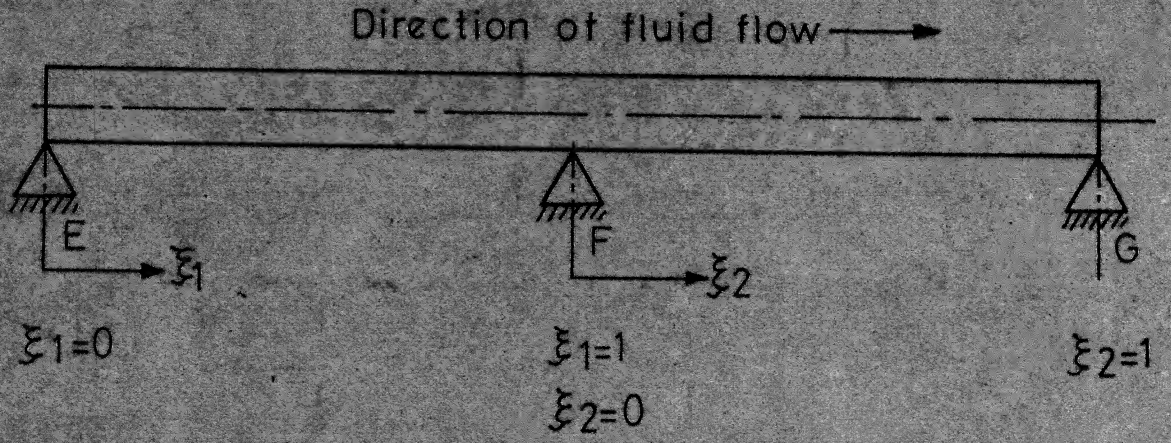

Figure A-2.1-A two span pipe on equi-spaced supports without rotational stiffness.

APPENDIX 2

DETERMINATION OF NATURAL FREQUENCIES OF A TWO SPAN PIPE CONVEYING FLUID USING FREQUENCY DETERMINANT

Consider a two span pipe resting on equi-spaced supports without rotational stiffness as shown in Figure A-2.1. Using equation (A-1.4), the displacement of the pipe, in non-dimensional form, can be written as

$$\bar{y}^1(\xi_1) = \sum_{n=1}^{4} C_n^1 e^{i\lambda_n \xi_1} \quad \text{for span EF,} \tag{A-2.1a}$$

and $$\bar{y}^2(\xi) = \sum_{n=1}^{4} C_n^2 e^{i\lambda_n \xi_2} \quad \text{for span FG,} \tag{A-2.1b}$$

where ξ_1 and ξ_2 are the non-dimensional co-ordinates along the length of the pipe for spans EF and FG, respectively. The coefficients C_n^1, C_n^2's are unknowns to be determined from boundary conditions.

The boundary conditions are

(a) for zero deflection at all the supports

$$\bar{y}^1(0) = 0, \tag{A-2.2a}$$

$$\bar{y}^1(1) = 0, \tag{A-2.2b}$$

$$\bar{y}^2(0) = 0, \tag{A-2.2c}$$

$$\bar{y}^2(1) = 0. \tag{A-2.2d}$$

(b) for zero moments at the supports E and G

$$\bar{y}''^1(0) = 0 \quad , \tag{A-2.2e}$$

$$\bar{y}''^2(1) = 0 \quad . \tag{A-2.2f}$$

(c) for continuity of slope and moment at the support F

$$\bar{y}'^1(1) = \bar{y}'^2(0) \quad , \tag{A-2.2g}$$

$$\bar{y}''^1(1) = \bar{y}''^2(0) \quad . \tag{A-2.2h}$$

Substitution of equation (A-2.1) in equations (A-2.2) yields a system of homogeneous equations

$$Q'C = 0 \tag{A-2.3}$$

where

$$Q = \begin{bmatrix}
1 & 1 & 1 & 1 & 0 & 0 & 0 & 0 \\
e^{i\lambda_1} & e^{i\lambda_2} & e^{i\lambda_3} & e^{i\lambda_4} & 0 & 0 & 0 & 0 \\
\lambda_1^2 & \lambda_2^2 & \lambda_3^2 & \lambda_4^2 & 0 & 0 & 0 & 0 \\
\lambda_1 e^{i\lambda_1} & \lambda_2 e^{i\lambda_2} & \lambda_3 e^{i\lambda_3} & \lambda_4 e^{i\lambda_4} & -\lambda_1 & -\lambda_2 & -\lambda_3 & -\lambda_4 \\
\lambda_1^2 e^{i\lambda_1} & \lambda_2^2 e^{i\lambda_2} & \lambda_3^2 e^{i\lambda_3} & \lambda_4^2 e^{i\lambda_4} & -\lambda_1^2 & -\lambda_2^2 & -\lambda_3^2 & -\lambda_4^2 \\
0 & 0 & 0 & 0 & 1 & 1 & 1 & 1 \\
0 & 0 & 0 & 0 & e^{i\lambda_1} & e^{i\lambda_2} & e^{i\lambda_3} & e^{i\lambda_4} \\
0 & 0 & 0 & 0 & \lambda_1^2 & \lambda_2^2 & \lambda_3^2 & \lambda_4^2
\end{bmatrix}$$

$$C = \{C_1^1 \quad C_2^1 \quad C_3^1 \quad C_4^1 \quad C_1^2 \quad C_2^2 \quad C_3^2 \quad C_4^2\}^t$$

and t denotes the transpose.

For non-trivial solution of equations (A-2.3), one gets

$$|Q'| = 0 \qquad \text{(A-2.4)}$$

Frequencies satisfying equation (A-2.4) give the natural frequencies of the two span pipe.

It is seen that for the case of a two span pipe, the order of the determinant $|Q'|$ is 8. In general, for an N-span pipe this order will be 4N. Thus, the method becomes unwieldy for large values of N.

APPENDIX 3

SOME PROPERTIES OF THE MATHIEU-HILL EQUATION

Consider the differential equation

$$\frac{d^2y}{dt^2} + \Omega_o^2 \left[1 - 2\delta f(t) \right] y = 0, \qquad \text{(A-3.1)}$$

where $f(t)$ is a periodic function with a period

$$T = \frac{2\pi}{\Omega} .$$

Since $\phi(t + T) = \phi(t)$, equation (A-3.1) does not change its form on addition of the period T to t. Therefore, if $y(t)$ is a solution of equation (A-3.1) then $y(t + T)$ is also its solution.

Let $y_1(t)$ and $y_2(t)$ be any linearly independent solutions of equation (A-3.1), then $y_1(t+T)$ and $y_2(t+T)$ are also its solutions, and consequently can be presented in the form of a linear combination of solution $y_1(t)$ and $y_2(t)$.

$$y_1(t+T) = a_{11}\, y_1(t) + a_{12}\, y_2(t), \qquad \text{(A-3.2a)}$$

$$y_2(t+T) = a_{21}\, y_1(t) + a_{22}\, y_2(t), \qquad \text{(A-3.2b)}$$

where a_{ij} are constants.

Thus, the addition of the period T to t results in a linear transformation of the initial system of solutions. If one takes some other linearly independent solutions instead of the initially chosen

solutions of $y_1(t)$ and $y_2(t)$, then the coefficients of the transformation in (A-3.2), generally, will change. In particular, one can try to choose solutions $y_1^*(t)$ and $y_2^*(t)$ such that the coefficients a_{12} and a_{21} in equation (A-3.2) vanish. The transformation in this case will take its simplest form and will be reduced to the multiplication of initially chosen solutions by certain constants†.

$$y_1^*(t+T) = \rho_1 \, y_1^*(t) \tag{A-3.3a}$$

$$y_2^*(t+T) = \rho_2 \, y_2^*(t) \tag{A-3.3b}$$

Now, the transformation of the type (A-3.2) can be reduced to the diagonal form (A-3.3), where the constants $\rho_{1,2}$ are determined from the characteristics equation

$$\begin{vmatrix} a_{11} - \rho & a_{12} \\ a_{21} & a_{22} - \rho \end{vmatrix} = 0$$

which can be written in the following form

$$\rho^2 - 2A\rho + B = 0 \tag{A-3.4}$$

where $A = \frac{1}{2}(a_{11} + a_{22})$,

and $B = a_{11} a_{22} - a_{12} a_{21}$.

Let $y_1(t)$ and $y_2(t)$ be two linearly independent solutions of equation (A-3.1) satisfying the initial conditions

---

† These are known as Floquet solutions.

$$y_1(0) = \alpha_1 \quad , \quad y_2(0) = \alpha_2,$$

$$\dot{y}_1(0) = \beta_1 \quad , \quad \dot{y}_2(0) = \beta_2 \quad , \tag{A-3.5}$$

where dots denote differentiation with respect to t.

Now, use of equations (A-3.5) in equations (A-3.2) results in

$$a_{11}\,\alpha_1 + a_{12}\,\alpha_2 = y_1(T), \tag{A-3.6a}$$

$$a_{11}\,\beta_1 + a_{12}\,\beta_2 = \dot{y}_1(T), \tag{A-3.6b}$$

$$a_{21}\,\alpha_1 + a_{22}\,\alpha_2 = y_2(T), \tag{A-3.6c}$$

$$a_{21}\,\beta_1 + a_{22}\,\beta_2 = \dot{y}_2(T) \tag{A-3.6d}$$

From equations (A-3.6), constants a_{ij} can be determined as

$$a_{11} = \frac{\alpha_2\,\dot{y}_1(T) - \beta_2\,y_1(T)}{\alpha_2\,\beta_1 - \alpha_1\,\beta_2},$$

$$a_{12} = \frac{\beta_1\,y_1(T) - \alpha_1\,\dot{y}_1(T)}{\alpha_2\,\beta_1 - \alpha_1\,\beta_2},$$

$$a_{21} = \frac{\alpha_2\,\dot{y}_2(T) - \beta_2\,y_2(T)}{\alpha_2\,\beta_1 - \alpha_1\,\beta_2},$$

and

$$a_{22} = \frac{\beta_1\,y_2(T) - \alpha_1\,\dot{y}_2(T)}{\alpha_2\,\beta_1 - \alpha_1\,\beta_2}$$

Using the values of a_{ij}, the constant B can be written as

$$B = a_{11}\,a_{22} - a_{12}\,a_{21}$$

or

$$B = \frac{y_1(T)\,\dot{y}_2(T) - y_2(T)\,\dot{y}_1(T)}{\alpha_1\,\beta_2 - \alpha_2\,\beta_1} \tag{A-3.7}$$

It can be shown that the constant B is always equal to unity. Since $y_{1,2}(t)$ are solutions of equation (A-3.1), then

$$\ddot{y}_1 + \Omega_o^2 \left[1 - 2\delta f(t)\right] y_1 = 0 \qquad \text{(A-3.8a)}$$

$$\ddot{y}_2 + \Omega_o^2 \left[1 - 2\delta f(t)\right] y_2 = 0 \qquad \text{(A-3.8b)}$$

Multiplying the first identity (A-3.8a) by $y_2(t)$, and the second identity by $y_1(t)$, and subtracting one from the other, one gets

$$y_1(t)\, \ddot{y}_2(t) - y_2(t)\, \ddot{y}_1(t) = 0$$

on integrating it, one obtains

$$y_1(t)\, \dot{y}_2(t) - y_2(t)\, \dot{y}_1(t) = C\,, \qquad \text{(A-3.9)}$$

where C is a constant.

Using initial conditions (at $t = 0$), C can be determined as

$$C = \alpha_1\, \beta_2 - \alpha_2\, \beta_1,$$

and at $t = T$, equation (A-3.9) gives

$$y_1(T)\, \dot{y}_2(T) - y_2(T)\, \dot{y}_1(T) = C = \alpha_1\, \beta_2 - \alpha_2\, \beta_1,$$

i.e., $B = 1$.

Thus, the characteristic equation (A-3.4) takes the form

$$\rho^2 - 2A\rho + 1 = 0\,, \qquad \text{(A-3.10)}$$

and its roots are related by

$$\rho_1\, \rho_2 = 1 \qquad \text{(A-3.11)}$$

It has already been shown that among the particular solutions of (A-3.1) two linear independent solutions $y^*_{1,2}(t)$ exist which satisfy equations (A-3.3)

$$y^*_k(t+T) = \rho_k\, y^*_k(t),\ k = 1,2.$$

These solutions, which acquire a constant multiplier by the addition of the period T to t, can be represented in the form

$$y_k(t) = \chi_k(t)\ e^{(t/T)\ \ln \rho_k},\ k = 1,2 \qquad (A\text{-}3.12)$$

where $\chi_{1,2}(t)$ are certain periodic functions of period T.

It follows from equation (A-3.12) that the behaviour of the solutions as $t \to \infty$ depends on the value of characteristic roots (more precisely, on the value of its moduli). In fact, taking into account that

$$\ln \rho = \ln |\rho| + i \arg \rho,$$

one can write equation (A-3.12) in the following form

$$y_k(t) = f_{1k}(t)\ e^{(t/T)\ln|\rho_k|},\ k = 1,2, \qquad (A\text{-}3.13)$$

where $f_{1k}(t)$ is the bounded function

$$f_{1k}(t) = \chi_k(t)\ e^{(it/T)\ \arg \rho}.$$

If the characteristic number ρ_k is greater than unity, then the corresponding solution (A-3.13) increases unboundedly with time. On the other hand, a characteristic multiplier less than unity implies a decaying solution. Finally, if the characteristic number is equal to unity, then the solution is periodic, i.e., it will be bounded in time.

If $|A| > 1$, then, as can be seen from equation (A-3.10), the characteristic roots will be real, and one of them will be greater than unity. In this case the general solution of equation (A-3.1) will unboundedly increase with time.

If $|A| < 1$, the characteristic equation has conjugate complex roots and since their product must be unity, their moduli will be equal to unity. The case of complex characteristic roots corresponds to the region of bounded solutions. On the boundaries separating the regions of bounded solutions, condition $|A| = 1$ must be satisfied [7].

For $|A| = 1$, multiple roots occur, moreover, it follows from equation (A-3.11), such roots can be either $\rho_1 = \rho_2 = 1$ or $\rho_1 = \rho_2 = -1$. In the first case, as seen from equation (A-3.3), the solution will be periodic with a period $T = \frac{2\pi}{\Omega}$; whereas in the second case the period will be 2T.

Therefore, the regions of unbounded solutions are separated from the regions of bounded solutions by the periodic solutions with period T and 2T. In other words, two solutions of identical period bound the region instability, and two solutions of different periods bound the region of stability.

Now, consider the differential equation of the form

$$\frac{d^2y}{dt^2} + 2\varepsilon \frac{dy}{dt} + \Omega_o^2 \left[1 - 2\delta f(t)\right] y = 0 \qquad \text{(A-3.14)}$$

where the second term represents viscous damping on the motion described by y.

Bolotin [7] has shown that the problem of finding the regions of instability for equation (A-3.14) is reduced to the determination of the conditions under which it has periodic solutions with period T and 2T. Here also, two solutions of an identical period bound the region of unboundedly increasing solutions and two solutions of different periods bound the region of damped solutions.

APPENDIX 4

ELEMENTS OF THE MATRICES D_{pp}, D_{cc}, D_{cp}, AND Z_a

(a) Matrix D_{pp} :

The elements of the matrix D_{pp} (order 8×8) are

$$d_{1,j} = 1,$$

$$d_{2,j} = \lambda_{1j}^2,$$

$$d_{3,j} = \lambda_{1j}\, e^{\lambda_{1j}/2}$$

$$d_{4,j} = (\lambda_{1j}^3 + \frac{1}{8}\Gamma_a \Omega^2 A_o)\, e^{\lambda_{1j}/2},$$

$$d_{4,j+4} = \frac{1}{8}\Gamma_a \Omega^2 B_o\, e^{\lambda_{2j}/2},$$

$$d_{5,j} = -\frac{1}{8}\Gamma_a \Omega^2 B_o\, e^{\lambda_{1j}/2},$$

$$d_{5,j+4} = (\lambda_{2j}^3 + \frac{1}{8}\Gamma_a \Omega^2 A_o)\, e^{\lambda_{2j}/2},$$

$$d_{6,j+4} = 1,$$

$$d_{7,j+4} = \lambda_{2j}^2,$$

$$d_{8,j+4} = \lambda_{2j}\, e^{\lambda_{2j}/2},$$

with $j = 1,2,3,$ and 4. The remaining terms of the matrix D_{pp} are zero.

(b) Matrix D_{cc} :

The elements of the matrix D_{cc} are same as the elements of the matrix D_{pp} but for the following changes

$d_{2,j} = \lambda_{1j}$,

$d_{7,j+4} = \lambda_{2j}$,

with j = 1,2,3, and 4.

(c) Matrix D_{cp} :

The elements of the matrix D_{cp} (order 16 × 16) are

$d_{1,j} = 1$,

$d_{2,j+4} = 1$,

$d_{3,j+8} = e^{\lambda_{1j}/2}$,

$d_{4,j+12} = e^{\lambda_{2j}/2}$,

$d_{5,j} = \lambda_{1j}$,

$d_{6,j+4} = \lambda_{2j}$,

$d_{7,j+8} = \lambda_{1j}^2 e^{\lambda_{1j}/2}$,

$d_{8,j+12} = \lambda_{2j}^2 e^{\lambda_{2j}/2}$

$d_{9,j} = e^{\lambda_{1j}/2}$,

$d_{9,j+8} = -1$,

$d_{10,j+4} = e^{\lambda_{2j}/2}$,

$d_{10,j+12} = -1$,

$d_{11,j} = \lambda_{1j} e^{\lambda_{1j}/2}$,

$d_{11,j+8} = -\lambda_{1j}$,

$$d_{12,j+4} = \lambda_{2j}\, e^{\lambda_{2j}/2},$$

$$d_{12,j+12} = -\lambda_{2j},$$

$$d_{13,j} = \lambda_{1j}^2\, e^{\lambda_{1j}/2},$$

$$d_{13,j+8} = -\lambda_{1j}^2,$$

$$d_{14,j+4} = \lambda_{2j}^2\, e^{\lambda_{2j}/2},$$

$$d_{14,j+12} = -\lambda_{2j}^2,$$

$$d_{15,j} = (\lambda_{1j}^3 + \tfrac{1}{4}\,\Gamma_a\,\Omega^2\,A_o)\, e^{\lambda_{1j}/2},$$

$$d_{15,j+4} = \tfrac{1}{4}\,\Gamma_a\,\Omega^2\,B_o\, e^{\lambda_{2j}/2},$$

$$d_{15,j+8} = -\lambda_{1j}^3,$$

$$d_{16,j} = -\tfrac{1}{4}\,\Gamma_a\,\Omega^2\,B_o\, e^{\lambda_{1j}/2},$$

$$d_{16,j+4} = (\lambda_{2j}^3 + \tfrac{1}{4}\,\Gamma_a\,\Omega^2\,A_o)\, e^{\lambda_{2j}/2},$$

$$d_{16,j+12} = -\lambda_{2j}^3,$$

with $j = 1,2,3$, and 4. The remaining terms of the matrix D_{cp} are zero.

(d) Matrix Z_a :

The elements of the matrix Z_a (order 8×8) are

$$z_{1,j} = 1,$$

$$z_{2,j} = -\lambda_{1j}^2,$$

$$z_{3,j+4} = e^{\lambda_{1j}/2},$$

$$z_{4,j+4} = -\lambda_{1j}^2 e^{\lambda_{1j}/2},$$

$$z_{5,j} = e^{\lambda_{1j}/2},$$

$$z_{5,j+4} = -1,$$

$$z_{6,j} = \lambda_{1j} e^{\lambda_{1j}/2},$$

$$z_{6,j+4} = -\lambda_{1j},$$

$$z_{7,j} = \lambda_{1j}^2 e^{\lambda_{1j}/2},$$

$$z_{7,j+4} = -\lambda_{1j}^2,$$

$$z_{8,j} = (\lambda_{1j}^3 + \frac{1}{4} r_a \Omega^2 A_o) e^{\lambda_{1j}/2},$$

$$z_{8,j+4} = -\lambda_{1j}^3,$$

with $j = 1,2,3,$ and 4. The remaining terms of the matrix Z_a are zero.